Hassen, Tewodros Wolde

Synchronization in Cognitive Overlay Systems

School of Electrical Engineering

Thesis submitted for examination for the degree of Master of Science in Technology.

Espoo, August 08, 2012

Thesis supervisor:

Prof. Olav Tirkkonen

Thesis instructor:

D.Sc. Jussi Poikonen

Aalto University
School of Electrical
Engineering

AALTO UNIVERSITY
SCHOOL OF ELECTRICAL ENGINEERING

ABSTRACT OF THE
MASTER'S THESIS

Author: Hassen, Tewodros Wolde

Title: Synchronization in Cognitive Overlay Systems

Date: August 08, 2012 Language: English Number of pages:8+85

School of Electrical Engineering
Department of Communications and Networking Technologies
Professorship: Radio Communications Code: S-72

Supervisor: Prof. Olav Tirkkonen

Instructor: D.Sc. Jussi Poikonen

The primary purpose of this thesis is to study the effect of synchronization problems in cognitive radio based overlay systems. In such systems the secondary transmitter should know the transmission timing of the primary transmitter for cooperation to take place between the two systems. The thesis also investigates the effect of relaying in overlay systems. By splitting the secondary transmission power into two parts by a ratio α, the secondary transmitter can relay the primary transmission while transmitting its own message. Another aim of the thesis is to study the effects of time and frequency offsets in the primary and the secondary systems. Hence, time and frequency synchronization issues are investigated for DVB-T and LTE systems individually. Cell search and selection procedures are also studied for LTE systems.
Two N200 Universal Software Radio Peripherals (USRPs) were used to transmit and receive the signal using the Gnu Radio platform and the captured signals were post processed in Matlab to study the effects of time offset and frequency offset of the devices. Moreover, a Matlab simulation was used to investigate the effect of timing offset between primary and secondary transmitters in overlay systems.

From the investigation of the overlay scenario with relay, we have found out that the relaying introduce a multi-path effect at the secondary receiver. If there is a delay between the primary and the secondary receivers, the components of the multi-path signal might be added-up in such a way that it is impossible to separate the primary and the secondary signals at the secondary receiver. Hence, we have implemented synchronization and equalization algorithms to estimate the delay and frequency offsets. We observed that the performance of the equalizer at the secondary receiver deteriorates for high delays and low α values.

Keywords: Synchronization, Cognitive Radio, Spectrum sharing, interweave, overlay, LTE, DVB-T, Gnu Radio

Acknowledgment

After pursuing it for over the last two years, I have finally completed my M.SC. studies. It has been such a journey full of excitements, ever changing challenges and new experiences. Many people have given me motivation and support throughout these times which was extremely important to accomplish my goals. I would like to dedicate this page to express my deepest gratitude to some of them.

First and Foremost, I would like to express my sincere gratitude to my supervisor Prof. Olav Tirkkonen for his continuous support and giving me the opportunity to work in the End-to-end cognitive radio testbed (EECRT) project and other researches over the years. I would like to thank him for his patience, motivation, enthusiasm, and immense knowledge. His insightful comments, and frank criticisms have bettered me throughout my learning process. Moreover, it has been a privilege to work with my instructor Dr. Jussi Poikonen. He was always there to guide me through the problems I faced in my research work. Besides, he helped me in structuring my thesis and in the daunting task of proof-reading it. Such a nice down-to-earth man! I also thank Kalle Rutik for his constructive ideas, comments and guidance. I am thankful for working with all the boys in project. Yehenewe, Li Yang, Gerardo and vishnu, thank you all for the fruitful discussions and the pleasant work atmosphere.

Last but not list, my greatest gratitude goes to my parents. Wolde and Geneye, your unwavering support and continuous encouragement has been huge throughout my life. Even if we are several miles apart, you two are my rocks during the times of despair .
Thank you all, you all have made things a bit easier for me!

Espoo, August 08, 2012,

Tewodros Hassen

Contents

Abbreviations

3GPP	Third Generation Project Partnership
ADC	Analog to Digital Converter
AWGN	Additive white Gaussian noise
BER	Bit error rate
BOF	Beginning of frame
BPSK	Binary phase shift keying
BS	Base Station
CAZAC	Constant Amplitude Zero Auto-Correlation
CDMA	Code Division Multiple Access
CFO	Carrier Frequency Offset
CP	Cyclic prefix
CR	Cognitive Radio
DAC	Digital to Analog Converter
DDC	Digital Down Conversion
DSO	Digital Switch Over
DUC	Digital Up Conversion
DVB-T	Digital Video Broadcasting-Terrestrial
FDD	Frequency Division Duplex
FFO	Fractional Frequency Offset
FFT	Fast Fourier Transform
ICI	Inter Carrier Interference
IF	Intermediate Frequency
IFFT	Inverse Fast Fourier Transform
IFO	Integer Frequency Offset
IOS	Internetwork Operating System
ISI	Inter Symbol Interference
LO	Local Oscillator
LOS	Line Of Sight
LTE	Long Term Evolution
ML	Maximum Likelihood
NLOS	Non line Of Sight
OFDM	Orthogonal Frequency Division Multiplexing
PDP	Power Delay Profile
PN	Pseudo Noise
PRBS	Pseudo Random Binary Sequence
PSK	Phase Shift Keyed
PSS	Primary Synchronization Sequence
QAM	Quadrature Amplitude Modulation
RF	Radio Frequency
RMS	Root Mean Square
SCFO	Sampling Carrier Frequency Offset
SDR	Software Defined Radio
SFN	Single Frequency Networks
SFO	Sampling Frequency Offset
SNIR	Signal to Noise and Interference ratio
SNR	Signal to Noise Ratio

Abbreviations

SSS	Secondary Synchronization Sequence
STO	Symbol Time Offset
TDD	Time Division Duplex
TDMA	Time Division Multiple Access
TPS	Transmission Parameter Signaling
TVWS	TeleVision White Space
UE	User Equipment
USRP	Universal Software Radio Peripheral
UWB	Ultra Wide Band
WiMax	Worldwide Interoperability for Microwave Access
WiFi	Wireless Fidelity
WLAN	Wireless Local Area Networks
WSD	White Space Devices
ZC	Zadoff-Chu

List of Figures

1 Introduction

1.1 Overview

Wireless communication has gone through dramatic development in the last century. It has proved to be important as a major development factor first as a form of wireless networks and more recently for computer networks (WiFi). The increase in demand for mobility and the recent transition of cellular networks from providing limited data to supporting mobile broadband services to accommodate the ever increasing demand of bandwidth-hungry services, put a huge strain on the capacity of the available licensed spectrum for the service. The international telecommunication union (ITU) has predicted that the spectrum demand for mobile communications would be six times more than the spectrum occupied at by the service at the moment [1].

On the other hand research [2][3] has revealed that there are cases of under utilization of the licensed spectrum in some wireless communication services. A good example is a TV broadcast system where there are a significant white spaces in the licensed spectrum [2]. Adaptability across the Internetwork Operating System (IOS) stack of the cellular network devices to be able to access the under-utilized spectrum resources in the unlicensed band is the new paradigm in wireless communication systems that quickly caught the interest of the research community in the communications arena in the recent years. In addition to exploiting the under-utilized spectrum resources, spectrum sharing by means of interference accommodation and mitigation is the other way forward to address the challenges faced in the development of mobile technology in the coming few years.

In its narrower sense, *Cognitive Radios* (CRs) are the new paradigm to deal with the aforementioned challenges associated with spectrum shortage. By making the unlicensed spectrum accessible to secondary systems using *underlay*, *interweave* or/and *overlay* spectrum sharing techniques [4], the scheme helps to increase spectrum efficiency in wireless communication systems. In the *interweave* spectrum access technique, the secondary system determines the spectrum that remains unused by the primary system. In the *underlay* approach, the secondary system transmits at signal power close to the noise level so that the primary is not affected by interference. The *overlay* approach increases flexibility on the signal level of the secondary transmitter. It employs some sort of cooperation between the primary and the secondary to mitigate interference at the primary receiver.

In its wider sense, a cognitive radio is capable of learning its environment, internal state and location and adapt its operation based on the changes in one of these parameters. Such a radio will also often incorporate software defined radio (SDR) functionality.

1.2 The Scope of the Thesis

In a digital communication system, data is transmitted by mapping bit sequences to symbols and symbols to sample functions of analogue wave forms. The analogue waveform passes through a band limited analogue channel (which can be modeled as incorporating also radio hardware non-idealities) where the signal is corrupted and noise is added. At the receiver, the symbol may be recovered by means of coherent detection, where all possible sample functions are known, or by non-coherent detection, where one or more characteristics of the sample function are estimated. In a coherent receiver, synchronization is the most commonly used technique for recovering the sample functions from the received waveform. These sample functions are then used as reference signals for correlation.

In cognitive overlay systems, symbol level synchronization between the primary and the secondary transmitters involves estimating the sample functions of the primary received signal at the secondary transmitter to determine symbol transmission interval of the primary transmitter. Based on this knowledge and using some mechanism to determine the primary codeword which is beyond the scope of this thesis, the secondary transmitter will be able to to design its own codewords accordingly and cooperate with the primary system by aligning the secondary codewords with the primary transmission.

The primary objective of this thesis is to show the effects of synchronization between the primary and the secondary systems in the overlay spectrum sharing scheme. However the research also covers time and frequency synchronization issues in the primary and the secondary systems independently. We investigated the 3GPP LTE down-link frame structure, implemented cell search and time and frequency synchronization algorithms and tested them using over-the-air transmission. Moreover, time and carrier frequency synchronization and channel equalization algorithms for the primary system, i.e the Digital video broadcasting-terrestrial (DVB-T), has been implemented and tested using over-the-air transmission set up in the laboratory using USRP N200 TX and RX boxes. Using a Matlab simulation, the performance of the *overlay* approach has been investigated for various delays between the primary and the secondary transmitters using DVB-T frames as a primary signal and a generic OFDM as a secondary system . The organization of the chapters of the thesis is as presented in the next paragraphs.

Chapter 2 explains the effects of a wireless channel in digital communication systems using the broader sense of the term 'channel' to include the effect of hardware non-idealities at radio ends. It proceeds to discuss the parameters of a wireless channel with a quantitative analysis of the the effects of the parameters on a wireless transmission system. Then the chapter closes by introducing wireless channel models used in different communications systems.

Chapter 3 sheds a light on the basics of cognitive radios (CRs) and software de-

fined radios (SDRs) in a brief introduction. It discusses the relation between CR and SDR and discusses usage scenarios of cognitive radios by citing spectrum sharing techniques as an example. The later part of the chapter presents a brief theoretical insight about cognitive radio channels.

Chapter 4 stands as the core chapter as it discusses the main essence of the thesis, textitsynchronization. Starting with background of synchronization in wireless communication systems, the chapter offers a thorough theoretical explanation about various time and frequency synchronization algorithms based on previous works on the topic. By narrowing the scope to a specific technology, the discussion goes on about synchronization algorithms for DVB-T and LTE systems. The chapter also reflects on synchronization between transmitters in a cognitive radio system by putting emphasis on cognitive radios in overlay systems.

Chapter 5 constitutes the measurement results and the observations. It starts by discussing the implementation aspects of the synchronization algorithms discussed in the previous chapter and the workarounds to address the problems at hand. It illustratively presents the results of the implementations and discusses about the observations.

Chapter 6 wraps up the thesis by reflecting on the big picture of what has been done in the thesis and discussing future possible work

2 Channel Effects in Wireless Communications

2.1 Introduction

In a broad sense a wireless channel can be defined as the radio propagation environment, including the transmitter and the receiver, through which information is transmitted, transported, and received. The characteristics of the wireless signal changes as it travels form the transmitter through the channel to the receiver. These changes in characteristics are mainly due to channel effects such as shadowing, multi-path effects, etc and hardware non-idealities at the transmitter and receiver, which introduces impairments in the received signal. For an error-free communication to take place, the magnitude of these impairments must be estimated and canceled from the received signal.

In mobile radio communication systems, information is transmitted in the air as a digitally modulated band-pass signal at a carrier frequency of f_c and can be expressed mathematically as:

$$s(t) = \mathbb{R}\{s_b(t) \cdot e^{j2\pi f_c t}\} \tag{1}$$

where s_b(t) is the complex envelop that encloses the modulating information. Since only the phase and amplitude of the carrier signal are modulated, we can use s_b(t) for our further discussion without loss of generality. In addition, in order to put more emphasis on the impairments from the channel effects and hardware non-idealities, we intentionally ignore to discuss distortions due to noise and other interferences. Path-loss is also neglected as it has little impact on synchronization and channel estimation which are the focal points of this project.

2.2 Impacts of hardware non-idealitlies

In software defined radios most of the signal processing task is done in the digital domain. As a result, the front-end of a reconfigurable radio uses minimal analog electronic components, which will have to process wide-band high dynamic range signals. A typical direct conversion radio implementation of this kind may be very sensitive to various mismatches and imperfections in the front-end. These imperfections are due to manufacturing defects, varying operating temperatures and the like, and may result in front-end non-idealities such as in-phase/quadrature-phase (IQ) imbalance; non-linearities in analog to digital converters (ADC), digital to analog converters (DAC) and amplifiers; phase noise and carrier frequency offset (CFO) due to local oscillator (LO) defects, etc. The front-end non-idealities are also commonly called radio frequency (RF) impairments [5][6]. If front-end non-idealities are not properly understood and compensated, they can easily become a limiting factor to the quality and performance of the radio device and the entire communication link. In particular, OFDM based communication systems are considered to be very sensitive to such non-idealities. As next generation wireless systems, many of them based on OFDM, will require more simplified, low cost, flexible and reconfigurable

radio front-ends, the use of cheaper components will increase, and as a result the effect of front-end non-idealities will become even more severe.

Rather than dealing with the effects of these non-idealities by using expensive front ends, it is easier and more economical to tolerate the effects in the analog domain and compensate them in the digital domain using suitable digital signal processing techniques. Some of the non-idealities associated with the front-end components are given below:

- DAC, ADC and Samplers: Common non-idealities are non-ideal passband response i.e. unintentional filtering, aliasing, quantization noise, jitter noise due to instabilities of the sampling clock, non linear distortion due to clipping in ADC, deviation in the representation of quantization levels in DAC and DC offsets. The differences in ADCs and DACs in the I and Q branch leads to IQ imbalance.

- Mixers: Common non-idealities are non-linear distortions such as out of band harmonics, in-band inter-modulation products. Mixers also result in finite isolation between the input, local oscillator and output ports, and DC offsets. The relative difference between the I and Q branch mixers also contribute to IQ imbalance.

- Local oscillator: Common non-idealities are phase noise due to random fluctuation of the oscillator phase, carrier frequency offset (CFO) and phase offsets due to differences between the local oscillators at transmitter and receiver. Also the deviation in amplitude and phase shift from the ideal settings results in IQ imbalance.

- Amplification stages (Low Noise Amplifiers (LNAs), Variable Gain Amplifiers (VGAs), power amplifier at transmitter): Common non-idealities are various non-linear distortion effects such as in-band interference, harmonic distortion and inter modulation distortion. The difference in I and Q branch amplifiers also result in IQ imbalance.

2.3 Parameters of wireless channels

In addition to the hardware non-idealities at the front-ends mentioned above, mobile radio propagation is substantially affected by unpredictable fluctuations in received signal power level due to multi-path propagation and shadowing. By multi-path propagation we refer to the property that multiple copies of a signal are received via distinctive transmission paths that are characterized by their own attenuation, phase shift and propagation delay. Multi-path propagation is a result of reflection, diffraction and scattering of the transmitted signal at natural or man-made objects. Figure 1 shows an example of a multi-path propagation. The constructive or destructive superposition of these multi-path copies, according to their phase-shift, results in linear time varying fluctuation of the signal power at the receiver. Let the

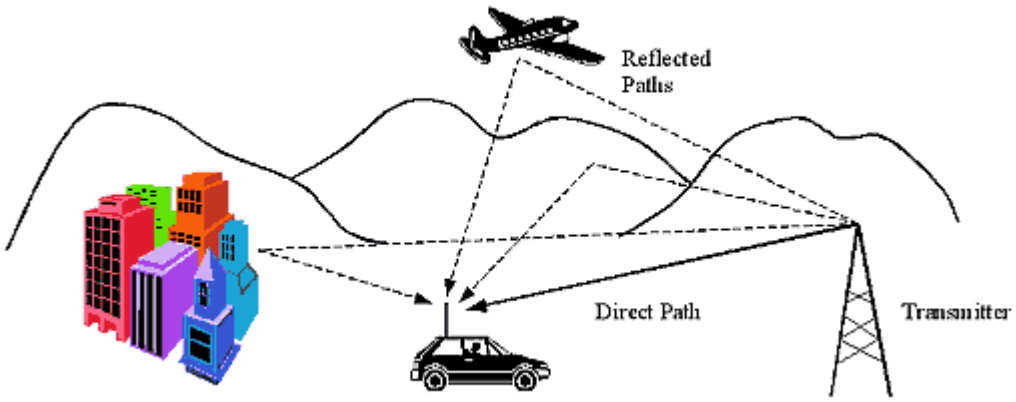

Figure 1: Illustration of Multi-path Propagation in a randomly varying geometry

attenuation and delay for each path be $\alpha_n(t)$ and $\tau_n(t)$ respectively. The signal at the receiver can be characterized as:

$$r(t) = \sum_n \alpha_n(t) s\left(t - \tau_n(t)\right) \tag{2}$$

Writing the transmit signal in its complex baseband form and substituting it in equation (2), we can get:

$$r(t) = \mathbb{R}\{\sum_n \alpha_n(t) s_b\left[t - \tau_n(t)\right] e^{j2\pi f_c[t-\tau_n(t)]}\} \tag{3}$$

Hence, the complex baseband representation of the the received signal is:

$$r_b(t) = \sum_n \alpha_n(t) s_b\left[t - \tau_n(t)\right] e^{-j2\pi f_c[\tau_n(t)]} \tag{4}$$

$$= \sum_n \alpha_n(t) e^{-j\theta_n(t)} s_b\left[t - \tau_n(t)\right] \tag{5}$$

where θ_n is the phase of n^{th} path.

Each component goes a phase shift of 2π in a matter of a distance of half a wavelength [7] while the amplitude remains almost unchanged for such a time scale. The large phase variations with small change in geometry together with the randomness of the incoming phases results in large variations in the amplitude of the received signal. Given the scale of the spacial change in which this variation occurs, this type of fading is called Small-scale Fading. Moreover, the mean received power which is averaged over the small-scale fading may still vary unpredictably as a result of attenuation of the propagation form obstructions like buildings, foliage and the terrain. Since these fluctuations occur over as a long range as hundreds of wave lengths, they are usually known as large-scale fading.

From the above discussion it should be clear that it is very difficult to describe a wireless channel in a rigorous fashion as it is governed by a number of unpredictable factors. For this reason, statistical characterization, using the channel parameters discussed in sections below, provides a good insight to study the properties of channels in wireless communication systems.

2.3.1 Excess Delay

A wireless channel can be fully expressed by its channel response h(τ,t) at time t for delayed Dirac delta impulse applied at time t - τ. In practice, there are a large number of multi-path components received via multiple paths. In digital signals at high rates, this multi-path propagation usually results in frequency selective fading and Inter Symbol Interference (ISI). Assuming only the first N multi-path components have significant power level at the receiver, the channel impulse response is characterized as:

$$h(\tau, t) = \sum_{l=1}^{N} \alpha_l(t) e^{j\theta_l(t)} \delta(t - \tau_l) \tag{6}$$

where α_l, θ_l and τ_l represent the time-varying attenuation, phase shift and delay of the l^{th} path. Assuming the path delays are arranged in increasing order, the excess delay, $\Delta\tau_l(t)$, is given as the difference between $\tau_l(t)$ and $\tau_1(t)$. Conventionally, the delay times are given relative to the time of arrival of the line-of-sight. i.e., $\tau_1(t) = 0$ hence, the excess delay is equivalent to $\tau_l(t)$ for $l > 1$.

2.3.2 Power Delay Profile

Power Delay Profile (PDP) is a statistical variable that characterizes the average received power level of the channel components in equation (6), that is, $E[\alpha_l^2]$. The individual average received power levels are added to give the cumulative received power level. However, in practice, the PDP is normalized so that the sum of received powers from each path is unity. PDP is also used to describe the average delay spread, which is the measure of time-dispersiveness of the channel and can be given as the second central moment of the PDP. The second central moment of the PDP is also referred to as the root-mean-square (RMS) delay spread and is given, weighted proportional to the reflected wave energies, as:

$$\tau_{RMS} = \sqrt{\frac{\sum_{n=0}^{N-1} P_n(\tau_n - \tau_m)}{\sum_{n=0}^{N-1} P_n}} \tag{7}$$

where τ_m is the average delay and is defined as:

$$\tau_m = \frac{\sum_{n=0}^{N-1} P_n \tau_n}{\sum_{n=0}^{N-1} P_n} \tag{8}$$

Again, $P_n = E[\alpha_n^2]$. The parameter τ_{RMS} in equation (7) is of great importance in evaluating the effect of multi-path distortions in the received signal. The ISI due to

time-dispersion is negligible if the symbol duration is larger than, for example, ten times the τ_{RMS} [7]. If τ_{RMS} values are larger than the symbol duration or even of the same order, some compensation procedures must be carried out at the receiver to mitigate possible performance degradation. Typical RMS delay profile values for different propagation environments are shown in Table 1 below according to [8].

Table 1: RMS delay for different propagation environments

Channel Model	Delay Spread τ_{RMS}
Urban micro cell	0.251 μs
Urban macro cell	0.65 μs
Suburban macro cell	0.17 μs

2.3.3 Coherence Bandwidth

The Coherence bandwidth (B_c) is the measure of the variation in the channel frequency response over a range of frequency components at a given time t. In other words, it is the measure of spectrum interval over which channel frequency response is flat. The channel frequency response at a given time t is defined as the Fourier transform of h(τ, t) with respect to τ and can be written as:

$$H(f,t) = \int_{\infty}^{\infty} h(\tau,t)\,\mathrm{d}\tau. \tag{9}$$

For transmitted signals with bandwidth less that B_c, the channel frequency response given by (9) is considered to be flat over the whole signal spectrum. Alternatively we can state that values of the channel frequency response at frequencies f_1 and f_2 are highly correlated if the separation between the frequencies is less than B_c. On the other hand, if the transmitted signal bandwidth is larger than B_c, the signal spectrum would be distorted. In this case, the channel might be referred to as frequency selective. Hence, whether a channel is flat or frequency selective largely depends on the bandwidth of the transmitted signal. In general a channel may be classified as frequency selective if its transmission bandwidth is greater than 50% of the coherence bandwidth [9].

There exists an inverse relation between B_c and τ_{RMS}. Using the uncertainty relationship discussed in [10] , B_c can be defined as:

$$B_{c(a)} \geq \frac{1}{2\pi\tau_{RMS}} \arccos(a) \tag{10}$$

where $B_{c(a)}$ is the minimal coherence bandwidth for which the channel power delay profile has an autocorrelation value of a.

2.3.4 Coherence Bandwidth and frequency domain reference signals

From the LTE frame structure, we know that the spacing between two adjacent sub-carriers, f_{space}, is 15 kHz [11]. In the frequency domain, the pilot symbols are placed at every 6th subcarrier. hence, separation between consecutive pilots, f_{space}, can be given as:

$$f_P = 6 \cdot f_{space} = 90 \text{ kHz}. \tag{11}$$

Using the uncertainty relationship described in [10] the bandwidth $B_{c(a)}$ in which the channel is constant is defined at $a = 0.9$ and at the value $a = 0.5$ for when the channel has changed. Based on these assumptions the coherence bandwidth for autocorrelation value of 0.5 can be calculated as:

$$B_{c(0.5)} \geq \frac{1}{2\pi\tau_{RMS}} \arccos(0.5) \tag{12}$$

$$= \frac{1}{2\pi 0.65\mu s} \arccos(0.5) = 256.4 \text{ kHz}. \tag{13}$$

Similarly, for the autocorrelation value of 0.9 we have

$$B_{c(0.9)} \geq \frac{1}{2\pi 0.65\mu s} \arccos(0.9) = 110.4 \text{ kHz}. \tag{14}$$

Equations (12) and (13) show that the spacing of the pilot symbols in frequency approximately corresponds to the bandwidth in which the channel is constant, furthermore the channel is estimated at least twice before the autocorrelation has the value 0.5.

2.3.5 Doppler Spread

In mobile communication environments, the movement of the receiver, the transmitter or the surrounding objects results in the spectral broadening of the received signal. In multi-path propagation conditions, there are a number of Doppler shifts, relative to the carrier frequency, which give raise to the Doppler spectrum. The measure of this spectral broadening is defined as the range of frequencies over which the received Doppler spectrum is essentially non-zero and is usually referred to as *Doppler spread*.

Let us assume a mobile receiver is moving at a speed of v_{rx} m/s and a wave is transmitted from a transmission station at a carrier frequency f_c. If the angle between the direction of the movement of the receiver and the direction of arrival of the wave is assumed to be ϕ, Doppler shift of the frequency component f_c is defined as:

$$f_d = \frac{f_{Dmax}}{\cos(\phi)} \tag{15}$$

where, f_d is the Doppler shift and

$$f_{Dmax} = \frac{f_c v_{rx}}{c} \tag{16}$$

where f_{Dmax} is the maximum Doppler frequency, v_{rx} is the velocity of the receiver and c is the speed of light.
In mobile communication systems, the maximum Doppler spread is used to characterize the rate of change of a radio channel. The measure of time interval during which the channel impulse response is time invariant is known as *coherence time* (T_c). Generally T_c can be calculated as:

$$T_{c(a)} \geq \frac{1}{2\pi f_{Dmax}} \arccos(a) \tag{17}$$

where $T_{c(a)}$ is the coherence time for which the auto-correlation value is a in time domain [9].

2.3.6 Coherence Time and Time Domain Pilot Signals

Taking the LTE system as an example once again, the relationship between pilot carriers spacing and the coherence time can be explained. From the LTE frame structure [11] we know that the duration of one slot is 0.5 ms. There are 6 OFDM symbols in one slot hence the symbol duration, T_{sym} can be calculated as:

$$\begin{aligned} T_{sym} &= \frac{T_{slot}}{N_{sym}} && (18)\\ &= \frac{0.5 \text{ ms}}{6} && (19)\\ &= 83.3\ \mu s && (20) \end{aligned}$$

where T_{slot} is slot duration and N_{sym} is the number of symbols per slot. Reference symbols are located every fourth OFDM symbol, but are distributed on different sub-carriers. Nevertheless, the channel can be estimated after each third OFDM symbol. Hence the spacing of reference symbols in the time-domain is given as:

$$T_{ref} = 3 \cdot T_{sym} = 0.25 \text{ ms}. \tag{21}$$

If we assume a receiver with a maximum speed of 120 km/h at a carrier frequency of 2.4 GHz, we will get a maximum Doppler shift of 266.67 Hz. Based on the assumption and using the uncertainty relationship described in Section 3.2 the coherence time, T_c, can be calculated for autocorrelation values of $a = 0.9$ and $a = 0.5$ respectively as shown below.

$$\begin{aligned} T_{c(0.5)} &\geq \frac{1}{2\pi f_{Dmax}} \arccos(0.5) && (22)\\ &= \frac{1}{2\pi 266.67 \text{ Hz}} \arccos(0.5) = 0.623 \text{ ms}. && (23) \end{aligned}$$

$$T_{c(0.9)} \geq \frac{1}{2\pi f_{Dmax}} \arccos(0.9) = 0.269 \text{ ms}. \tag{24}$$

Equations (20) and (21) show that the spacing of the reference symbols in time is less than the coherence time. Furthermore the channel is estimated at least two times before the autocorrelation of the channel estimates has the value 0.5.

2.4 Channel Models in Wireless Communications Systems

The effects of the aforementioned channel parameters on the received signal can be modeled such that the resulting profile of the signal at the receiver can be obtained from the profile of the transmitted signal. This model of the medium between the transmitter and the receiver is called *channel model*.

Based on the different scenarios at the receiver, different channel models can be developed to study system performance at the receiver. For example, the DVB-T standard [12] considers three scenarios at the receiver to model a channel. The scenarios under consideration are Portable Reception (P1), Fixed Reception (F1) and Single Path Reception (Gaussian). Corresponding to the scenario at hand, an appropriate channel model should be selected. In this section we will study channel models which can generally be applied to both LTE and DVB-T standards. In addition, the DVB-T2 specific Memoryless Rayleigh Channel with erasures [12] will also be covered in brief detail. The channel

2.4.1 Gaussian channel

Model of a Gaussian channel describes a case in which the transmitted signal reaches the receiver through a direct, single path. The received signal is subject to a definite level of noise. The channel is affected only by Additive White Gaussian Noise (AWGN) which is mainly produced at the receiver itself. Since the sub-carriers of the transmitted signal are normalized at the transmitter, the signal-to-noise ratio (SNR) is controlled by varying the noise variance, δ_n^2. The average energy of one OFDM symbol can be given as:

$$E_s = \frac{N_{BW}}{N_{IFFT}} \tag{25}$$

hence, the SNR is set to be the ratio of E_s and the noise variance, i.e,

$$SNR = \frac{E_s}{E_N} = \frac{N_{BW}}{N_{IFFT}} \frac{1}{\delta_n^2} \tag{26}$$

2.4.2 Ricean channels

The channel model for mobile reception can be generated from the following equation where s(t) and r(t) are input and output signals respectively.

$$r(t) = \frac{\rho_o s(t) \sum_{i=1}^{N} \rho_i e^{-j\theta_i} s(t - \tau_i)}{\sqrt{\sum_{i=1}^{N} \rho_i^2}}, \tag{27}$$

where:

- the first term before the sum represents the line of sight ray
- N is the number of echoes

- θ_i is the phase shift from scattering of the i^{th} path
- ρ_i is the attenuation of the i^{th} path
- τ_i is the relative delay of the i^{th} path

The Ricean factor K (the ratio of the power of the direct path (the line of sight ray) to the reflected paths) is given as:

$$K = \frac{\rho_o^2}{\rho_i^2} \tag{28}$$

2.4.3 Rayleigh Fading Channels

As discussed in section 2.2, when a signal is transmitted in an environment with obstacles resulting in non line-of-sight (NLOS) propagation, more than one transmission path will appear as a result of the reflections. The signal at the receiver is then the superposition of the signals via individual paths with their own delay and the corresponding phase shift. For a given path, a change in delay, τ_n, of $\frac{1}{f_c}$ results in a phase change of 2π radians. Considering the fact that the distance between the transmitter and the receiver are very large relative to the wave length of the carrier frequency, it is reasonable to assume that the phase shift is uniformly distributed between 0 and 2π rad and the phases of each path are independent. When there are large number of paths, each path may be modeled as complex Gaussian random variable by applying central limit theorem [13, pp. 542-543]. This model is called the *Rayleigh fading channel*.

A complex Gaussian random variable is of the form: $Z = X + jY$, where X and Y are zero mean, independent and identically distributed Gaussian random variables. Assuming that the random variables are circularly symmetric, the probability distribution of the magnitude of random variables turns out to be:

$$p(z) = \frac{z}{\sigma^2} e^{\frac{-z^2}{2\sigma^2}}, \qquad z \geq 0 \tag{29}$$

where $p(z)$ is the Rayleigh distribution and z is the fading coefficient.

Hence, the Rayleigh channel model can be generated from the following equation where s(t) and r(t) are input and output signals respectively.

$$r = k \sum_{i=1}^{N} \rho_i e^{-j\theta_i} s(t - \tau_i), \text{ where } k = \frac{1}{\sqrt{\sum_{i=1}^{N} \rho_i^2}} \tag{30}$$

2.4.4 Memoryless Rayleigh channel with erasure

This channel model is used to study the behavior of the Bit Interleaved Coded Modulation (BICM) module of DVB-T2 system over multi-path channels. It models the destructive interference caused by Single Frequency Networks (SFN) in DVB-T2

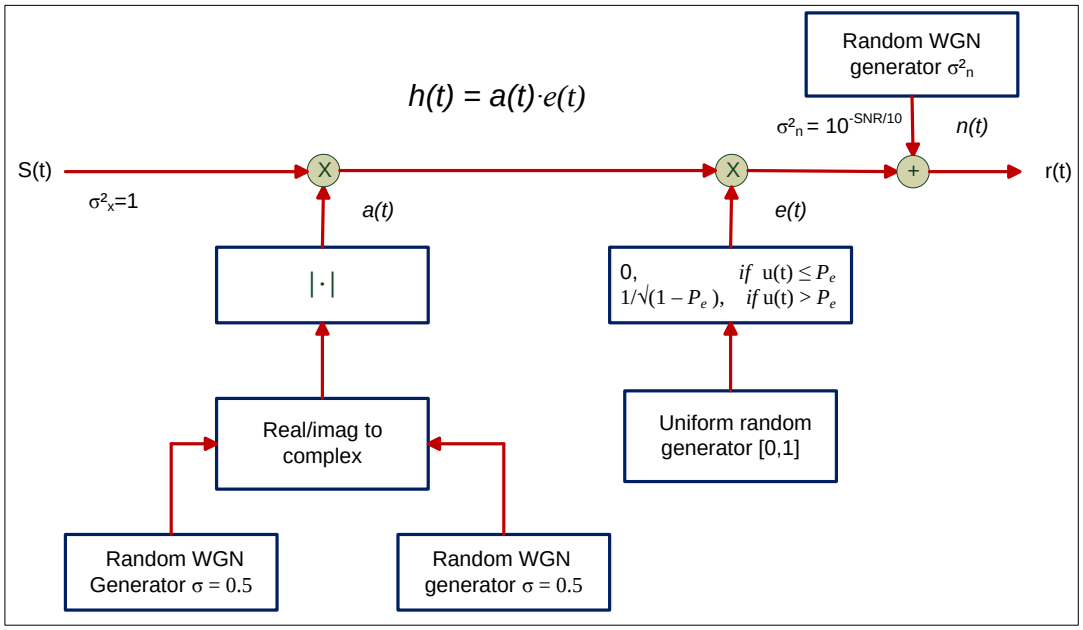

Figure 2: Memoryless Rayleigh channel with erasures

systems. The principle is based on modeling the concatenation of the frame builder, OFDM modulator, wireless channel, OFDM demodulator and frame extraction so as to give raise to a flat fading equivalent channel [12]. On top of the classical Rayleigh fading discussed above, erasure events distort the transmitted signal. If a properly designed interleaver is inserted between the QAM mapper and the OFDM modulator, the erasure event can be modeled by a discrete random process, E_t, taking a value of 0 and 1 with probability P_e (erasure probability) and 1 - P_e respectively. Hence, the equivalent flat fading coefficient h can be modeled as a Rayleigh process concatenated with E_t. The discrete time representation of the complex baseband received signal is of the form:

$$r_t = \rho_t E_t s_t + n_t \tag{31}$$

where n_t is a complex white Gaussian noise with spectral density $\frac{N_o}{2}$. Figure 2 above depicts the way the equivalent channel is simulated.

3 An overview on Cognitive Radios

Due to exponential increase in broadband wireless demands in recent years, interest is rapidly growing in issues related to spectrum access and spectrum efficiency. The emergence of software-defined radios and the realization that new levels of computational performance applied to radios creates exciting new possibilities for wireless devices. This has resulted in explosive growth in interest in cognitive radios. The term cognitive radio was first coined by Joe Mitola [14]. The concept and the term cognitive radio quickly caught the interest of many in the research and development arena of the communications field.

Since the introduction of the term in 1997, a number of definitions have been provided by different industries and standardization bodies. The IEEE-USA Board of Directors defined cognitive radio as a radio frequency transmitter/receiver that is designed to intelligently detect whether a particular segment of the radio spectrum is currently in use, and to jump into (and out of, as necessary) the temporarily unused spectrum very rapidly, without interfering with the transmissions of other authorized users [15]. Whereas, ITU's Radio Communication Study Group defined it as a radio or system that senses, and is aware of, its operational environment and can dynamically and autonomously adjust its radio operating parameters accordingly.

3.1 Motivation

The radio frequency spectrum is used by variety of services such as terrestrial wireless communications, satellite wireless communications, broadcasting services or navigation systems. The frequency bands licensed to different services show different occupancy rates. Some frequency bands are unoccupied most of the time, others are partially occupied while the rest are heavily occupied. Due to this unevenly distributed load among different licensed frequency bands, the existing paradigm of fixed allocation of a spectrum band to a licensed user results in overloading in some services and under-utilization in others. In today's wireless communication networks, a significant portion of the spectrum is under-utilized because of fixed spectrum allocation approach. Due to this lack of flexibility in resource allocation and spectrum access a significant temporal and spacial spectral holes throughout the network left unused hence under-utilization of the already scarce resources. Moreover, unlicensed users can not access the resource even if they have little or no effect on the licensed (primary) users.

Conventional digital transceivers as depicted in Figure 3, include the analog *RF front-end* module responsible for transmitting/receiving the Radio Frequency (RF) signal from the antenna and down-converting the signal from RF to Intermediate Frequency (IF) on receive path (or up-conversion of the IF signal into RF signal, in case of transmit path). The middle section includes the Analog-to-Digital/Digital-to-Analog Converter (ADC and DAC) block, the demodulating Digital Down Conversion (DDC) and modulating Digital Up Conversion (DUC) blocks. The baseband

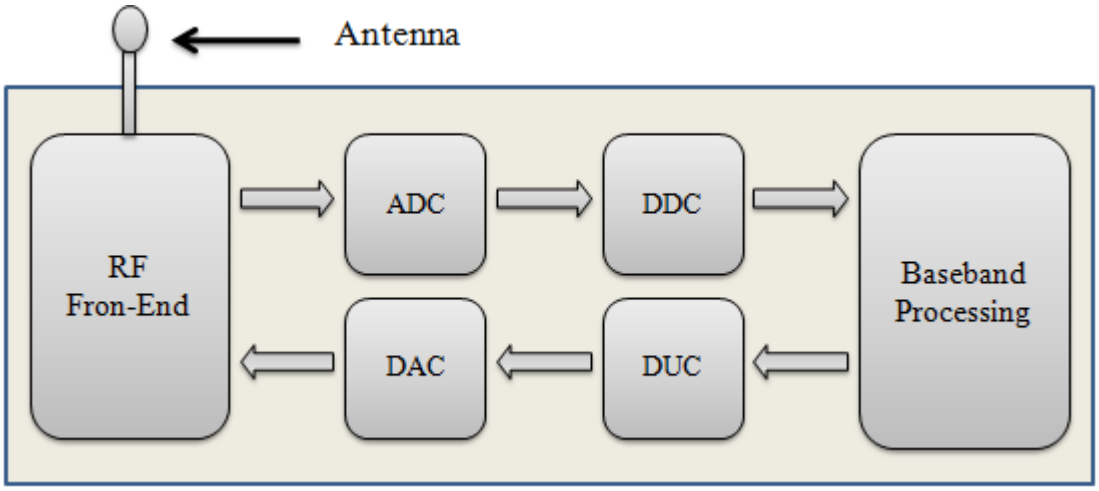

Figure 3: Generic digital transceiver

section performs baseband operations such as (connection setup, equalization, frequency hopping, coding/decoding and correlation) and implements link layer protocols. The continuous evolution of wireless access schemes is demanding new hardware updates each time. Mobile users, on the other hand, need technology-neutral roaming capabilities. This technical requirement is bringing a new variant of radio systems which rely on software-reconfigurability running on generic hardware with Digital Signal Processors (DSPs) and general purpose microprocessors. Cognitive radio technology is a new paradigm for wireless networks which provides a number of capabilities to improve the usefulness and effectiveness of wireless communications by changing the existing paradigms in the field. It enables network components change their parameters to adapt to their environment and utilize the available radio frequency spectrum in a fair-minded way without harmfully violating the right of others and provide highly reliable communication for all users of the network.

3.2 Software Defined Radios (SDR) and Cognitive radios

Software-Defined Radios (SDRs) are radios whose functional modules, such as modulation/demodulation, signal generation, coding and link-layer functions, can be implemented in software. In other words, the coding, modulation type and frequency band can be modified solely by changing software. This capability of SDR devices enables upgrading the modules, and hence the devices, mainly by software updates whenever the wireless access protocol is changing.

Unlike the conventional radios, which have operating parameters fixed during design time, physical layer operating parameters that affects the radio frequency emission can be altered in SDRs by changing software parameters without changing the hardware components.

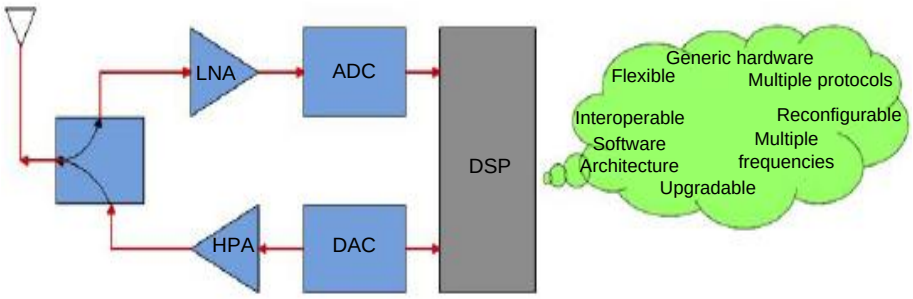

Figure 4: Pictorial interpretation of cognitive radio

Hence, Cognitive radios are SDRs with added capabilities of sensing the spectral environment and learn to dynamically alter their physical layer behaviors to follow complex strategic adaptations to the environment.

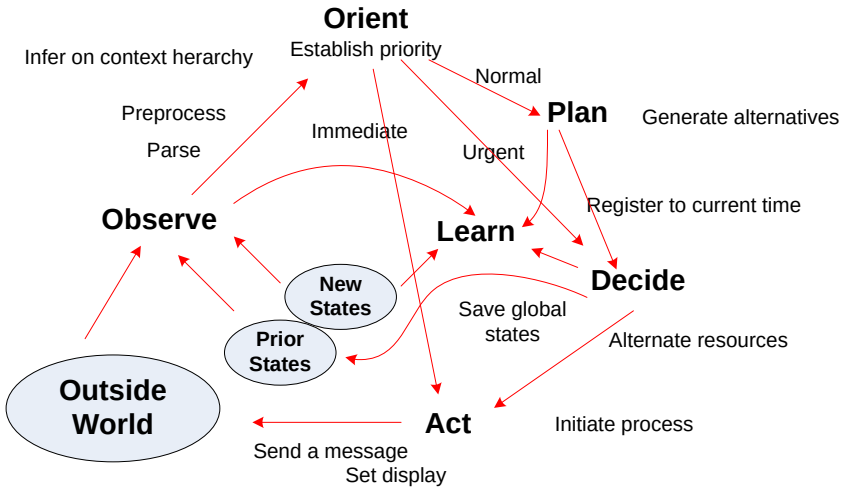

Figure 5: Cognitive cycle [16]

3.3 A Cognitive radio usage scenario: Spectrum Sensing based access

Wireless communication systems require spectrum for their operation but interference poses a serious threat if systems in close geographical proximity use the same band simultaneously. This leads to a global spectrum regulation system in which

a given spectrum band is exclusively allocated for a certain service licensed to use that band at any given location. But this kind of allocation of the scarce resource results in under-utilization due to unfair distribution among different services. This can clearly be seen from the allocation of the TV spectrum. A larger amount of spectrum is allocated to TV broadcast systems (on the order of 300 - 400 MHZ) even though large chunks of that spectrum remain unused most of the time [2]. On the other hand, the total spectrum currently occupied by or recommended for mobile communications systems is around 230 - 430 Mhz depending on the geographic region [17]. However, the rapid transition in cellular networks from limited data mobile telephony to universal broadband mobile services in recent times led to a huge capacity demand that can not be accommodated by the spectrum resources that are allocated to these systems. One approach of research interest to tackle the aforementioned problem is a cognitive radio scenario where spectrum sensing is employed for dynamic and flexible access. In this approach, the spectral environment is sensed and any unused resource allocated to the primary system is assigned to a secondary system. The other approach to dynamic spectrum access is to allow secondary systems to access spectrum resources that have been allocated to a primary system under restrictions that the secondary usage does not harmfully interfere with the primary service.

Three different paradigms of dynamic primary-secondary spectrum access have been discussed and are presented in the following sections.

3.3.1 The interweave approach

In the interweave paradigm, the secondary system determines the white spaces or spectral holes in time, frequency and geographic location that remain unused by the primary system. The motivation of the idea stems from studies that showed large parts of the licensed spectrum are not utilized most of the time [2][3]. A television white space can be discussed as a good example in this regard.

Television broadcasting services operate in the VHF and UHF portions of the radio frequency, on a licensed basis. Regulators prohibit the use of these bands for unlicensed devices. Most regulators, however, are necessitating the adoption of digital transmission by all TV stations that were using analogue transmission. The US has already completed this *Digital Switchover (DSO)* by June 2009, while UK is planning to complete by 2012. Similar steps are in progress (or already finished) in the remaining Europe. This transition has freed up a significant amount of spectrum for other services.

The other major benefit of the DSO is the opportunity to use the licensed TV bands for unlicensed wireless devices when licensed users are not needing them. There are suitable geographical locations which could not be accessed by some channels without interfering with their adjacent/co-channels, but still these channels could be used by low power devices without disturbing similar primary users. These

secondary devices, also known as *White Space Devices (WSDs)*, should be equipped with state-of-the-art cognitive capabilities to avoid any harmful interference to the protected incumbent services. The name *Television White Space (TVWS)* came from the broadcast coverage color map, where different colors indicating different signal levels, while geographical areas without TV signals are left white. Thus TVWS can be defined as:
Geographical locations where there is no TV signal and the broadcasting frequency can be used for secondary purposes without causing any interference to the performance of the TV broadcasting in the remaining areas and other incumbent services anywhere.

In Europe, the TVWS is located in the 470-790MHz bands - which is traditionally a high quality signal, far better than the 3G and WiFi signals, that is able to travel long distances and penetrate shadowing walls. It is also very promising for many potential services such as last mile wireless broadband access in rural areas.These gaps change with time and geographic location, and can be exploited by secondary users for their communication. Hence, the utilization of spectrum is improved by opportunistic frequency reuse over the spectrum holes. The interweave technique requires knowledge of the activity information of the non-cognitive (primary) users in the spectrum. One could also consider that all the users in a given band are cognitive, but existing users become primary users, and new users become secondary users that cannot interfere with communications already taking place between existing users.

3.3.2 The Underlay approach

The underlay approach comprises of techniques enabling cognitive radio communications based on the assumption that the cognitive part has knowledge of the interference caused by its transmitter to the primary receivers. One of the basic requirements in this scenario is that the secondary user cannot significantly interfere with the communication of the existing primary users. Under this cognitive radio model, parallel non-cognitive and cognitive transmissions may occur only if the interference generated by the cognitive devices at the primary receivers does not drag the SNR at the primary below a certain threshold. The interference constraint for the non-cognitive users may be met by using multiple antennas to guide the cognitive signals away from the non-cognitive receivers, or by using a wide bandwidth over which the cognitive signal can be spread below the noise floor, then de-spread at the cognitive receiver. The latter technique is the basis of both spread spectrum and Ultra-Wide-Band (UWB) communications.

The interference caused by a secondary transmitter to a primary receiver can be estimated via reciprocity if the secondary transmitter can overhear a transmission from the primary receiver. Alternatively, the secondary transmitter can remain very conservative in its output power level to ensure that interference at the primary receivers remain below the prescribed threshold. In the later case, since the interference constraints in underlay systems are typically quite restrictive, this limits the

secondary users to short range communications. The underlay paradigm is most common in the licensed spectrum however it can also be used in unlicensed bands to provide different classes of service to different users.

3.3.3 The Overlay approach

The assumption in this paradigm is that the cognitive transmitter has knowledge of the primary users' codebooks and possibly the messages as well. The codebook information can be obtained in a periodic brodcast from the primary users or by following a uniform standard for communication using a publicly known codebook. There are a number of alternatives to obtain a message from the primary user at the cognitive receiver. One way is to decode the message at the cognitive receiver. However this approach might be impractical for overlay systems built based on assumptions that the secondary receiver knows the primary message when the primary transmitter starts transmission. Nonetheless, the assumption holds for a message retransmission where the cognitive user hears the first transmission and decodes it, while the intended receiver cannot decode the initial transmission due to fading or interference.

The other way of obtaining the primary message at the cognitive receiver could be the primary user send its message to the secondary prior to its transmission. The primary user's message and/or codebook can be used in a variety of ways to either cancel or mitigate the interference seen at the secondary and primary receivers. On the one hand, this information can be used to completely cancel the interference due to the primary signals at the secondary receiver by sophisticated techniques like dirty paper coding. Moreover, the secondary users can utilize this knowledge and assign part of their power for their own communication and the remainder of the power to assist (relay) the primary transmissions.

By choosing an optimum secondary transmission-to-relaying-power-ratio, the decrease in signal-to-noise ratio (SNR) at the primary users due to the interference caused by the secondary transmitters can be compensated by the increase in SNR at the primary users due to the assistance from the secondary relay signal. This guarantees that the primary user's rate remains unchanged while the secondary user allocates part of its power for its own transmissions. Note that the overlay paradigm can be applied to either licensed or unlicensed band communications. In licensed bands, cognitive users would be allowed to share the band with the licensed users since they would not interfere with, and might even improve, their communications. In unlicensed bands cognitive users would enable a higher spectral efficiency by exploiting message and codebook knowledge to reduce interference.

To summarize the three approaches, an interweave cognitive radio is a smart wireless communication system that periodically scans the radio spectrum, intelligently detects occupancy in the different parts of the spectrum and then opportunistically communicates over spectrum holes with minimal interference to the active

users. While underlay and overlay techniques permit concurrent cognitive and non-cognitive communication, avoiding simultaneous transmissions with non-cognitive or existing users is the main goal in the interweave technique. We also point out that the cognitive radio approaches require different amounts of side information: underlay systems require knowledge of the interference caused by the cognitive transmitter to the non-cognitive receiver(s), interweave systems require considerable side information about the primary user activity and overlay systems require a large amount of side information (non-causal knowledge of the non-cognitive user's codebook and possibly its message). Apart from device level power limits, the cognitive user's transmit power in the underlay and interweave approaches is decided by the interference constraint and range of sensing, respectively. While underlay, overlay and interweave are three distinct approaches to cognitive radio, hybrid schemes can also be constructed that combine the advantages of different approaches. For example, the overlay and interweave approaches are combined in [18]. Since cognitive radio networks are based on the notion of minimal interference, the interference channel provides a fundamental building block to both the capacity as well as encoding and decoding strategies for these networks.

3.3.4 White Space Access Mechanisms in Interweave Approach

Cognitive secondary access to Television white spaces (TVWS) involves detection of the available spectrum holes in the TV-bands and to use the spectrum based on the regulatory requirements, which basically protect incumbent services from harmful interferences. Three cognitive techniques have been proposed to help WSDs find empty channels [30]:

1. Geo-location with databases
2. Spectrum sensing
3. Beacons

Currently, the geo-location assisted by database seems to be a more promising short-term solution for incumbent detection and interference avoidance.

3.3.5 Geo-location Databases

In this approach, the WSDs are required to consult a centralized (or regional mirror) *geo-location database* to determine if there are any TVWS (free channels) they can use without causing interference to other services. ECC requires that the WSDs have to recognize and indicate their current location before sending the query. There are few essential parameters yet to be decided in the future: the location precision, how often the devices should contact the database and the quality of the database itself. Too precise location requirement imposes unnecessary complexity to the WSDs, while contacting the server at short time intervals shortens the battery life of the devices.

With this scheme, WSDs are not allowed to transmit before they receive notifications from the database about the available white spaces, if any, in their position. This requires that the WSDs make initial connectivity to the database by some other way than the white space frequencies. Currently, the *master-slave* communication architecture is proposed to alleviate this problem. A *master* device, most likely an access point or a base station, having access to the location information will connect to the database via Internet. Then it in turn serves the inquiries of the *slave* WSDs at its vicinity.

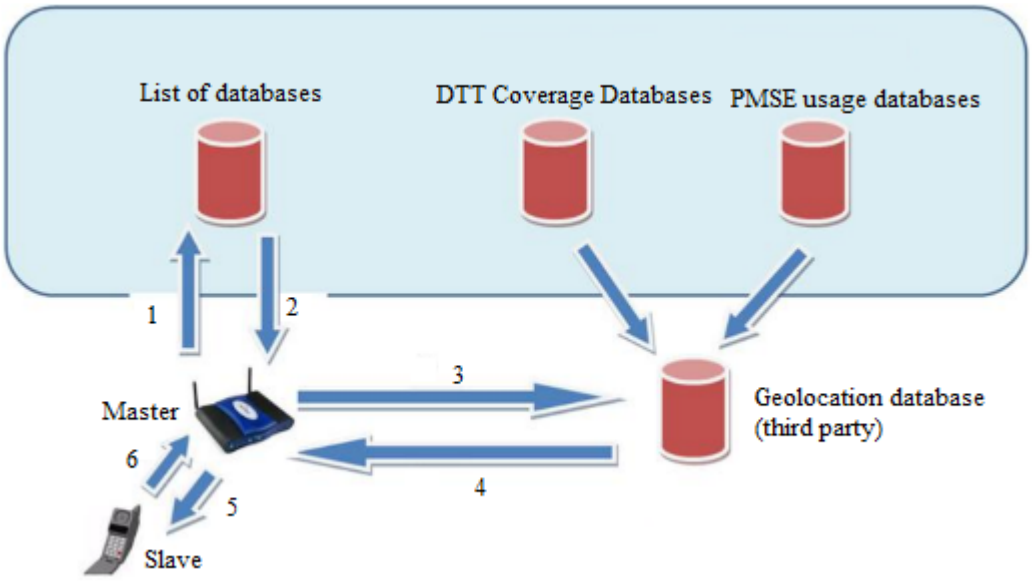

Figure 6: Possible geolocation database proposed by Ofcom [31].

The database scheme might work well for protecting services whose coverage plan is more or less fixed and deterministic, the protection of mobile incumbent services such as wireless-microphone, however, may need more sophisticated approaches like sensing.

3.3.6 Spectrum Sensing

Spectrum Sensing enables unlicensed devices detect the presence of any protected incumbent services in licensed channels, which appear to be white spaces. Spectrum sensing involves measuring the signal levels of the potential channel, based on the regulatory requirements. FCC, for instance, requires the *"TV bands devices [unlicensed WSDs] be capable of sensing analog TV signals, digital TV signals and wireless microphone signals at a level of -114 dBm within defined receiver bandwidths"*. While this level is referenced to an omni-directional receive antenna of 0dBi gain, other approaches for sensing antenna are allowed as far as they maintain the same performance, with respect to the sensing threshold.

Up on finding a vacant channel, the WSDs may also be required to sense the adjacent channels to find out, if any, transmission power constraints. Certain services like radio astronomy in the band 608-614MHz, which are technically difficult to detect, might need special protection (or even exclusion) from these sensing procedures.

Spectrum sensing, if it is standalone, has very important advantage that it doesn't need connection to a centralized database server. This eliminates the need for extra communication infrastructures like the Internet. The down-side of this scheme, however, is that sensing signals may be vulnerable to what is called the *hidden terminal* problem shown in Figure 7.

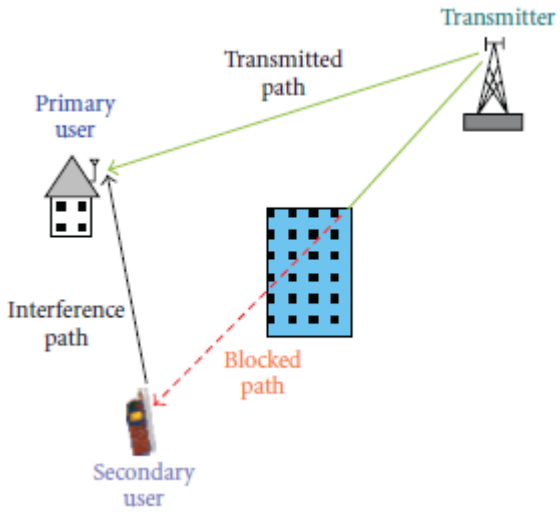

Figure 7: Hidden-terminal problem of sensing-based cognitive radio. [32]

While the unlicensed cognitive device is trying to sense the signal from the primary transmitter, which is located on the other side of the shadowing building, it may conclude that there is no primary transmitter nearby and may start transmitting on the same channel. In this scenario, the licensed users, which are still receiving from the transmitter and located at the vicinity of the WSD, will suffer from chronic interference.

3.3.7 Beacons

A third proposal for spectrum white space detection is using beacons. Unlicensed devices transmit only when they receive the beacons that carry information whether the channel is vacant or not. The beacons can be broadcasted by the TV stations, or a different unlicensed fixed transmitter using TV bands. Using beacons increases the probability of detection at lower threshold values, that would otherwise need more complex sensing systems.

This approach needs a dedicated infrastructure that broadcasts beacons and it should be operated depending on statistics from the licensed incumbent services.

When beacons are lost for example due to shadow-fading, the hidden-terminal problem, explained above, may happen.

3.4 Cognitive Radio Channels

The cognitive channel model [19],[20] describes scenarios in which multiple terminal pairs intend to communicate concurrently in the presence of interference. The users are not assumed to be cognitive - they do not monitor the activity or decode messages of other users. However, it is commonly assumed that all terminals know the channel gains and the codebooks of all the encoders. The identified problem here is to determine the highest rates that can simultaneously be achieved with arbitrarily small error probability at the desired receivers, i.e., to determine the capacity region. This performance can serve as a benchmark to evaluate the gains of cognition. Even for the smallest interference network consisting of two transmitter-receiver pairs, this problem has remained unsolved for decades, emphasizing that one of the fundamental problems in networks - coping with and exploiting interference - is not yet entirely understood. Based on the two-transmitter, two receiver scenario, shown in Figure 6(a), we discusses the basic theory of interference channels briefly in the next paragraphs. We assume that each encoder t for t = 1, 2 wishes to send one of M_t messages, denoted W_t, to its receiver at rate R_t. In an interference channel, transmission at each user is affected by a random disturbance of the channel and the transmission of the other user. The following two steps are important in determining the capacity region of the interference channel. i,e,

1. Propose a specific encoding and decoding scheme, and evaluate its achievable rate region.

2. Determine a boundary of the rate region that cannot be exceeded by any encoding scheme.

If the two regions meet, then the capacity region is known and the planned encoding scheme is said to be capacity-achieving. Based on the interference at the receivers, different regimes can be identified. In cases when the interference is strong, the received interfering signal component carrying the unwanted message is strong enough so that this message can be decoded and can be canceled from the received signal,

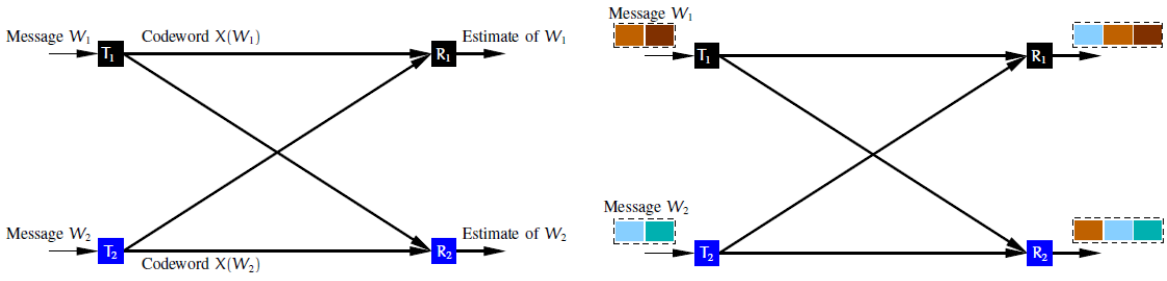

Figure 8: (a) Interference channel and (b) Rate splitting

allowing for interference-free decoding of the desired information. This approach leads to the capacity in strong interference [21]. But, in general cases the interference is not strong enough to allow for decoding of the unwanted message without negatively affecting its rate. In this case, rate-splitting [20] can be used at the encoders to allow the receivers to decode a part of the unwanted message. Rate-splitting is known for achieving the best rates [22]. In this scheme, each transmitter divides its message into two sub-messages and encodes them separately. A receiver decodes one sub-message of the other user and cancels a part of the interference. This will increase the rate for its communication, but will lower the rate for the other communicating pair due to the additional decoding requirement. Hence, there is a compromise between sending a message only to the desired receiver and allowing partial decoding at the other. The idea of rate-splitting is depicted in Figure 6(b). These results have generally been specialized to the interference channel with additive white Gaussian noise.

4 Synchronization Aspects in Cognitive and conventional Wireless Systems

4.1 Synchronization in Communications systems

In any communication system, the process of constructing the receiver requires the knowledge of some information about the transmitted signal and the communication channel. Typical examples of necessary information at the receiver includes the channel phase response, the carrier frequency, the timing of the arriving information and the carrier phase. However, in practical situations these information are not available beforehand and it must be estimated from the received signal. The carrier frequency at the receiver deviates from the nominal carrier frequency at the transmitter due to various reasons. The Doppler effect which arises from the relative movement of the receiver with respect to the transmitter can be cited as an example. Moreover, hardware non-idealities discussed in section 2.2. cause carrier frequency offset at the receiver. Therefore these discrepancies in system parameters between the transmitter and the receiver should be estimated and corrected at the receiver to improve the system performance to an acceptable level. Similarly, in a real-life communications environment, it takes a finite amount of time for the information-bearing electromagnetic wave to travel from the transmitter to the receiver. The transmission delay due to the propagation environment results in symbol timing mismatch between the transmitter and the receiver. Hence, we need to know the correct symbol timing at the receiver to tackle the performance degradation due to timing mismatch. The carrier phase offset of a received signal primarily consists of three components: the channel phase response, phase due to timing offset and phase noise (jitter) from the transmitter local oscillator. It should be estimated and compensated in cases of coherent demodulation.

In order to model the aforementioned discrepancies, we need to augment the simple non-dispersive channel model we employ in the previous chapter. The received signal in the model is given as:

$$r(t) = Av(t-\tau)\cos\left[2\pi\left(f_c + \Delta f\right)(t+\tau) + \theta\right] + n(t) \tag{32}$$

where $v(t)$ is the baseband signal and the new parameters Δf and τ are used to model the deviation of the received carrier frequency from the nominal carrier frequency and the transmission delay, respectively. The process of estimating these parameters is called *synchronization*.

4.1.1 Effect of synchronization errors in communication systems

In this section we investigate the impacts of time and frequency synchronization errors on the performance of a simple communication system by taking a Binary Phase Shift Keying (BPSK) transmission as an example. In BPSK systems the

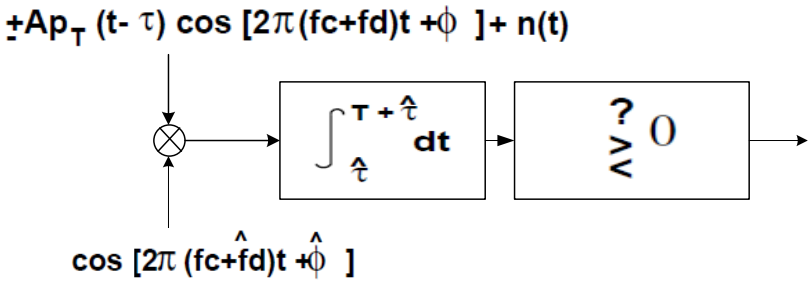

Figure 9: A BPSK modulator with estimated parameters

received signal can be given as:

$$r(t) = \pm A p_T(t-\tau)\cos\left[2\pi(f_c+\Delta f)(t+\tau)+\theta\right]+n(t) \quad (33)$$

$$= \pm A p_T(t-\tau)\cos\left[2\pi(f_c+\Delta f)t+\phi\right]+n(t) \quad (34)$$

where n(t) is AWGN with spectral density $N_0/2$ and ϕ is the combination of the phase response, the phase due to timing offset and phase noise. Let us assume that we obtain the estimates $\widehat{\Delta f}$, $\hat{\tau}$ and $\hat{\phi}$ of the parameters Δf, τ and ϕ employing a certain synchronization algorithm. Hence, the compensation at the receiver can be done using the estimated parameters as shown in the block diagram shown in Figure 9 above. When $\tau - \hat{\tau} \leq T$ the bit error probability can be given as:

$$P_b = Q\left(\alpha\sqrt{\frac{2E_b}{N_0}}\right) \text{ where,} \quad (35)$$

$$\alpha = \frac{1}{T}\int_{max(\tau,\hat{\tau})}^{T+min(\tau,\hat{\tau})} \cos\left[2\pi\left(\Delta f - \widehat{\Delta f}\right)t + \left(\phi - \hat{\phi}\right)\right] dt \quad (36)$$

α takes values less than or equal to unity where equality holds only if $\Delta f = \hat{\Delta f}$, $\tau = \hat{\tau}$ and $\phi = \hat{\phi}$. Hence, from equation (3) we can see that any error in the estimated parameters pushes the bit error probability figure above the optimal error probability. We can also see that if the estimation error in Δf, $|\Delta f - \widehat{\Delta f}|$, is much smaller than the data transmission rate $\left(\frac{1}{T}\right)$, then

$$\alpha \approx \left(1 - \frac{\Delta\tau}{T}\right)\cos\left(\Delta\phi\right), \quad (37)$$

where $\Delta\tau = \tau - \hat{\tau}$ and $\Delta\phi = \phi - \hat{\phi}$. Hence errors in estimating the frequency offset and the time delay cause a significant degradation of the bit error rate performance. Other metrics to measure the performance of synchronization algorithms will be discussed in this chapter in association with OFDM based synchronization algorithms.

4.2 Timing and Frequency Synchronization in OFDM systems

OFDM has emerged as one of the most promising radio access technologies in the last couple of decades. Its application ranges from wired communications such as

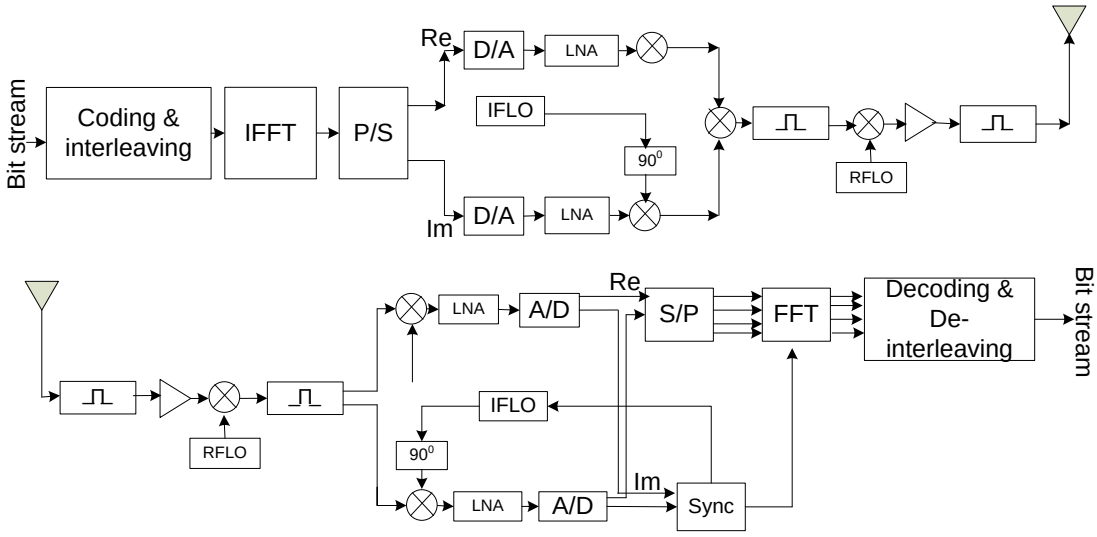

Figure 10: A simplified OFDM system model [33]

DSL to wireless local area networks (IEEE 802.11a/g) and digital audio and video broadcasting. OFDM has also gained a significant ground in mobile communications technologies as in, for example, mobile WIMAX and LTE.

In OFDM communications data is divided into small chunks at the transmitter and sent through a number of narrow-band sub-channels which are orthogonal in both time and frequency domain. The OFDM signal is created by taking the inverse Fourier transform of the Quadrature Amplitude Modulated (QAM) or Phase Shift Keyed (PSK) symbols at the baseband. The block diagram of OFDM transmitter and receiver adapted from [33] given in Figure 8 (top and bottom respectively) above illustrates the baseband, discrete-time OFDM system model under investigation. The complex data symbols are modulated by means of an inverse fast Fourier transform (IFFT) on parallel sub-carriers. The resulting OFDM symbol is transmitted over a discrete-time channel, whose impulse response we assume is shorter than T samples.

To avoid inter-symbol interference (ISI), cyclic prefixes are added at the start of each symbol. This can be done by appending the last G samples of the symbol as a prefix. It is required that the length of the cyclic prefix (T_G) should be longer than the delay spread of the channel to avoid performance degradation due to ISI. Hence, the length of the transmitted OFDM symbols is this cyclic prefix plus the body (FFT-length sample). The insertion of a cyclic prefix can be shown to result in an equivalent parallel orthogonal channel structure that allows for simple channel estimation and equalization. Despite the increase in transmission energy and the decrease in data rate associated with the cyclic prefix, the advantage from these properties generally outweighs its disadvantage [7]. After CP insertion, the OFDM symbols are up-converted to radio frequency (RF) and transmitted through the channel. At the receiver, the signal is down-converted to intermediate frequency (IF) and synchronization is performed to determine the arrival time of the OFDM

symbols and to correct the frequency offsets.

Transmitting data in narrow sub-bands allows robustness in multi-path fading channel conditions and in the presence of impulse noises. However, it requires the cost of accurate synchronization of the sub-carrier frequencies at the OFDM transmitter and receiver. This is due to the fact that as the spacing between the sub-carriers getting narrower, the orthogonality of the sub-carriers becomes more sensitive to frequency offset. Even if some symbol timing estimation error would be tolerated when cyclic prefix is used to extend the symbol, the frequency offset estimate should be quite accurate to avoid inter carrier interference (ICI). On the other hand the error from the symbol timing estimation, unless the estimate falls beyond the range of the CP length, results only in phase rotation in the frequency domain which requires a trivial process to compensate. Frequency offset results in loss of orthogonality between the sub-carriers which causes ICI. There are three major synchronization [9] errors in OFDM systems: Symbol time offset (STO), carrier frequency offset (CFO), and sampling clock frequency offset (SCFO). When the symbol time is not located in the range of CP samples, ISI is introduced. In time-selective channels, CFO, and SCFO will introduce additional inter-carrier interference (ICI) on top of the ISI. Symbol timing offset and frequency offset will be discussed in the following paragraph followed by synchronization techniques in the next section.

Now, let us consider that we have two unknowns at the receiver: The arrival time of the OFDM symbol and the carrier frequency at which it is transmitted (a difference in the local oscillators in the transmitter and receiver gives rise to a fractional or integer shift in the sub-carriers). The symbol arrival time is modeled as a delay in the channel impulse response $\delta(k-\theta)$, where θ is the integer-valued unknown arrival time of a symbol. The fractional frequency offset is modeled as a complex multiplicative distortion of the received data in the time domain, $e^{j2\pi\epsilon k/N}$ where ϵ denotes the difference in the transmitter and receiver oscillators as a fraction of the inter-carrier spacing and N represents the FFT length. We assumed that the transmitter and the receiver are stable such that all sub-carriers experience the same shift. Based on the previous assumption that the channel is non-dispersive and that the transmitted signal is only affected by complex additive white Gaussian noise (AWGN), the signal at the receiver can be modeled as:

$$r(k) = s\left(k-\theta\right) e^{j2\pi\epsilon k/N} + n(k) \tag{38}$$

where two other synchronization parameters are not accounted for in this model. First, an offset in the carrier phase may affect the symbol error rate in coherent modulation in the absence of channel estimation. If the data is differentially encoded, however, this effect is eliminated. An offset in the sampling frequency will also affect the system performance. We assume that such an offset is negligible.

Much research has been done to estimate and correct the time and frequency offsets in OFDM systems based on a number of different approaches. Most time

and frequency synchronization algorithms take advantage of the cyclic nature of the time domain signal or use specially designed training symbols for the synchronization purpose. Some of the time and frequency synchronization technique are discussed in the following sections.

4.2.1 Symbol Timing and Frequency synchronization techniques

In this section we investigate different existing approaches to estimate the starting time of a symbol transmission and timing offset. In [33], symbol timing estimation was done based on a search for a unique training sequence with identical halves each with a duration of half OFDM symbol time. Such a sequence in the time domain is resulted by transmitting Pseudo-Noise (PN) sequences on even frequencies and zeros on odd frequencies. That means QPSK constellation points are transmitted on even frequencies. At the receiver complex base band samples, r_m, are taken by multiplying the down converted (IF) signal by quadrature and in-phase oscillators and passing it through a low pass filter followed by sampling.

Let us analyze the unique synchronization sequence as it arrives at the receiver. Let L be the number of samples in the first half of the training sequence. The two halves of the sequence are identical except the phase shift caused by the the frequency offset between the transmitter and the receiver. At each potential frame starting point, the summation of the products of L samples in the first half and the conjugate of corresponding samples in the second half can be given as:

$$P(d) = \sum_{m}^{L-1} \left(r^*_{d+m} r_{d+m+L} \right) \tag{39}$$

where d is the possible frame starting time. At the starting point of the symbol, the product of each pair of samples gives the power of the samples and an approximately constant phase, $2\pi\Delta$f, which is similar for all of the products. This results in maximizing equation (39). From equation (39) a timing metric can be defined as:

$$M(d) = |p(d)|^2 \tag{40}$$

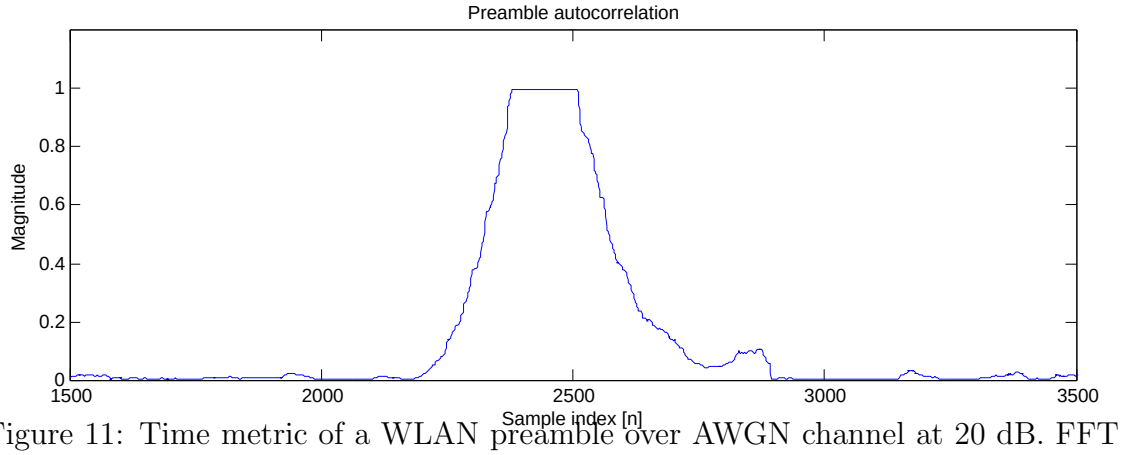

Figure 11: Time metric of a WLAN preamble over AWGN channel at 20 dB. FFT length of the system is 512 and CP length is 64.

Figure 11 above shows an example of a timing metric we observed for a generic wireless local area network (WLAN) signal (L = 256 and CP = 64) transmitted over AWGN channel at a total SNR of 15 dB. The time metric attains a plateau of length which is equal to the length of the guard interval minus delay spread of the channel. The starting time of the frame can be anywhere within the range of the plateau without risking any interference. However this ambiguity in identifying the exact sampling time poses problem in practical implementations. A number of signal processing approaches have been employed to avoid this ambiguity so that one can get a single relatively dominant peak that can be easily detected. In the Wireless Local Area Network (WLAN) GNU Radio implementation presented above, for example, matched-filtering of the normalized correlation output with a filter of unity coefficient was used to get a single peak at the edge of the plateau as shown in Figure 12 below.

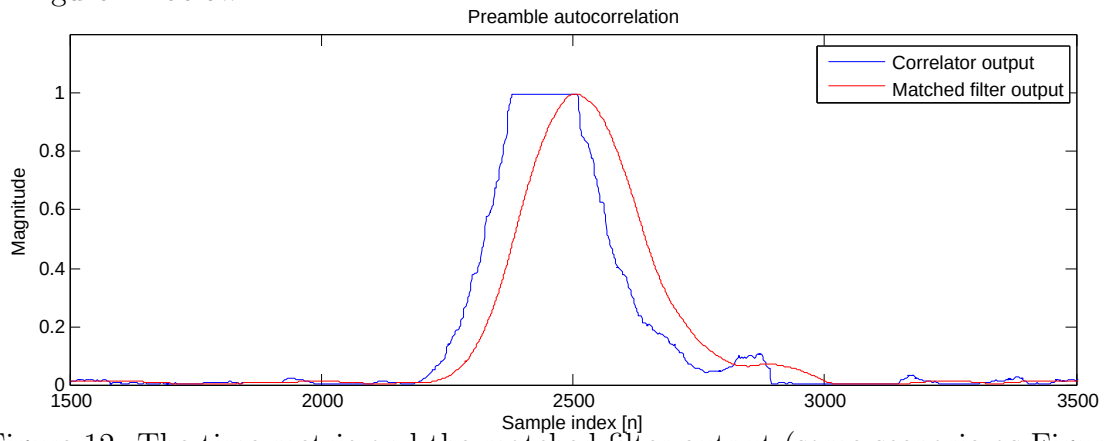

Figure 12: The time metric and the matched filter output (same scenario as Figure 9).

The frequency offset can be estimated by exploiting the following fact. The only difference between two samples that are L/2 samples apart from each other in the

PN sequence is a phase difference of

$$\phi = 2\pi\Delta f\frac{T}{2} \quad (41)$$

$$= \pi\Delta f T \quad (42)$$

We can find the phase at the point where we find the peak (symbol starting time) since at that point the correlation samples are identical and the phase of the correlation output, if there is any, is due to the frequency offset between the transmitter and the receiver. Hence,

$$\hat{\phi} = \text{angle}(P(d)) \quad (43)$$

and consequently,

$$\Delta f = \frac{\hat{\phi}}{\pi T} \quad (44)$$

Equation (44) gives the estimate for the fractional frequency offset. By estimating the fractional frequency offset and correcting it by multiplying the samples by $\exp^{-j2t\phi/T}$ we can avoid adjacent carrier interference and preserve orthogonality between consecutive sub-carriers. This is usually referred to as coarse frequency synchronization.

The synchronization algorithm in [33] requires a second PN sequence to estimate the shift in frequency bins (integer frequency offset). In this technique, after the two PN sequences are compensated for fractional frequency offset, they are transformed to the frequency domain. Let their FFTs be $x_{1,k}$ and $x_{2,k}$ and let the differentially-modulated PN sequence on the even frequencies of the second training symbol be v_k. The PN sequence will appear at the output except it will be shifted by positions because of the uncompensated frequency shift of $2z/T$ where z is an integer. Note that because there is a guard interval and there is still a frequency offset, even if there were no differential modulation between training symbols 1 and 2 (i.e., PN sequence), there would still be a phase shift between $x_{1,k}$ and $x_{2,k}$ of $2\pi\left(T+T_g\right)2z/T$. Since at this point the integer is unknown, this additional phase shift is unknown. However, since the phase shift is the same for each pair of frequencies, a metric similar to equation (39) can be used. Let X be the set of indices for the even frequency components. The number of even positions shifted can be calculated by finding $\hat{g}$ to maximize

$$B(g) = \frac{|\sum_{x\in X} x^*_{1,k+2g} v^*_k x_{2,k+2g}|^2}{2(\sum_{x\in X}|x_{2,k}|^2)^2} \quad (45)$$

with integer spanning the range of possible frequency offsets and being the number of even frequencies with the PN sequence. Then the final frequency offset estimate can be given as

$$\widehat{\Delta f} = \frac{\hat{\phi}}{\pi T} + \frac{2\hat{g}}{T} \quad (46)$$

In the non data-aided category of time and frequency synchronization as in [34], we exploit the cyclic nature of the received symbol to find the symbol starting

time and the frequency offset. In the next paragraphs we investigate the maximum likelihood time and frequency offset estimation method based on the cyclic prefix of the OFDM symbol. Assume we have M OFDM symbols each with N + L samples where N is the FFT length and L is the CP length. The starting time of a given symbol within the total block of received samples is however unknown due to the uncertainty at the receiver of the transmission delay θ. Let the indices of the received

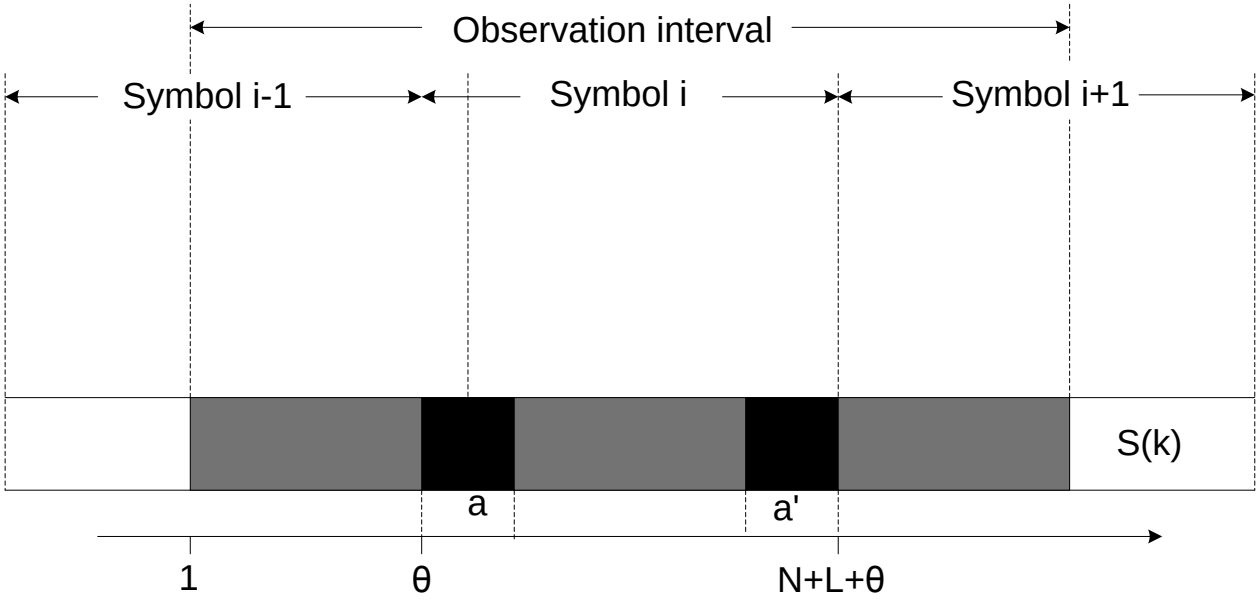

Figure 13: Model of OFDM symbols in time domain [34]

symbol samples be denoted as $a = \{\theta, \theta+1, \theta+2, ..., \theta+L-1\}$. Samples of indices a and a + N are mutually correlated as they are the cyclic prefix and their copies while the remaining samples are uncorrelated. Hence,

$$E\{r(k)\, r^*(k+m)\} = \begin{cases} \sigma_s^2 e^{-j2\pi\varepsilon}, & \text{if } m = N. \\ 0, & \text{otherwise.} \end{cases} \tag{47}$$

where $k \in a$, σ_s^2 is symbol power and ε is the difference in carrier frequency between the transmitter and the receiver. Based on the correlation properties of the observed symbols in r a log-likelihood function is developed [34].

$$\Lambda(\theta, \varepsilon) = \frac{\sum_{k=\theta}^{\theta+L-1} r(k)\, r^*(k+N) \cos\left(2\pi\varepsilon + \arg\left(\sum_{k=\theta}^{\theta+L-1} r(k)\, r^*(k+N)\right)\right)}{\frac{\rho}{2}\sum_{k=\theta}^{\theta+L-1} |r(k)|^2 + |r(k+N)|^2} \tag{48}$$

where,

$$\rho = \frac{E\{r(k)\, r^*(k+N)\}}{E|r(k)|^2 E|r(k+N)|^2} \quad (49)$$

$$= \frac{\sigma_s}{\sigma_s + \sigma_n} \quad (50)$$

$$= \frac{SNR}{SNR+1} \quad (51)$$

The metric used to estimate θ and ε can be found by running a correlation of the received signal with the delayed version of itself.

$$\gamma(m) = \frac{\sum_{k=m}^{m+L-1} r(k)\, r^*(k+N)}{\frac{\rho}{2}\sum_{k=m}^{m+L-1} |r(k)|^2 + |r(k+N)|^2} \quad (52)$$

The maximum of the likelihood function with respect to ε is found when the cosine term is equal to one in equation (48). This gives the ML estimation [34] of ε as:

$$\hat{\varepsilon}_{ML}(\theta) = \frac{-1}{2\pi} \arg\left(\sum_{k=\theta}^{\theta+L-1} r(k)\, r^*(k+N) \right) \quad (53)$$

Substituting equation (52) in equation (48) we get the compressed likelihood function with respect to ε such that,

$$\Lambda(\theta, \hat{\varepsilon}_{ML}) = \frac{\sum_{k=\theta}^{\theta+L-1} r(k)\, r^*(k+N)}{\frac{\rho}{2}\sum_{k=\theta}^{\theta+L-1} |r(k)|^2 + |r(k+N)|^2} \quad (54)$$

Then, ML estimation of θ and ε found to be

$$\hat{\theta}_{ML} = \arg\max_{\theta} \Lambda(\theta, \hat{\varepsilon}_{ML}) \quad (55)$$

$$\hat{\varepsilon}_{ML} = \frac{-1}{2\pi} \arg\left(\sum_{k=\hat{\theta}_{ML}}^{\hat{\theta}_{ML}+L-1} r(k)\, r^*(k+N) \right) \quad (56)$$

The performance of the maximum likelihood estimator is mainly affected by the SNR value and the length of the cyclic prefix (L). As we increase the length of the cyclic prefix, the frequency offset estimation improves proportionally. This is because of the fact that we use the average of the phases of the metric in equation (52) at the CP samples to find the frequency offset. As we increase the SNR, the probability of detecting a false peak decreases proportionally thus increasing the performance of the estimator. The CP length is known at the receiver, and the SNR can be fixed. Basically, the metric $\gamma(m)$ provides the estimates of θ and ε. Its energy-normalized magnitude determines the peaks that locate the symbol starting point. The phase at each peak point is proportional to $\hat{\varepsilon}_{ML}$. Figure 14 shows the portion of the output of equation (52) for DVB-T test stream investigated in the lab. The peaks show the time estimates for each symbol. The phases at the corresponding time instants are

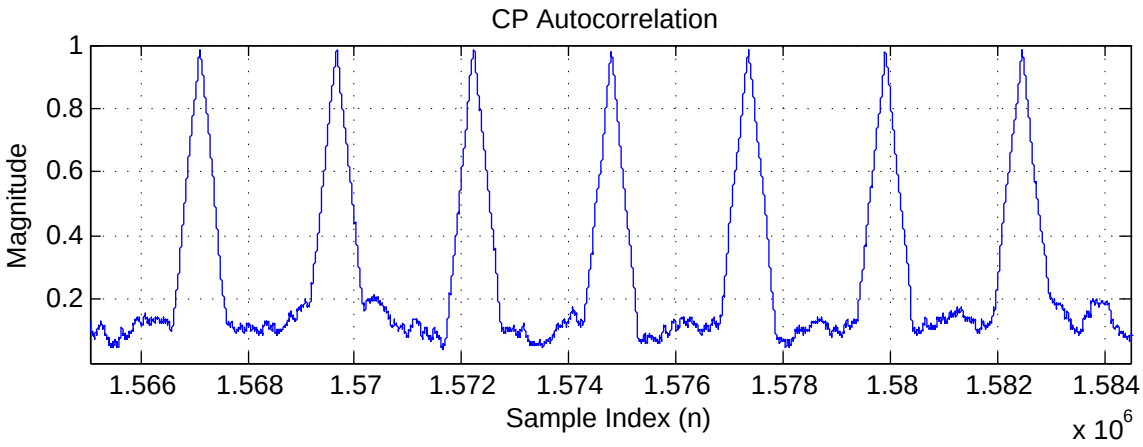

Figure 14: Portion of received samples at a 2K-mode, 1/4-guard interval DVB-T signal at 20dB SNR

used to determine the frequency offset in the system. If ε is a priori known to be zero, the log-likelihood function for θ becomes a real function as the phases at time instant θ is zero, hence

$$\Lambda(\theta) = \frac{\Re\{\sum_{k=\theta}^{\theta+L-1} r(k)\, r^*(k+N)\}}{\frac{\rho}{2}\sum_{k=\theta}^{\theta+L-1} |r(k)|^2 + |r(k+N)|^2}. \tag{57}$$

The next two sections will be devoted to discussion about time and frequency synchronization schemes in two OFDM based technology standards: LTE and DVB-T.

4.3 Synchronization in 3GPP LTE Down-link

Like in all mobile communication systems, a terminal in an LTE system must perform a certain procedure to establish connection with the network. This procedure includes cell search, cell selection, extraction of system information and random access and is generally known as LTE initial access. As soon as an LTE terminal is switched on it measures and keeps a list of the signal from the neighboring cells so as to choose one among them as its serving base station. Once the serving base station is selected, the User Equipment (UE) must remain synchronized to its serving Base Station (BS) in time in order to extract the system information transmitted to it. Cell search and synchronization in LTE are performed using primary and secondary synchronization signals. Before going to details about the primary and secondary signals and how the synchronization procedures are performed, we will discuss the down-link LTE frame structure briefly in the following section.

4.3.1 Down-link LTE frame structure

The 3GPP LTE uses OFDMA as its multiplexing scheme in the down-link. In OFDMA users are allocated a specific number of sub-carriers for a predetermined

amount of time. The smallest unit in this time-frequency grid that can be scheduled is known as resource block. The resource block, in a generic LTE frame structure, is a grid of 12 sub-carriers in the frequency dimension and 7 OFDM symbols in the time dimension, that gives a total of 84 resource elements.The generic frame structure is used with FDD. Alternative frame structures are defined for use with TDD. However, TDD is beyond the scope of this thesis. Figure 7 below shows the physical layer configuration of a generic LTE. As shown in the figure, OFDM

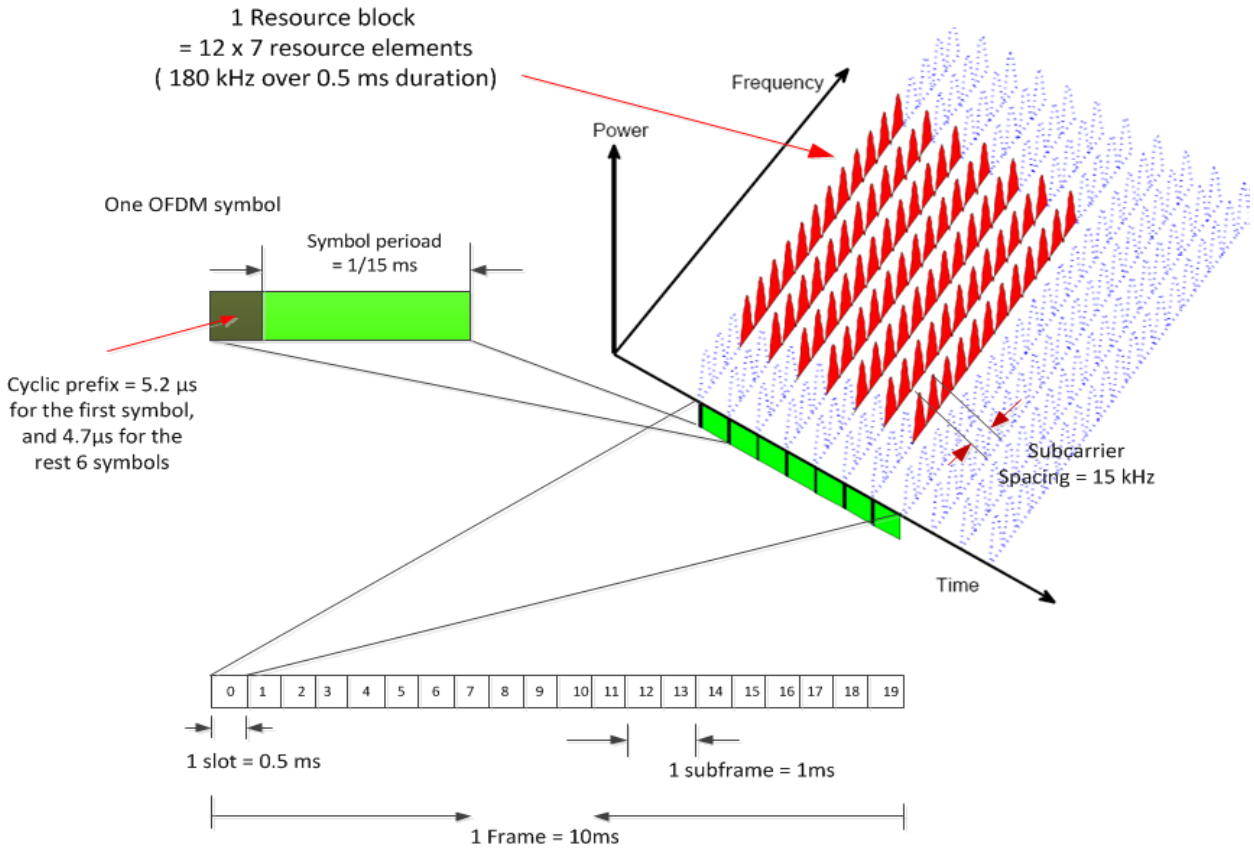

Figure 15: Physical layer configuration of a generic LTE

symbols in time domain are structured into an LTE frame. The LTE frame consists of 10 sub-frames of duration 1 ms. Each sub frame consists two time slots of 0.5 ms duration each. In a time slot there are 7 OFDM symbols with a useful part duration of 0.067 ms. Hence, there are a total of 140 OFDM symbols in a frame of 10 ms duration.

4.3.2 Primary and Secondary Synchronization signals

As mentioned in the previous sections, the primary and secondary synchronization signals are crucial in LTE cell search and frame timing synchronization procedures. Independent of the defined channel bandwidth, 6 resource blocks around the DC in the frequency domain are reserved for the transmission of the synchronization signals. With a carrier separation of 15 kHz, a total frequency range of $6 \times 12 \times 15kHz = 1.08MHz$ is reserved around the DC for the synchronization signals. From the reserved 72 sub-carriers, 62 are used for transmitting the synchronization signal. This simplifies the signal processing computations at the terminal by allowing as low FFT length as 64 and lower sampling rate. In the time domain, they are transmitted every fifth sub-frame in order to perform the time synchronization on a 5 ms interval basis. In 3GPP LTE standard, there are three unique primary synchronization sequences and 168 secondary sequences. By scrambling the secondary sequences with the primary we can get 504 possible sequences that would identify a cell uniquely in the network.

The primary signals are used to perform the 5 ms timing synchronization between the BS and UE. They are transmitted in the last OFDM symbol of the first time slot of the first (sub-frame 0) and the fifth sub-frames in a radio frame. The type of signal used for primary synchronization is a Zadoff-Chu (ZC) sequence which has a constant amplitude zero auto-correlation (CAZAC) property. The constant amplitude property helps to minimize the peak-to-average ratio while the zero auto-correlation achieves good time domain properties. Equation (58) shows how to generate the ZC sequences used for primary synchronization.

$$d_u(n) = \begin{cases} \exp^{(-j\frac{\pi un(n+1)}{63})}, & n = 0, 1, ..., 30. \\ \exp^{(-j\frac{\pi u(n+1)(n+2)}{63})}, & n = 31, 32, ..., 61. \end{cases} \tag{58}$$

where u is the root index which is a quantity dependent on the selected local cell ID. In our discussion we use the term local cell ID to describe an ID that identifies a cell locally in a given cell group. In the hierarchical network approach, the network is divided into a number of cell groups of each containing three cells. The cells in a given group have a cell ID that uniquely identifies them locally. However the cell IDs are repeated for cells in other cell groups. In the LTE 3GPP standard it is specified that there are 168 such cell groups and 504 unique cell IDs.

Once the 5 ms timing synchronization is achieved using the primary signals, the secondary synchronization signals are used to determine frame timing and the cell group IDs in order to uniquely identify a cell in the network. The secondary signals are always transmitted one symbol period prior to the primary signal as shown in Figure 16

The Secondary Synchronization Sequence (SSS) is formed by interleaved concatenation of two length 31 sequences $s_0^{(m_0)}$ and $s_1^{(m_1)}$ which are dependent on the selected local cell ID as in the case of the Primary Synchronization Sequence (PSS). In the first sub-frame, $s_0^{(m_0)}$ is mapped to the even-numbered sub-carriers and $s_1^{(m_1)}$

is mapped to the odd-numbered sub-carriers and vise-versa in the sixth sub-frame. The combination of the indices m_0 and m_1 uniquely identifies one of the 168 cell groups. Depending on the sub-carrier index, even or odd, another scrambling sequence is used for sequences $s_0^{(m_0)}$ and $s_1^{(m_1)}$. In case of even index sub-carriers, the scrambling sequence employed is $c_0(n)$ and for odd index sub-carriers, it is $c_1(n)$. Depending on the sub-frame number, additional scrambling sequence is used for the sequence mapped to the odd-numbered sub-carriers. For sub-frame 0, it is $z_1^{(m_0)}(n)$ and and for sub-frame 5, $z_1^{(m_1)}(n)$ is used. Each of these two scrambling sequences depends on the indices m_0 and m_1 , which define the cell group. The generation of the SSS is summarized in equation (59) shown below.

$$d(2n) = \begin{cases} s_0^{(m_0)}(n)c_0(n), & \text{in subframe 0} \\ s_1^{(m_1)}(n)c_0(n), & \text{in subframe 5} \end{cases} \tag{59a}$$

$$d(2n+1) = \begin{cases} s_1^{(m_1)}(n)c_1(n)z_1^{(m_0)}(n), & \text{in subframe 0} \\ s_0^{(m_0)}(n)c_1(n)z_1^{(m_1)}(n), & \text{in subframe 5} \end{cases} \tag{59b}$$

Matlab code for the generation of the primary and secondary synchronization sequences is given in Appendix B.

4.3.3 Timing synchronization in LTE systems

In order for the LTE terminal to extract the system information transmitted from the base station and to locate the pilots exactly, the frame timing between the transmitter and the receiver should be synchronized. As mentioned in the previous sections, primary synchronization signals play an important role in frame timing synchronization. The synchronization process is done by auto-correlation of the received signal by each of the primary synchronization signals in the time domain. Due to strong auto-correlation properties of the primary synchronization signals in the time domain, we should get dominant peaks every 5 ms where the primary synchronization signals are located. Hence, the primary signals enable us to achieve

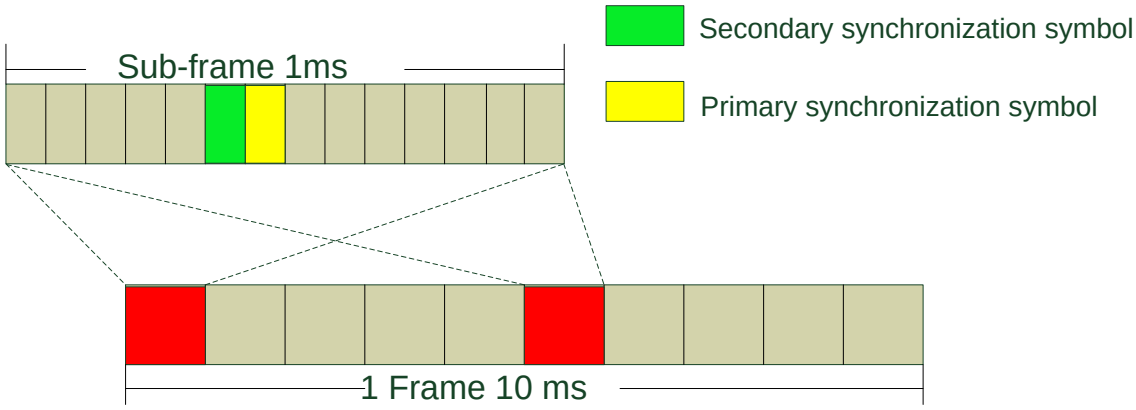

Figure 16: Primary and Secondary synchronization symbols in a LTE frame

the half-frame synchronization. In order to find the starting time of the full frame however, we should exploit the properties of the secondary synchronization signals. As shown from equation (59), since the secondary signals in the first and the sixth sub-frame are modulated with different scrambling sequences, correlation of the received signal with both of these sequences would uniquely tell whether the symbol is in the first or sixth sub-frame thus the offset from the starting time of the frame.

4.3.4 Frequency synchronization in LTE systems

LTE down-link transmission utilizes OFDM as the physical layer technique which enables high data rate transmission in frequency selective fading scenarios [23]. However, one of the drawbacks of OFDMA is its sensitivity to CFO. Given a carrier frequency of 2.5 GHz, a typical frequency drift of 10 Parts Per Million (PPM) of the local oscillator results in an offset of 25 kHz. In LTE, which employs a fixed sub-carrier spacing of 15 kHz, such an offset corresponds to 1.67 sub-carrier spacings. This offset causes ICI and phase distortion in the received signal if left uncorrected. In this section we will describe a two stage CFO estimation scheme for down-link LTE.

1. Fractional Frequency Offset (FFO) estimation: As mentioned in several occasions in this chapter, the FFO is responsible for ICI by destroying orthogonality between sub-carriers. So, it should be compensated before the received signal is transformed to the frequency domain. The maximum likelihood estimation method discussed in section 4.2.1 shall be used to estimate the FFO. The ML estimator of the FFO given in Equation (52) can be extended to a sub-frame basis as:

$$\hat{\varepsilon}_{ML} = \frac{-1}{2\pi} \arg \left(\sum_{l}^{N_{sf}} \sum_{k=\hat{\theta}_{ML}}^{\hat{\theta}_{ML}+L-1} r_l(k)\, r_l^*(k+N) \right) \tag{60}$$

   where N_{sf} is the number of OFDM symbols in a sub-frame.

2. Integer Frequency Offset (IFO) estimation: Once the FFO estimation has been performed, we assume the fractional part of the CFO has been mostly corrected. The integer part of the CFO has two effects on the received signal. The first is the frequency bin shift, that is, the symbol transmitted on sub-carrier k-ε_{IFO} is received on sub-carrier k. The second effect is a phase rotation proportional to the OFDM index l. These two effects can be compensated once the IFO is estimated, for example by the ML estimator proposed in [24]. The symbols used for estimation can be either pre-defined pilots or PSK modulated data symbols. In our context, we choose to use the synchronization signals for estimation, leading to the following IFO estimator:

$$\hat{\varepsilon}_{IFO} = \arg\max_{i} \left\{ \Re \left[e^{\frac{j2\pi i N_g}{N}} \cdot \sum_{k} \left(R^*_{SSS,k+i} R_{PSS,k+i} \right) \left(X^*_{SSS,k} X_{PSS,k} \right)^* \right] \right\} \tag{61}$$

where PSS and SSS are the primary and secondary synchronization sequences respectively, k is the sub-carrier index of the synchronization sequences and N_g is the guard length. Since the synchronization sequences are found only in the first and sixth sub-frame, the estimation of IFO can only be carried out in these sub-frames.

4.4 Synchronization in DVB-T systems

In a typical DVB-T receiver, a pre-FFT acquisition stage is required to obtain the OFDM symbol timing, the OFDM symbol length, that is, size of the Fast Fourier Transformation (FFT), and the cyclic prefix length, where the latter two parameters are adjustable by the transmitter. The principle of the pre-FFT synchronization is based on the availability of the cyclic prefix in the OFDM symbols [34] while post FFT frequency synchronization and tracking involves the use of reference signals distributed in the frame structure. The OFDM Frame structure will be discussed in the next section to help explain the synchronization process in the DVB-T system.

4.4.1 The DVB-T Frame Structure

In DVB-T frame structure, the transmitted signal is organized as frames comprise of OFDM symbols. One frame consists of 68 OFDM symbols and 4 such frames constitutes a super frame [25]. Each symbol is a set of N = 6 817 carriers in the 8K mode and N = 1 705 carriers in the 2K mode and transmitted with a duration T_S. A symbol is composed of two parts: a useful part with duration T_U and a guard interval with a duration Δ. The guard interval consists of a cyclic continuation of the useful part, T_U, and is appended at the front.

In addition to the transmitted data, an OFDM frame contains scattered pilot cells, continual pilot carriers and Transmission Parameter Signaling (TPS) carriers. These pilots can be used for frame synchronization, frequency synchronization, time synchronization, channel estimation, transmission mode identification and can also be used to follow the phase noise.

The continual and scattered pilots are modulated according to a Pseudo Random Binary Sequence (PRBS),w_n, corresponding to their respective carrier index n. This sequence also governs the starting phase of the TPS information. The PRBS is initialized so that the first output bit from the PRBS coincides with the first active carrier. A new value is generated by the PRBS on every used carrier (whether or not it is a pilot). Reference information, taken from the reference sequence, is transmitted in scattered pilot cells in every symbol. Scattered pilot cells are always transmitted at the "boosted" power level. Thus the corresponding modulation is given by: $\Re\{c_{m,l,n}\} = 4/3 \times 2(1/2 - w_n)$ and $\Im\{c_{m,l,n}\} = 0$ where m is the frame index, n is the frequency index of the carriers and l is the time index of the symbols. For the symbol of index l (ranging from 0 to 67), carriers for which index n belongs to the subset

$$n = N_{\min} + 3(l \mod 4) + 12p \text{ where, } p \geq 0, n \in [N_{\min}; N_{\max}] \tag{62}$$

are the positions of the scattered pilots. $N_{\min}$ and $N_{\max}$ represent the first and the last carrier indices in a given mode respectively. p is an integer that takes all possible values greater than or equal to zero, provided that the resulting value for k does not exceed the valid range [$N_{\min}$; $N_{\max}$]. The location of the continual pilots in 2K and 8K modes are given in Appendix C.

4.4.2 Timing synchronization in DVB-T system

The typical timing synchronization algorithm takes advantages of the presence of a long cyclic prefix to find the starting time of a symbol. This algorithm uses the ML method discussed in section 4.2.1 The result of the auto-correlation between the received signal and its delayed version gives dominant peaks at the starting point of each symbol. Once the starting time of the symbol is known, we can locate the TPS pilots in the symbol and decode the information in it to determine the starting time of the frame. The TPS pilots are organized into blocks of 68 bits, and each bit is transmitted on several sub-carriers within one OFDM symbol. Hence, 68 symbols, that is, one OFDM frame in DVB-T, are required to transmit a whole TPS block. Hence, typical frame synchronization requires a time in a range of 17 up to 84 OFDM symbols depending on the very first received OFDM symbol in the frame.

4.4.3 Frequency synchronization in DVB-T system

In addition to timing offset estimation, the phase due to fractional frequency offset can be determined and used to correct the FFO in time domain. Hence, only CFOs which are integer multiples of the sub-carrier spacing will remain in the OFDM signal in the frequency domain. The recovered OFDM symbols are transformed by means of the FFT, which acts as a matched filter for the OFDM signal. The post-FFT synchronization obtains estimations for the integer part of the CFO and the SCFO in frequency domain, which are then compensated in time-domain OFDM signal in order to reduce ICI. The phase rotation in the frequency domain caused by the time offset is estimated and compensated by using the continual pilots.

The above discussed synchronization methods for different technologies can be used in primary-secondary cognitive radio spectrum sharing either for white space sensing in licensed spectrum in interweave approach or transmission timing interval detection in overlay approaches.

4.5 Synchronization in Cognitive radio networks

Timing synchronization problem has gained a new aspect in cognitive radio and has been developed as one of the most challenging issues in cognitive radio systems. In the interweave cognitive radio approach, timing synchronization is not such a challenge that needs to be addressed as it is in the overlay approach. Nonetheless it would be wise to briefly discuss how white space spectrum access works in this subsection. In interweave cognitive radio systems, the secondary system needs to

determines spectrum holes or spectrum white spaces in time, frequency and/or geographic location that left vacant by the primary system. This strategy is based on cognitive radios that can detect the usage of spectrum resources in order to discover spectrum usage opportunities. White spaces can be determined by spectrum sensing [26][27], or in case of rather static spectrum usage of the primary system by means of Geo-location combined with access to a spectrum usage database [28]. In the later case, synchronization between White Space Devices (WSD) and a spectrum usage database might be a point of discussion.

In the cognitive overlay approach, where the secondary uses the same spectrum as the primary system at the same time, the secondary system should know the message and the transmission timing of the primary system in advance. This allows the secondary system to design its own transmitted signal such that interference from the primary system to the secondary receiver can be mitigated. At the same time, the secondary system can cooperate with the primary system by relaying the primary signal; this enables the secondary system to compensate for interference that it causes to the primary receivers. For all this to work properly however, the secondary system must be time-synchronized to the primary system. In the following subsections, white space access and general synchronization aspects of cognitive radio spectrum sharing in interweave and overlay approaches will be discussed.

4.5.1 General Synchronization Aspects of Interweave Cognitive Radio Systems

As discussed in chapter 3, we use techniques such as Geo-location databases, spectrum sensing and beacons to access white spaces available in a licensed spectrum, specifically a TV band. In this section we will try to address the synchronization aspects associated with each of the techniques.

Geo-location database synchronization process aims to ensure the same data content among several participating entities, possibly having different sets of content. TVWS database synchronization can be performed in two ways: *Unidirectional synchronization/centralized synchronization* and *bidirectional database synchronization.* The *Unidirectional synchronization/centralized synchronization* scheme is working only with the authorized government database, i.e., the commission's Consolidated Data Base System (CDBS) and the universal licensing system (ULS). In a unidirectional synchronization, all of the contents from the CDBS/ULS will be placed in other clearinghouse/databases, which also implies any content in the clearinghouse/database entities that do not exist in the CDBS/ULS database will be deleted.This is applied only to the registered incumbent devices in the CDBS/ULS. This scheme also is suitable with the hierarchical database within the same database service provider.

Bidirectional database synchronization is suitable for non-registered TVBDs, the contents of which will be merged with all the participating databases. However, the

security module should make sure that no unauthorized data will be injected into the database.There are several other factors that need to be taken care of when implementing the database synchronization, i.e., how frequently this synchronization of data will be conducted, speed of implementation, security, performance, and the immediate update of data [29].

In beacon based white space spectrum access, each WSD shall maintain a beacon period start time (BPST). The device shall derive all times for communication with its neighbors based on the current BPST. The device shall adjust its BPST in order to maintain super frame synchronization with its slowest neighbor. A device shall synchronize with such a device before it sends its first beacon. When a device receives a beacon from a neighbor, the device determines the difference between the beacon's actual reception time and the expected reception time. The beacon's actual reception time is an estimate of the time that the start of the beacon preamble arrived at the receiving device's antenna. The expected reception time is determined from the information in the received beacon and the receiving device's BPST. If the difference is positive, then the neighbor is slower. In order to maintain frame synchronization with a slower neighbor, the device shall delay its BPST by the difference, but limited to a maximum adjustment of a specified amount per frame.

4.5.2 Synchronization in Overlay Cognitive Radio Systems

The issue of synchronization between the primary and the secondary systems is one of the challenges in cognitive overlay spectrum sharing . There are a number of ways to deal with the time synchronization problem in such systems. One approach would be synchronization of the primary and the secondary symbols at the primary transmitter. In another approach, synchronization of the primary and the secondary waveforms can also be performed at the secondary receiver. These approaches will be discussed in the following sections.

Synchronization at the Secondary Transmitter: In this approach the secondary transmitter tap the primary signal and looks for the symbol starting time of the primary symbols. After the secondary transmitter determines the symbol starting time and transmission intervals of the primary transmitter, it synchronizes its transmission to the primary transmitter before sending its aggregate signal. This approach simplifies the synchronization at the secondary receiver as there will only be a single channel and conventional synchronization techniques discussed in the previous sections can be applied. Let $x_p(t)$ and $x_s(t)$ be the primary and the secondary signals respectively at the secondary transmitter. The combined primary-secondary waveform x(t) can be written as:

$$x(t) = x_p(t) + x_s(t + \tau) \tag{63}$$

where τ is the timing offset between the primary and the secondary symbol transmission. In the presence of AWGN the discrete channel impulse response for Equation

(63) can be given as:

$$h(n) = |x_p|\,\delta(n) + |x_s|\,\delta(n+D) + w(n) \tag{64}$$

where D is the delay in samples between the primary and the secondary OFDM symbols and w(n) is a AWGN. From the equivalent channel frequency response equation, H(k), shown below we can examine and counteract the effect of the delay in the phase and the amplitude of the aggregate signal.

$$H(k) = |x_p| + |x_s|\,e^{\frac{-j2\pi Dk}{N}} + W(k) \tag{65}$$

where k is the sub-carrier and N is the FFT length. As an example the phase and the magnitude of the channel frequency response at SNR of 15 is shown in Figure 17 below for a delay of 20 samples. Performing the synchronization at the secondary

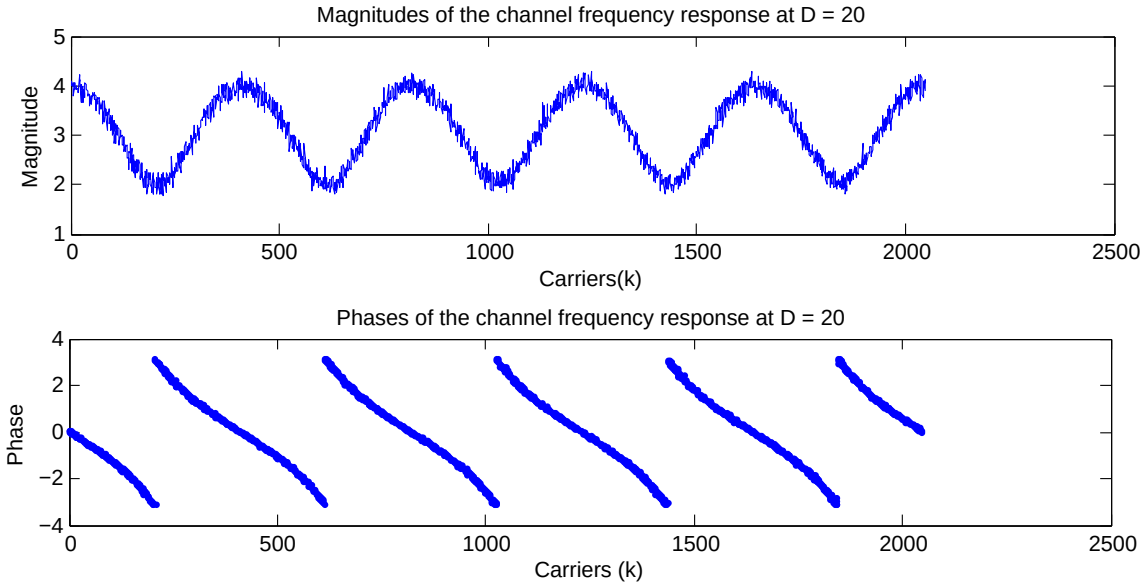

Figure 17: Magnitude and Phase of channel frequency response at delay of 20 samples

transmitter helps to take computational complexity off the receiver thus enabling simple and less expensive receivers with a better battery life.

Synchronization at the Secondary Receiver: In this approach, synchronization is preformed on the waveform as it reaches the secondary receiver. In overlay systems with relaying, the secondary transmitter splits its power to transmit its own message and to relay the primary signal. Hence, the secondary transmitter sends an aggregate of the primary and the secondary signals. Since the primary system is also transmitting, the aggregate signal from the secondary transmitter and the primary signal from the primary transmitter reach the secondary receiver with some timing offset to each other. The secondary receiver estimates the phase response of the multi-path channel and uses it to construct the primary signal. Once the

primary signal is constructed, the secondary receiver cancels it from the aggregate signal to find the residual signal.

5 Measurement observations and discussions

In the following sections, laboratory observations for synchronization and equalization tests in LTE and DVB-T systems will be discussed. Moreover, simulation examples of synchronization in cognitive overlay systems will be presented with a DVB-T primary and a generic OFDM secondary. The laboratory setup for each measurement, the measurement results and result discussions are presented in the sections coming below.

5.1 Timing, Frequency Synchronization and Cell search in 3GPP LTE

When an LTE mobile unit is powered on, it has to search for the available radio cells and lock to one of them to continue further communication. Multiple mobile unit users simultaneously try to access the same set of radio cells and also, the UE mobile unit begins it search blindly without any knowledge of the bandwidth it has allocated. Hence the initial cell search procedure must also be implemented in timing and frequency synchronization. This research presents how a LTE mobile unit performs this cell search and identifies the strongest available radio cell near it. The timing and frequency synchronization that is required as part of this cell search procedure is also performed. Cell search is a basic function of any cellular system, during which timing and frequency synchronization is obtained between the mobile unit and the network. Successful execution of the cell search and selection procedure as well as acquiring initial system information is essential for the UE before taking further steps to communicate with the network. LTE uses a hierarchical cell-search procedure in which an LTE radio cell is identified by a cell identity. LTE systems consist of 504 unique physical layer cell identities. To accommodate and manage this large amount, the cell identities are divided into 168 unique cell layer identity groups. Each group further consists of three physical layer identities. A detailed discussion on primary and secondary sequence generation and resource mapping is presented in Section 4.3.1.

5.1.1 Cell search procedure

The cell search procedure is performed using the primary and the secondary sequences in a two step process. To begin with, the MATLAB representation of the three primary synchronization signals (see Appendix for MATLAB code to generate PSS and the SSS) is presented here. The PSS signals are Zadoff-Chu sequences with their center made zero at the DC. Each one has their amplitudes on the unit circle at different cyclically shifted phases.

5.1.2 Simulation scenario and test setup

For the measurements, a multi-cellular environment with 4 BSs and a UE is assumed. The scenario is illustrated as shown in Figure 18 below. In the simulation scenario

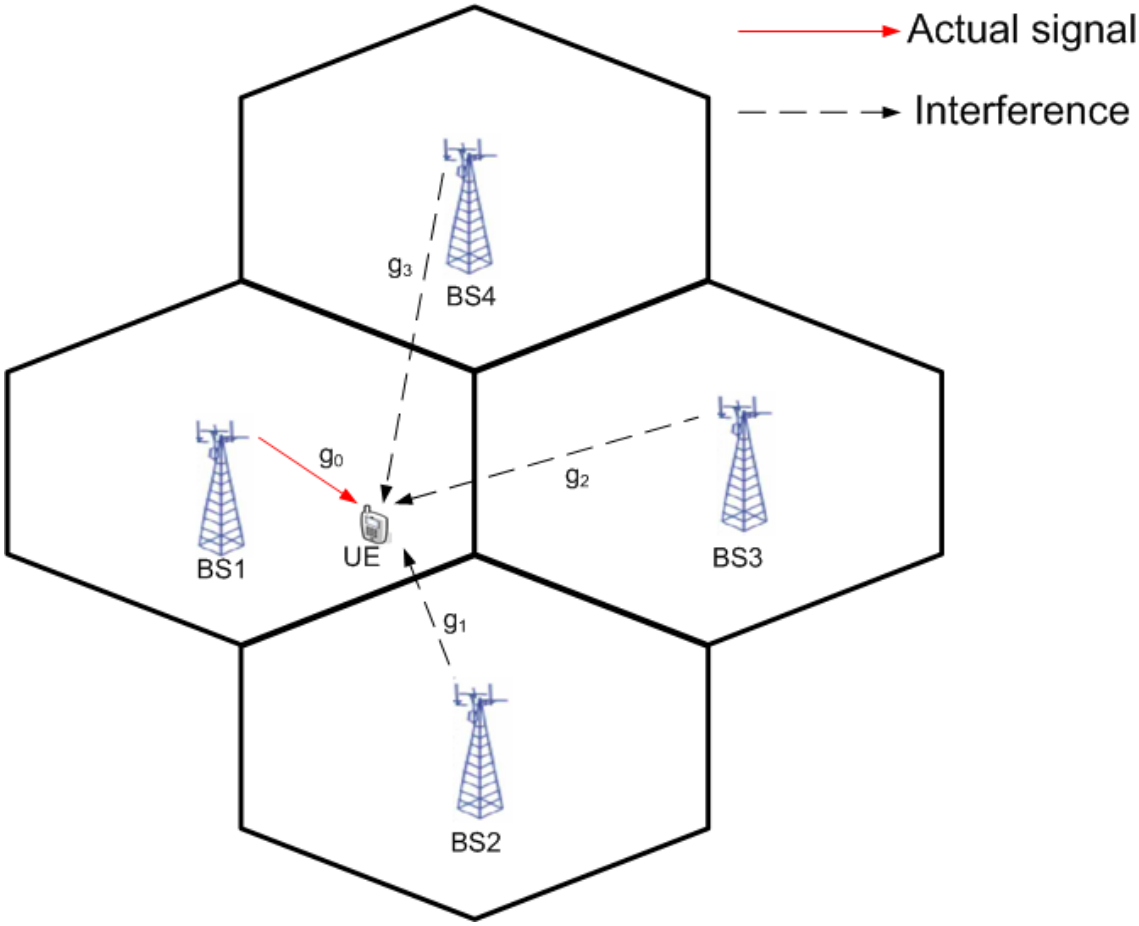

Figure 18: Simulation scenario for LTE cell search and synchronization

Primary sequences of root index 29, 34 and 25 were used at BSs 1, 2 and 3 respectively. Moreover, of the possible 168 unique secondary sequences, 4 PN-polynomials were selected. A channel gain $g_0 = 1$ dB is assumed between BS1 and the receiver while a random channel gain between 0 and 1 dB is assumed for channel gains g_1, g_2 and g_3 in Figure 18. The simulated transmitted signals from the three BSs are combined and transmitted via a Universal Software Radio Peripheral (USRP N200) using the Gnuradio platform. The transmit-receive setup used in the laboratory is shown in Figure 19 below.

The determination of sub-frame transmission interval is performed by cross-correlation of the received signal with each of the three PSs and comparing the correlation magnitudes obtained. In addition, according to the aforementioned channel gains between the UE and the three BSs, the test determines that the signal from BS1 (root index 29) is the strongest at the UE and thus selects BS1 as the serving cell. Figure 20 below shows the cross correlation of the received signal with each of the three PSs. Each secondary sequence was scrambled with the 3 primary sequences. Hence, there are 12 scrambled sequences.

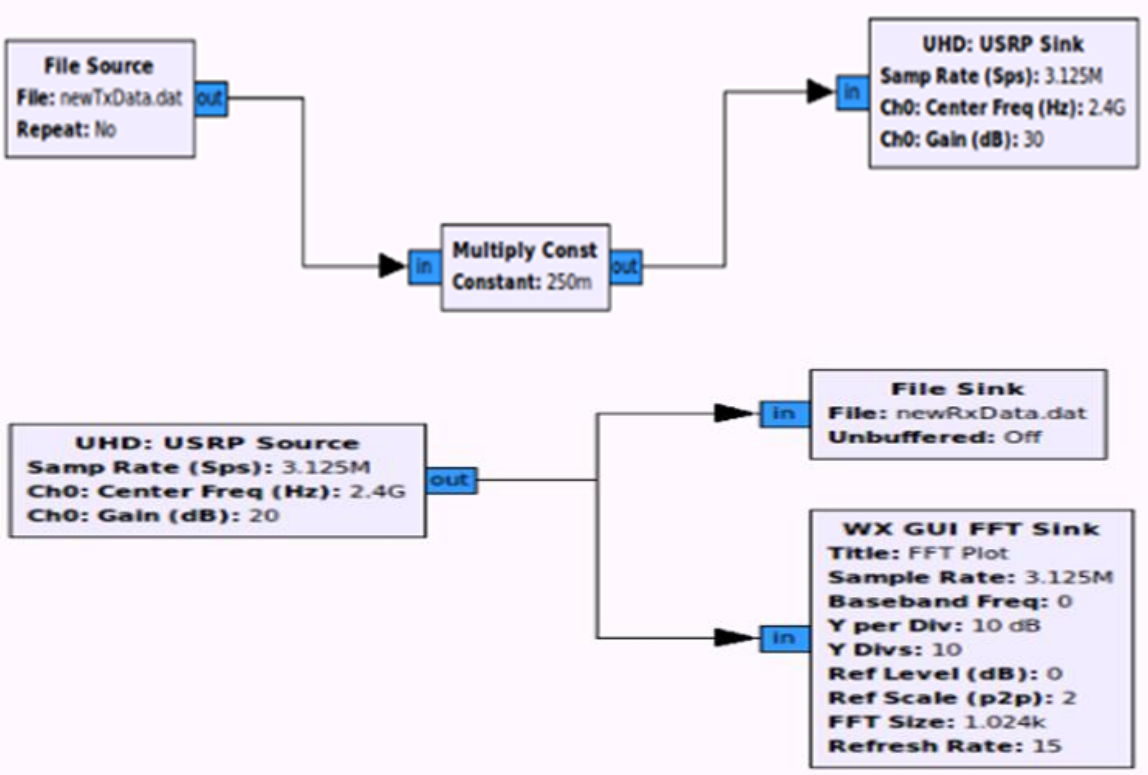

Figure 19: Test setup for LTE cell search and synchronization measurements

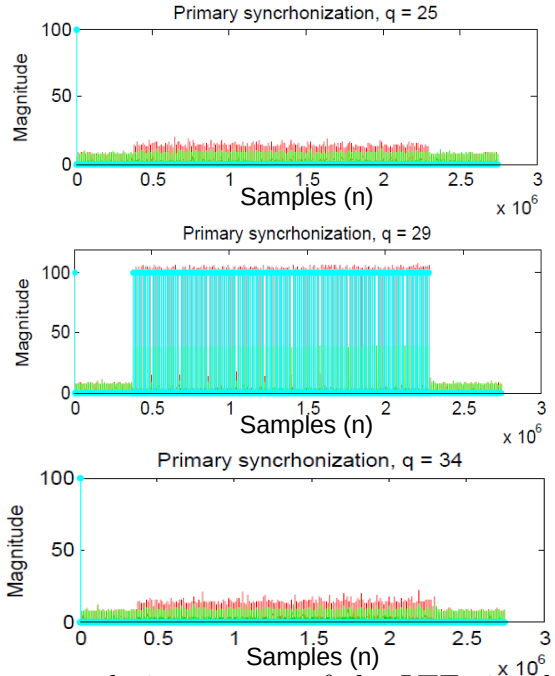

Figure 20: Cross-correlation output of the LTE signal with primary sequences of root index 29, 25, 34

A closer look at the plot of the cross-correlation of the received signal with the primary sequence of root index 29 (Figure 20 top-left) reveals more details as shown in Figure 21.

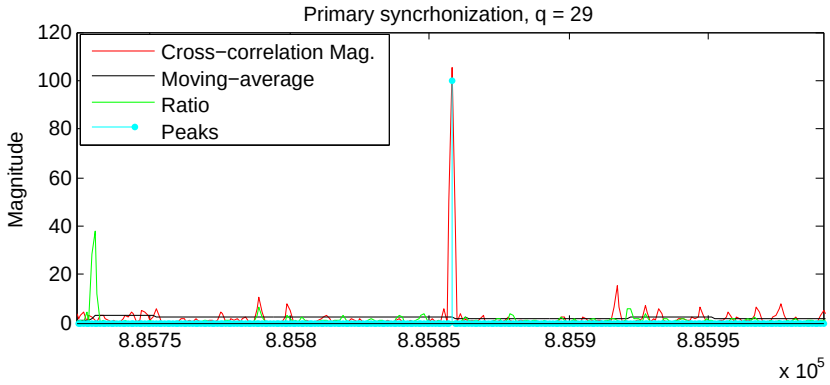

Figure 21: Output of the peak detector algorithm

A peak detection algorithm detects the correlation peaks by comparing the output of the cross-correlation with its own moving average (the output of the moving average filter). The algorithm starts to look for a peak if the cross-correlation magnitude is greater than the moving average by a pre-defined factor called the *rise threshold* and stops the search when the correlation magnitude falls below a certain threshold called the *fall threshold* detecting a single peak in the interval. The detected peak positions indicate a half frame interval in LTE symbol transmission.

Once the primary sequence that gives the maximum cross-correlation magnitude is identified (in our case it is root index 29), The secondary sequences which are

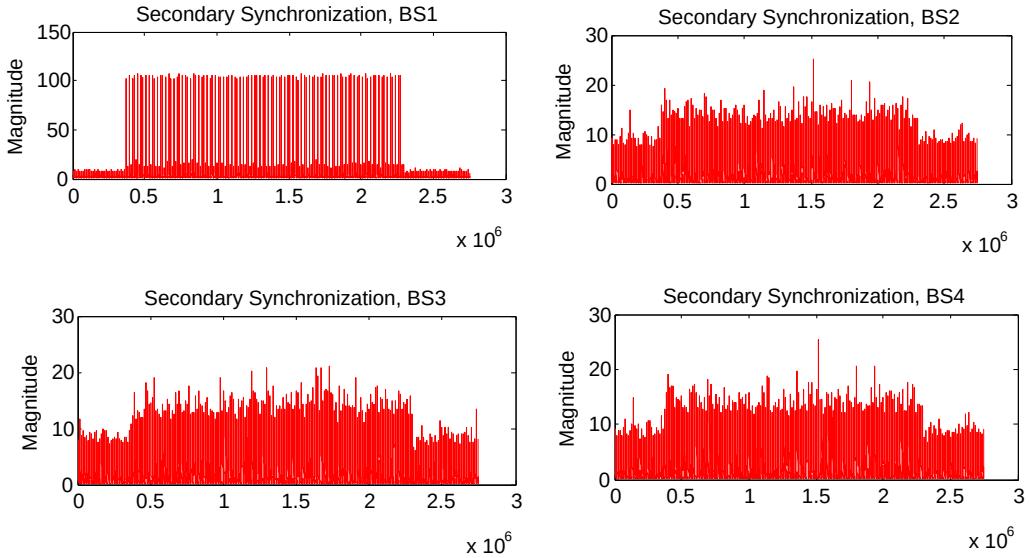

Figure 22: Cross-correlation output of the received signal with secondary sequences

scrambled with this particular primary sequence are used to perform cross-correlation with the received signal to find the peaks as shown in Figure 22 above that determine the serving cell and transmission frame interval. Thus a total of seven correlations were needed to estimate the frame transmission starting time and identify a cell uniquely at the UE.

5.1.3 Fractional Frequency Offset Estimation and Correction

By correlating the received signal with the delayed version of itself in the time domain, the phases at the CP samples tells the the phase introduced due to the fractional frequency offset between the transmitter and the receiver. By taking the moving average of these phases at the CP samples, the phase introduced due to FFO can be estimated from equation (56) and FFO compensation can be done by de-rotating the OFDM symbols with the resulting phase.

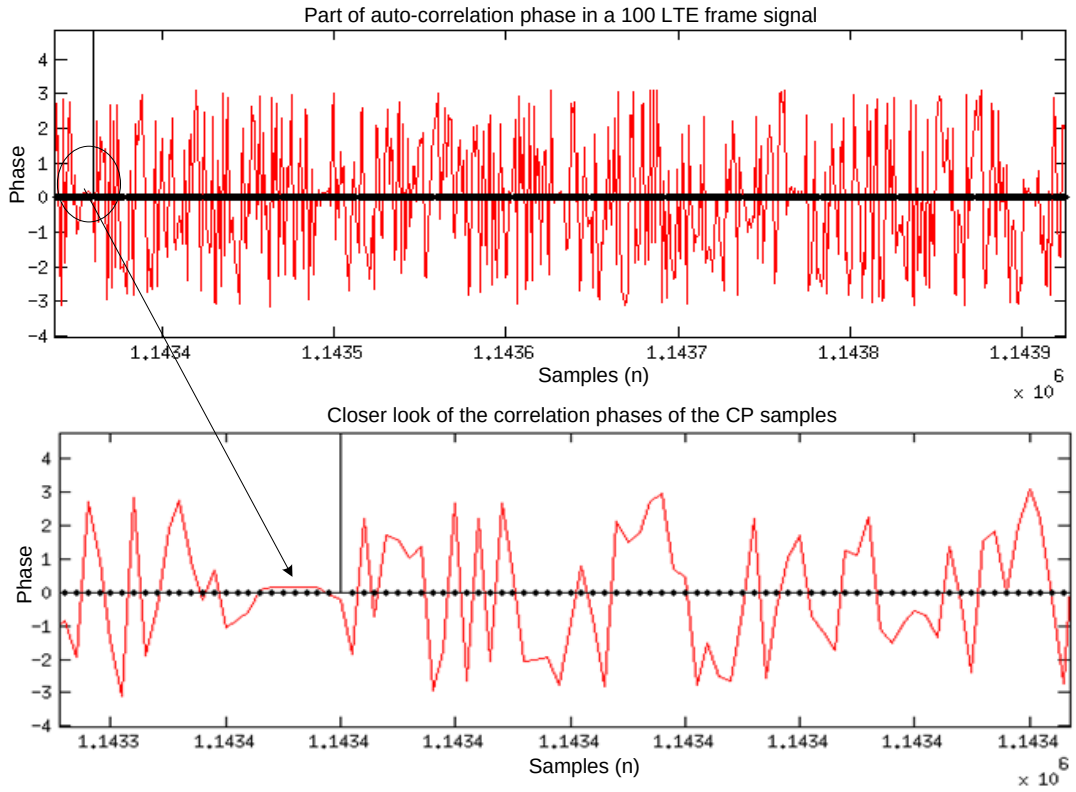

Figure 23: Phase of the auto-correlation of the LTE signal after phase correction

Figure 23 shown above depicts the phase of the auto-correlation of 100 LTE frames after the received signal is de-rotated by the estimated phase. As it should be, the average phase over the CP samples is zero (as indicated by the vertical lines). In the frequency domain, the sampling offset introduces a linearly increasing phase over the sub-carriers. The slope of the increment was obtained by estimating the channel using the primary synchronization sequences. After equalizing the received signal by the reciprocal of the channel, which is AWGN in our experiment, the BPSK

constellation diagram of the received signal at 15dB SNR looks as shown in Figure 24 below. The short length of the CP in LTE system poses a challenge in LTE

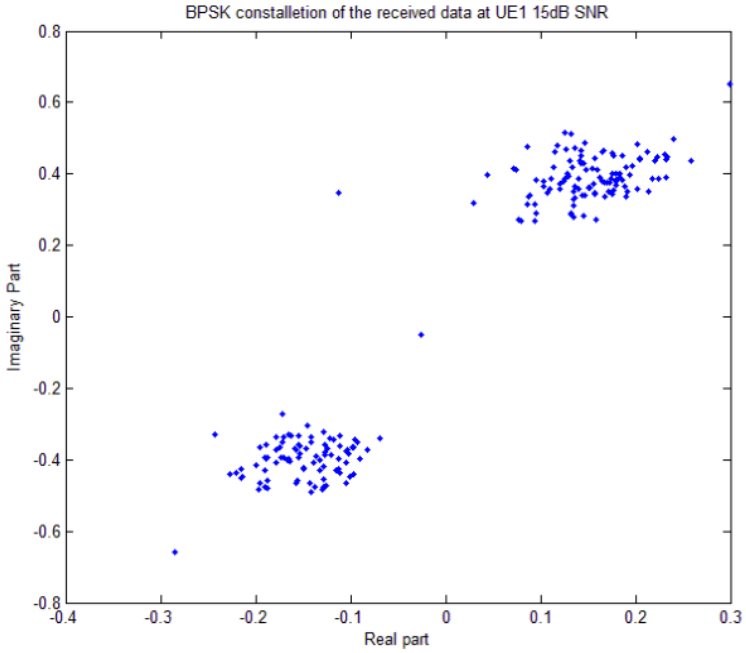

Figure 24: BPSK constellations symbols of LTE signal after synchronization and equalization

FFO estimation. since averaging of the phases over the CP length would not be a good approximation of the actual phase rotation caused by the FFO and resulted in residual phase.

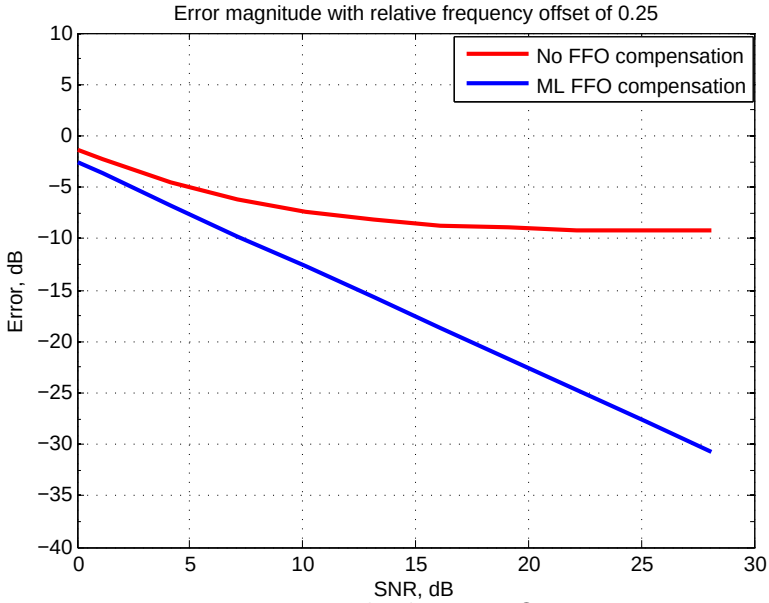

Figure 25: Error magnitude due to FO in DVB-T system

In our test we have taken the average of the phase estimates over a sub-frame. This approach improves the phase estimation significantly by removing the residual phase. The error magnitude of the constellation with and without FFO compensation is depicted in Figure 25 shown above.

5.2 Timing and Frequency Synchronization in DVB-T systems

The setup for this test was arranged in such a way that DVB-T signal of Mode 2K and bandwidth 7 Mhz was transmitted from Rohde&Schwartz SMBV100A vector signal generator at sampling rate of 8 MSamples/second and 5 super-frames (20 frames) were captured at the USRP N200. The receiver setup in the gnu-radio is depicted in Figure 26 below. The captured signal was then post processed in Matlab to verify the algorithms.

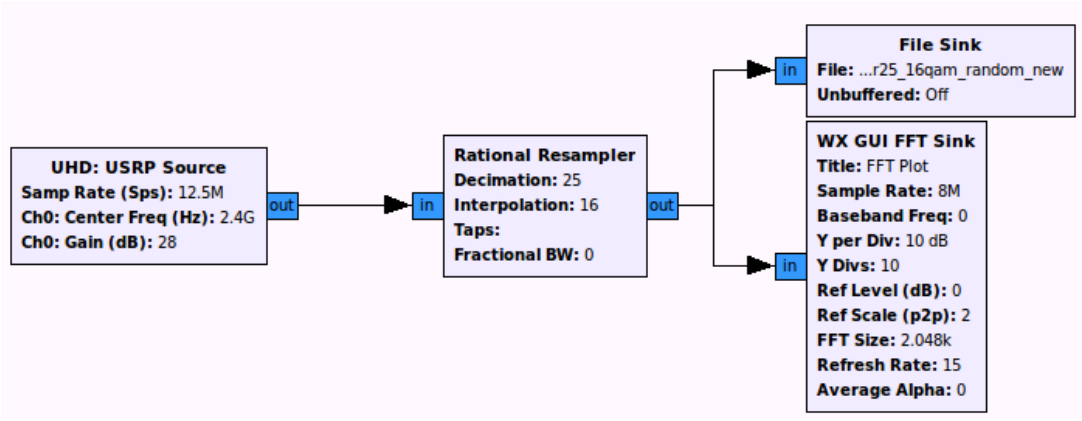

Figure 26: Test setup at the receiver for DVB-T synchronization measurements

5.2.1 Time synchronization in DVB-T systems

The DVB-T symbol starting time was estimated by time domain auto-correlation of the received signal with itself delayed with FFT length. As a result correlation peaks can be found at the end of each OFDM symbol a shown in Figure 27. The peaks are detected using the peak detection algorithm discussed in section 5.2.3. Sampling can be done either by taking only the first peak from the peak detector and cutting out symbols of FFT length or using all the peaks from the peak detector. The former approach was adopted for tackling conditions when there when there are a large number of false peak detections. Besides determining the starting time of a DVB-T symbol, it is necessary to know which symbol we received as the scattered pilots that we used for channel estimation and equalization are different in different symbols. Although this information is normally found by decoding the TPS, a quicker and simpler approach is used in this research. The approach is based on the fact that

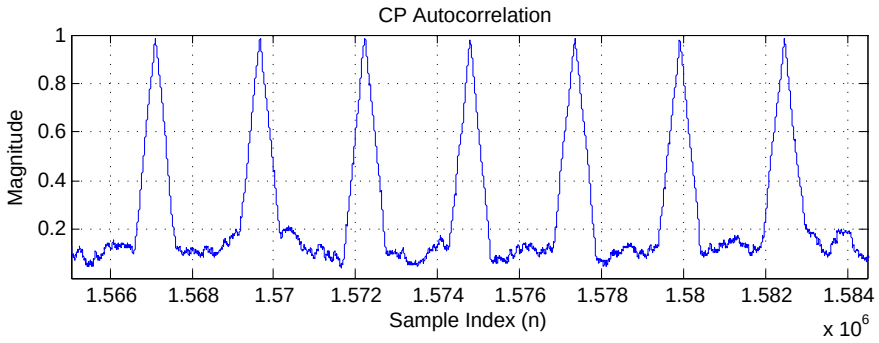

Figure 27: Auto-correlation output of the DVB-T signal

the position of the scattered pilots are repeated after four OFDM symbols. By performing four correlations with the received symbol for the possible for scattered pilot positions and comparing the resulting magnitude, the positions of the scattered pilot in a given OFDM symbol can be determined.

5.2.2 FFO Estimation and compensation in DVB-T

Investigating the phase of the auto-correlation that we have discussed in the previous section, we can see that the phases are nearly constant at the CP samples (as indicated by the vertical lines which indicate the last CP samples in the OFDM symbols in Figure 28 below). This constant phase represents the phase introduced due to fractional frequency offset. A moving average filter was used over the phases at the CP samples to estimate the phase due to FFO. The phase of the auto-correlation of the received signal after it was de-rotated by the estimated phase is depicted in Figure 29 below. Figure 30 below shows the error magnitude of the

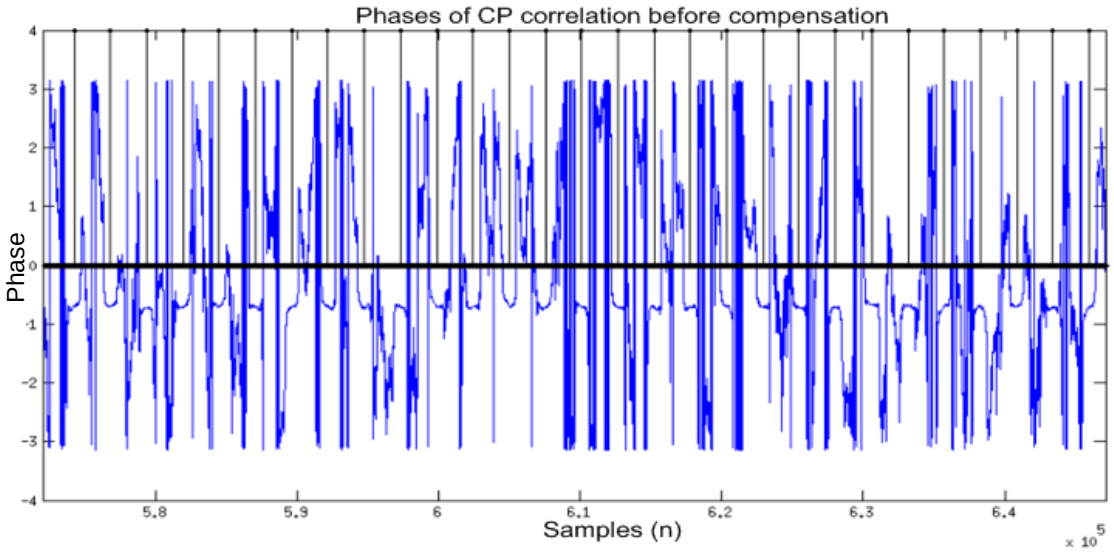

Figure 28: The phase of the auto-correlation output the DVB-T signal

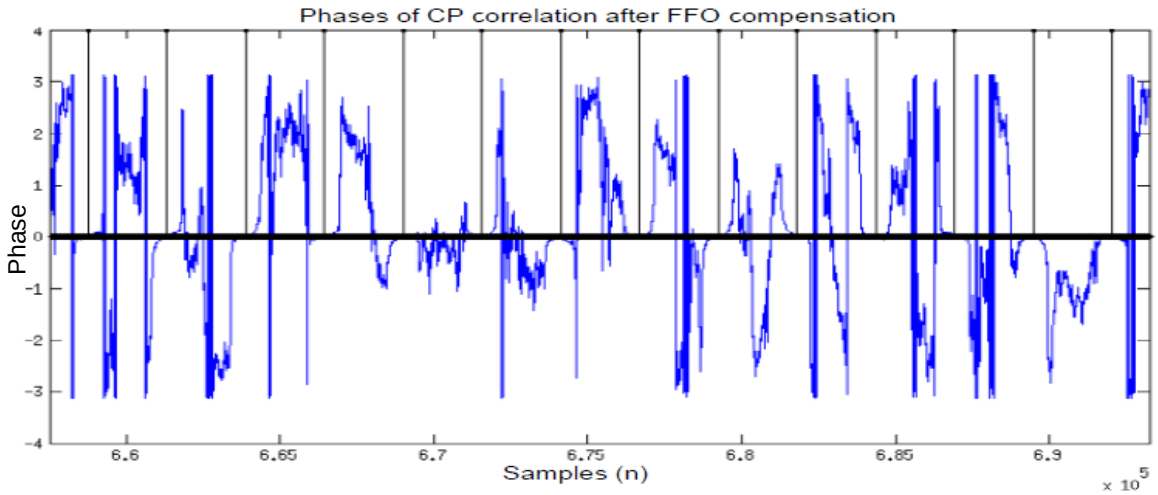

Figure 29: Phase of the auto-correlation output after phase correction

constellation points versus SNR with ML FFO compensation and without any FFO compensation at relative $FFO = 0.4$. In comparison with the LTE system discussed in the previous section, the relative FFO is increased in the DVB-T system for the same device frequency offset. This is due to the difference in carrier spacing of the two systems. As a result, the performance lose due to FFO is slightly greater in error magnitude plot in Figure 30 than in Figure 25.

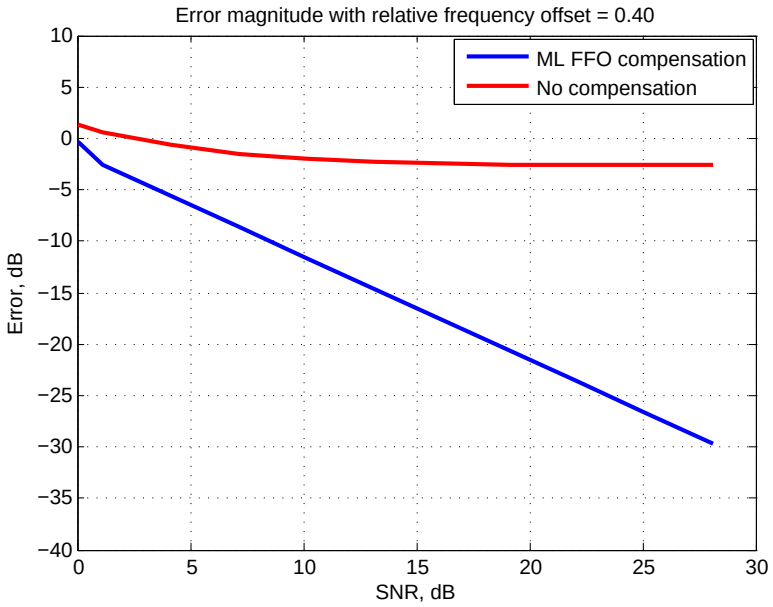

Figure 30: Error magnitude due to FO in DVB-T system

5.2.3 Channel Estimation and equalization

The scattered pilots are used to estimate the channel and the phase introduced by the sampling time offset between the transmitter and the receiver. This phase increases linearly across the sub-carriers as shown in Figure 31 below and results in circular rotation of the constellation points. The phases at the pilot positions were estimated from the pilots and Linear interpolation was performed to calculate the phase rotations at the payload symbols.

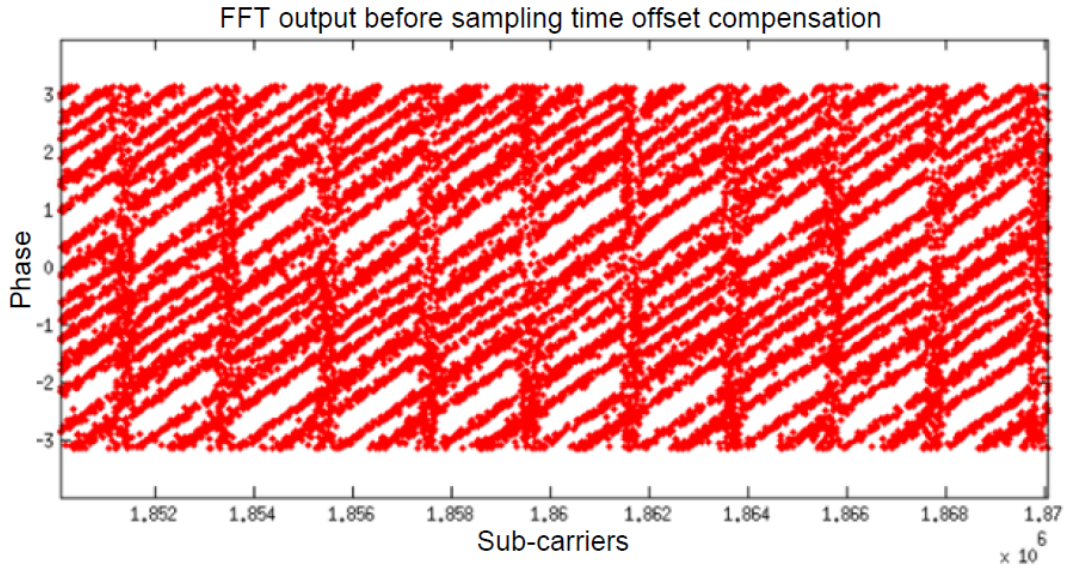

Figure 31: Phase due to sampling offset plotted against sub-carriers

To correct the phase distortion, the constellation symbols are de-rotated by the estimated phases. After equalization of the received signal by the reciprocal of the AWGN channel, the 16 QAM constellation diagram of the received signal at 20dB SNR looks as shown in Figure 32 below.

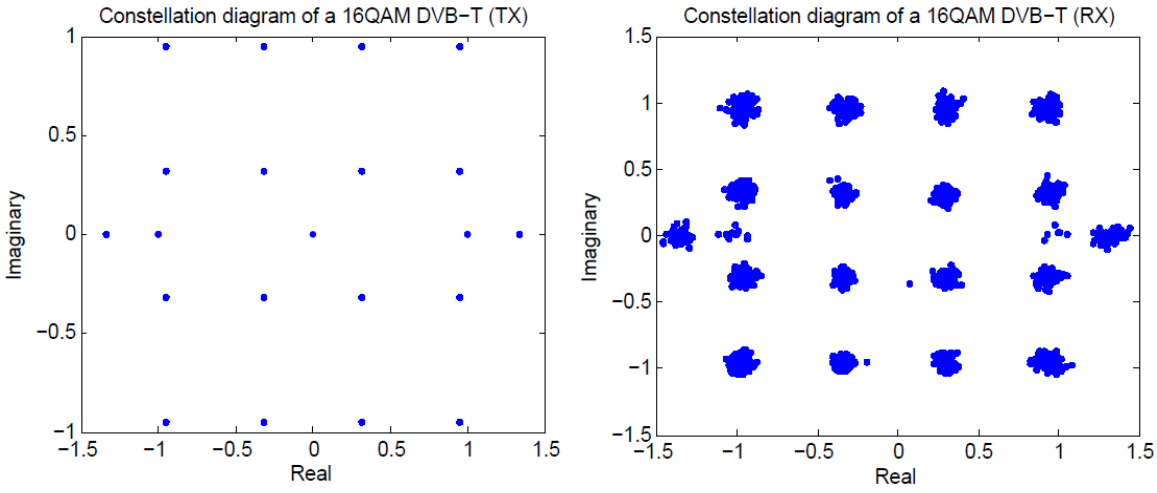

Figure 32: 16QAM constellation symbols of a DVB-T signal after equalization

5.3 Synchronization in Cognitive Overlay systems

In this section an example of synchronization in cognitive overlay networks will be discussed with the help of Matlab simulations using a DVB-T signal as a primary and an OFDM as a secondary. The secondary signal is suppressed at frequencies that carry the primary pilots so that the secondary signal will not be canceled out during primary equalization. The simulation runs for 10, 12, 14 and ∞ dB power ratios between the primary and the secondary transmitters. To protect the QoS of the primary system the power of the transmitter is split into αP_{sec} and (1 - α)P_{sec} where P_{sec} is the power of the secondary transmitter. The power αP_{sec} is used to transmit the desired secondary signal and (1 - α)P_{sec} is used to relay the primary signal. The primary codeword is assumed to be known at the secondary transmitter for relaying and simulations were performed for different delays between the primary and the secondary transmitters.

5.3.1 Simulation Results for Time Synchronization between Primary and Secondary Transmission

The receiver considers the primary signal and its overlayed delayed version as multi-path signals with delay τ. The phase response of the multi-path channel at $\tau = 10$ samples was estimated using the scattered pilots in the DVB-T signal and interpolated for payload sub-carriers. The resulting phase is depicted as shown in Figure 33. The phase response is used to correct the phase distortion introduced due to

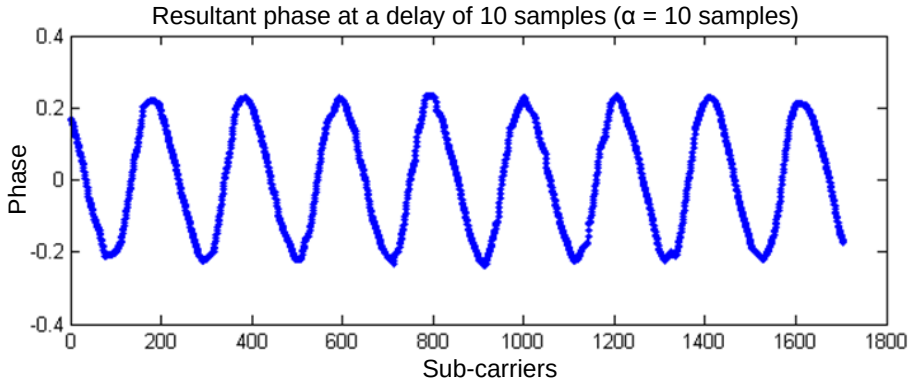

Figure 33: Phase response of the relayed overlay channel

the delay.

5.3.2 Simulation Results for Frequency Offset Correction in Overlay Transmission

When estimating the frequency offset in the primary system, we can assume the secondary as a deterministic noise and the relay signal as a multi-path component. The delay between the paths can be corrected if it is not greater than the duration of the cyclic prefix. It is also evident that the mean and variance of the frequency

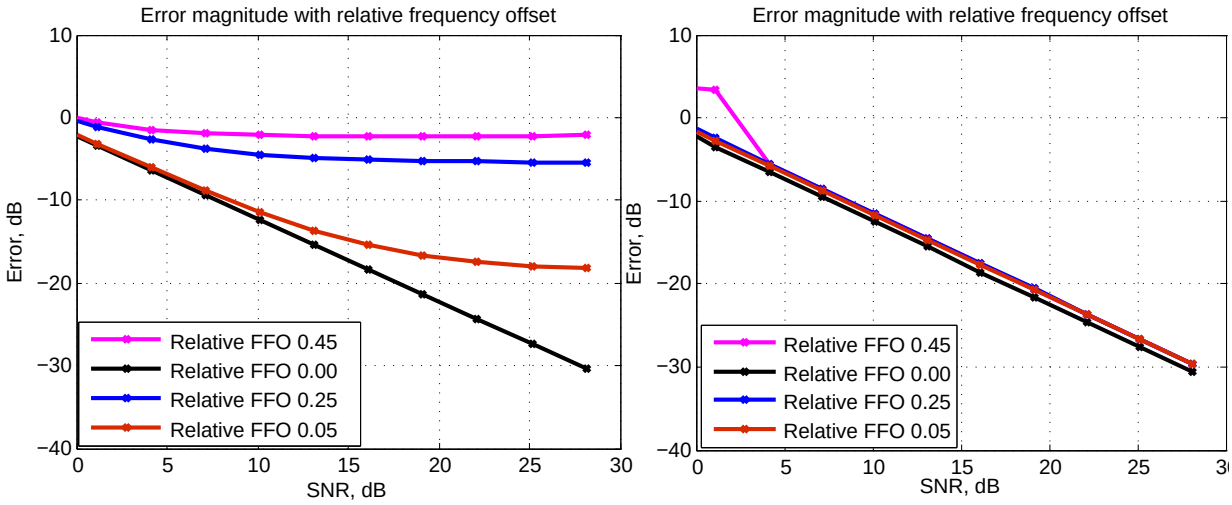

Figure 34: Error Magnitude versus SNR for various relative FFOs before (left) and after FFO compensation

offset estimate do not depend on the received frequency coefficients, hence the FFO estimation algorithm [34] used in the previous sections can also be applied here. Simulation results of the performance measures at the primary receiver are presented in Figure 34 as an example. By simulation we can show the difference between the estimated frequency offset and the actual frequency offset at a given SNR value. Figure 35 below shows the estimated FFO ploted against the actual FFO at SNR values of 3 dB and 15 dB.

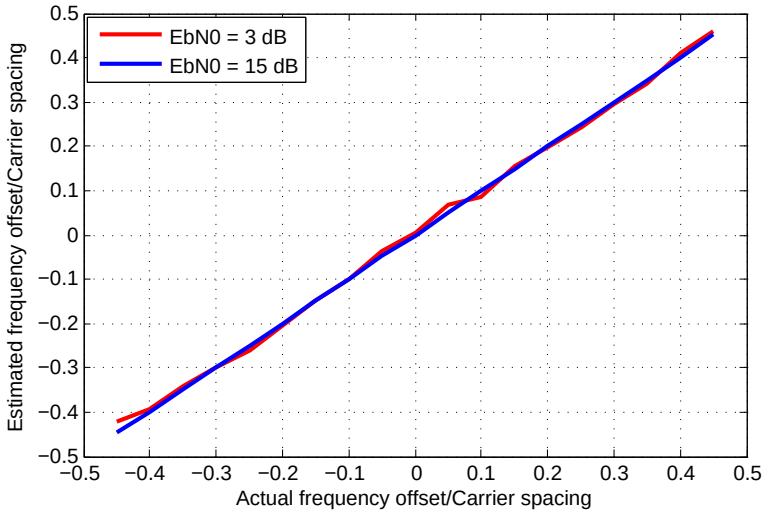

Figure 35: Relative frequency offset estimate versus Relative frequency offset

The combined primary-secondary QPSK constellation points at the receivers before and after phase correction is given in Figure 36 shown below.

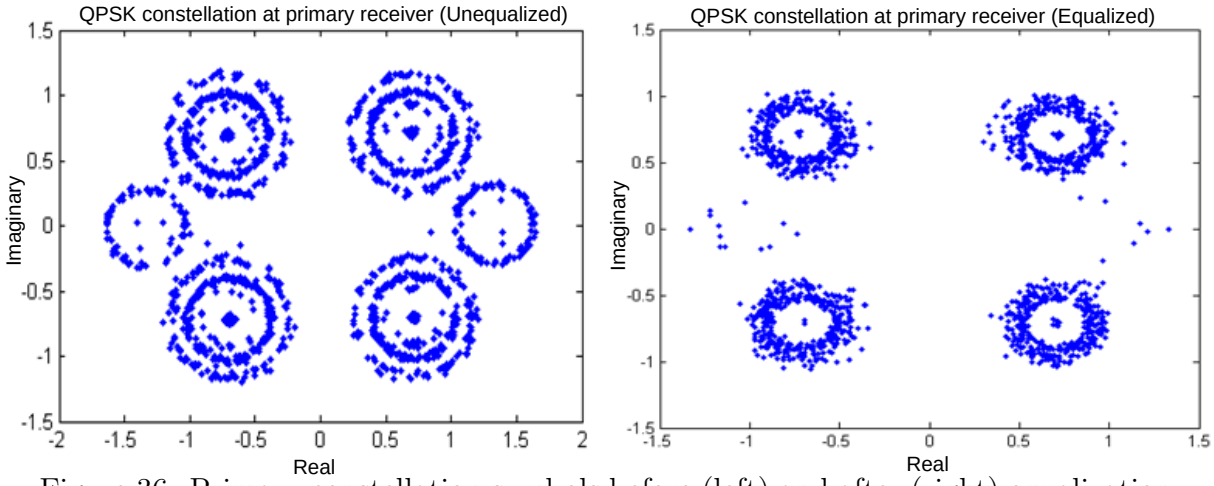

Figure 36: Primary constellation symbols before (left) and after (right) equalization

As discussed in section 4.4, there are three types of pilots in the primary (DVB-T): Continual, Scattered, and TPS pilots. Since we used the continual and scattered pilots for channel estimation and equalization purposes, the secondary signal at these pilot positions have been suppressed. On the other hand, because the TPS pilots has not been used for any purpose in this simulation, secondary transmission has been allowed on top of the TPS pilots. Figure 36 (right) shows rotation of these pilots after equalization. At the secondary receiver, the equalized combined signal was quantized and modulated before subtracted form the un-quantized signal. The resulting residual signal, which is the secondary OFDM, was rotated by a certain phase. This phase can be estimated by the help of the pilots in the OFDM signal and used to correct the phase distortion caused by the rotation due to timing offset. Figure 37 below shows the before and after equalization plots of the secondary signal at the respective receiver.

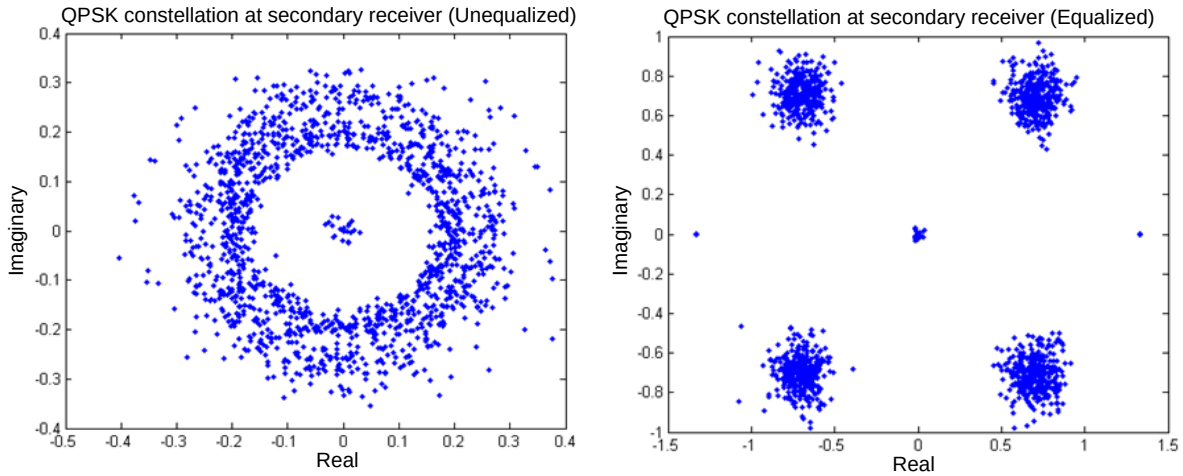

Figure 37: Secondary constellation symbols before (left) and after (right) equalization)

Bit error rate (BER) curves for the primary and secondary signals for various delay, primary-to-secondary (P_{pr}/P_{sec}) ratio values and modulation types are shown in the simulation plots discussed below. The simulation assumes a AWGN channel. The X-axis of the plots represents SNIR with respect to the primary signal (blue curve) and SNR with respect to the secondary signal (Red curves). The secondary power splitting ratio has been calculated automatically as in [43] taking the cognitive radio channel coefficients as one. The noise has been calculated from a given primary SNR and the primary transmission power. Based on the noise value, the primary power and the secondary power, alpha can be adjusted in such a way to mitigate the effect of the interference caused by the secondary signal at the primary receiver. After the optimal α is found, the noise at the secondary can be calculated from the desired secondary signal, αP_{sec}, for a given SNR value at the secondary receiver.

Figure 38 below shows the BER curves of the primary and the secondary signals

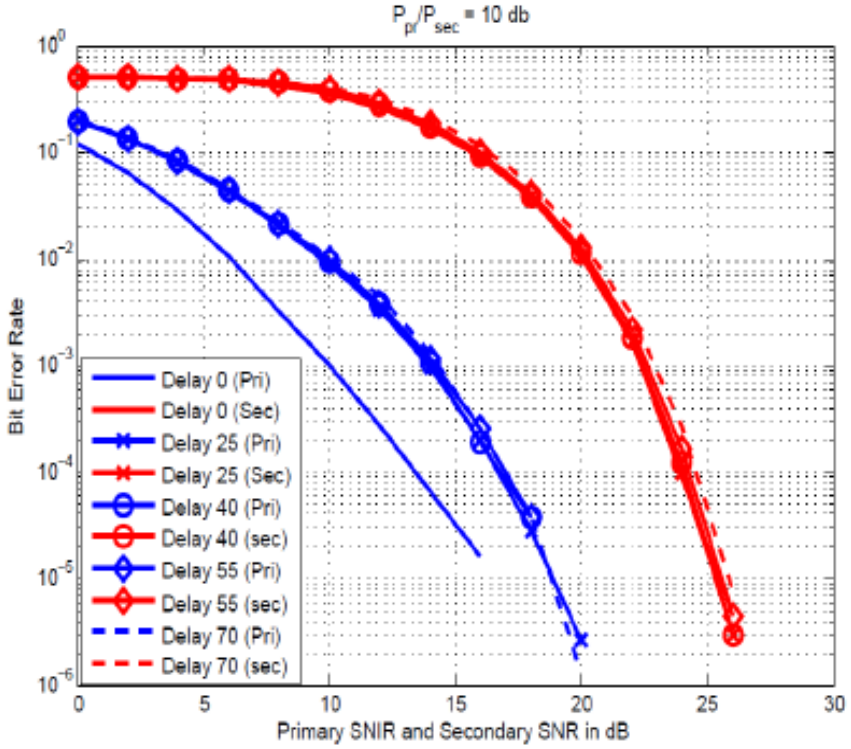

Figure 38: Primary (QPSK) and secondary (QPSK) BER curves for varying delay values

for primary-secondary transmission power ratio of 10 dB. The modulation type used in this case is QPSK for both the primary and the secondary. From the figure we observe SNIR loss of 4 dB for power ratio of 10 dB between the primary and the secondary transmitters. This loss in SNIR resulted from the delay introduced between the primary and the secondary systems. This can be explained by the fact that α calculation for achievable rates assumes coherent combining of the primary and the relaying signals [43]. However, when there is delay between the primary

and the secondary transmission, the relaying and the primary signals add up non-coherently hence a weaker combined signal. As a result the portion of the secondary transmission power used for relaying the primary message does not compensate all the interference from the secondary transmitter.

In ideal conditions, given α we can determine the relaying power of the secondary transmitter required to maintain the target SNR at the primary receiver. However, due to non-Gaussian nature of the interference, we observe SNIR loss as we increase the signal power of the secondary message.

6 Conclusion and future work

This master's thesis has investigated, studied and simulated the synchronization issues in cognitive radio spectrum sharing by taking the *overlay* approach as an example. The research covers an analysis of the effects of channel, hardware non-idealities and timing offset on the received primary and secondary signals independently using a laboratory TX-RX setup. For the secondary system which is an LTE down-link signal, cell search and synchronization algorithms have been implemented and tested by transmitting LTE frames over the air under AWGN channel conditions. In the process, we have shown the properties of Zadoff-Chu sequences whose correlation properties make it an excellent choice for the primary synchronization signal. We also demonstrated the issues of timing and frequency synchronization and also channel estimation under scenarios similar to actual networks.

Similarly for the primary system which is a DVB-T signal, we have observed the effects of the actual channel and the transmitting and receiving hardwares (USRP N200) on the received signal. We have implemented time and frequency synchronization algorithms to correct these effects. By investigating the primary and the secondary systems independently the thesis highlights the importance of timing and frequency synchronization for successful demodulation of received data in the respective systems. The other aspect of the thesis has dealt with the synchronization issues between the primary and the secondary transmitters in the overlay spectrum sharing scheme. Using a Matlab simulation, we have observed the effects of different time offsets between the transmitters on the performance of the primary and the secondary systems. The thesis also investigated the effect of relaying. By splitting the secondary transmission power into two parts by a ratio α, the secondary transmitter can relay the primary transmission while transmitting its own message. We have observed the effect of various α values on the performance of the primary and the secondary systems.

References

[1] ITU. Estimated spectrum bandwidth requirements for the future development of IMT-2000 and IMT-Advanced, ITU-R Report M.2078, 2006.

[2] Federal Communications Commission Spectrum Policy Task Force. Report of the Spectrum Efficiency Working Group. November, 2002.

[3] Shared Spectrum Company. Comprehensive Spectrum occupancy measurements over six different locations. August, 2005.

[4] A. Goldsmith, et al. "Breaking Spectrum Gridlock with Cognitive Radios: An Information Theoretic Perspective" *Proceedings of the IEEE*, Vol. 97, No.5, pp. 894-914, May 2009.

[5] E. Cetin, I. Kale, and R.C.S. Morling. "Living and dealing with RF impairments in communication transceivers." *In Proc. IEEE International Symposium on Circuits and systems (ISCAS), New Orleans, LA*, May, 2007, pp. 21-24

[6] G. Fettweis, et al. "Dirty RF: A new paradigm." *In Proc. IEEE Personal, Indoor and Mobile Radio Communications (PIMRC), Berlin, Germany*, September, 2005.

[7] C.J. Kuo, M. Morelli and M. Pun. *Multi-Carrier Techniques for Broadband Wireless Communications: A Signal Processing Perspective.*, London, Covent Garden, 2007.

[8] 3GPP, *Technical Specification Group Radio Access Network; Spatial channel model for Multiple Input Multiple Output (MIMO) simulations (Release 6)* , 2003.

[9] T.S. Rappaport. *Wireless Communications: Principles & Practice*, Prentice-Hall, Inc., Upper Saddle River, NJ, 2002.

[10] B.H. Fleury. "An Uncertainty Relation for WSS Processes and Its Application to WSSUS." *IEEE Transactions On Communications*, Vol. 14, N0. 12, December, 1996.

[11] 3GPP. Technical Specification Group Radio Access Network; Evolved Universal Terrestrial Radio Access (E-UTRA); Physical Channels and Modulation (Release 8), May, 2008.

[12] ETSI. 102 831 V1.1.1 DVB-T2 Document A133: Implementation guidelines for a second generation digital terrestrial television broadcasting system (DVB-T2) (draft TR), June, 2010.

[13] S. Haykin. *Adaptive Filter Theory*. Prentice-Hall, Inc., Upper Saddle River, NJ, USA, 1995.

[14] J. Mitola. "Software Radios-survey, Critical Evaluation and Future Directions." *IEEE National Telesystems Conference*, May, 1992.

[15] IEEE-USA Board of Directors. Improving Spectrum Usage Through Cognitive Radio Technology. November, 2003.

[16] J. Mitola. "Cognitive Radio for Flexible Mobile Multimedia Communications." *IEEE Mobile Multimedia Conference*, pp. 3-10, 1999.

[17] H. Takagi, B. Walke. *Spectrum Requirement Planning in Wireless Communications: Model and Methodology for IMT-Advanced*, John Wiley & Sons, Inc., New York, NY, USA, 2008.

[18] Z. Wu and B. Natarajan. "Interference Tolerant Agile Cognitive Radio: *Maximize Channel Capacity of Cognitive Radio*" *Communications and Networking Conference*, pp. 1027-1031, January, 2007.

[19] H. Sato. "Two user communication channels" *IEEE Transactions on Information Theory*, Vol. 23, pp. 295-304, May, 1977.

[20] A. B. Carleial. "Interference channels" *IEEE Transactions on Information Theory*, vol. 24, pp. 60-70, January, 1978.

[21] M. H. M. Costa and A. E. Gamal. "The capacity region of the discrete memoryless interference channel with strong interference" *IEEE Transactions on Information Theory*, Vol. 33, pp. 710-711, May, 1977.

[22] T. Han and K. Kobayashi. "A new achievable rate region for the interference channel" *IEEE Transactions on Information Theory*, Vol. 27, pp. 49-60, January, 1981.

[23] 3GPP. Technical specification group radio access network; (E-UTRA) and (E-UTRAN); overall description; stage 2, May, 2008.

[24] D. Toumpakaris, J. Lee, and H. Lou. "Estimation of integer carrier frequency offset in OFDM systems based on the maximum likelihood principle" *IEEE Transactions on Broadcasting*, Vol. 55, No.1, pp.95-108, March 2009.

[25] ETSI. ETSI EN 300 744: Digital Video Broadcasting (DVB); Framing structure, channel coding and modulation for digital terrestrial television (DVB-T), December 2010.

[26] P. Kolodzy, et.al. "Next generation communications: *Kickoff meeting*" *in Proc. DARPA*, October, 2001.

[27] R. Matheson. "The electrospace model as a frequency management tool" *Int. Symposium On Advanced Radio Technologies*, Boulder, Colorado, USA, Mar. 2003, pp. 126-132.

[28] A. L. Drozd, I. P. Kasperovich, C. E. Carroll, and A. C. Blackburn. "Computational electromagnetics applied to analyzing the efficient utilization of the RF transmission hyperspace" *in Proc. IEEE/ACES Int. Conf. on Wireless Communications and Applied Computational Electromagnetics*, Honolulu, Hawaii, USA, Apr. 2005, pp. 1077-1085

[29] Thomas C. Jepsen, *Distributed Storage Networks: Architecture, Protocols and Management*, John Wiley and Sons Ltd, 2003.

[30] ECC. Report 159: Technical and Operational Requirements for the Possible Operation of Cognitive Radio Systems in the 'White Spaces' of the Frequency Band 470-790 MHz, Sept. 2010.

[31] Ofcom consultation. "Implementing Geo-location", Nov. 2010, <`http://stakeholders.ofcom.org.uk/binaries/consultations/geolocation/summary/geolocation.pdf`>

[32] M. Nekovee. "A Survey of Cognitive Radio Access to TV White Spaces" *International Journal of Digital Multimedia Broadcasting*, Volume 2010. <`http://www.quasarspectrum.eu/images/stories/Documents/publications/Nekovee_journal2010.pdf`>

[33] T. M. Schmidl and D. C. Cox. "Robust Frequency and Timing Synchronization for OFDM." *IEEE Transactions On Communications*, Vol. 45, No. 12, pp.1613-1621, Dec. 1997.

[34] J. van de Beek, M. Sandell and P. O. Börjesson. "ML Estimation of Time and Frequency Offset in OFDM Systems." *IEEE Transactions On Signal Processing*, Vol. 45, No. 7, pp.1800-1805, Jul. 1997.

[35] H. Nogami and T. Nagashima. "A Frequency and Timing Period Acquisition Technique for OFDM Systems." *Personal, Indoor and Mobile Radio Commun.(PIRMC)*, pp. 1010-1015, Sept. 1995.

[36] P. H. Moose. "A Technique for Orthogonal Frequency Division Multiplexing Frequency Offset Correction." *IEEE Transactions On Communications*, Vol. 42, No. 10, Oct. 1994.

[37] J. Sachs, et.al. "A Cognitive Cellular Systems Within the TV Spectrum." *Cognitive Wireless Systems (UKIWCWS), 2009 First UK-India International Workshop on*, pp. 1-12, Apr. 2010.

[38] F. A. Khan, et.al. "Outage Analysis of Causal Cognitive Radio Channel." *IEEE Symposium on New Frontiers in Dynamic Spectrum*, Vol., No., pp.1-6, 10-12 Dec. 2009.

[39] G. Kramer. "Outer bounds on the capacity of Gaussian interference channels" *IEEE Transactions on Information Theory*, Vol. 50, No. 3, pp. 581-586, March 2004.

[40] G. Kramer. "Review of rate regions for interference channels" *in Proc. 2006 Int. Zurich Seminar on Communications, Zurich, Switzerland*, pp. 162-165, Feb. 2006.

[41] R. Etkin, D. Tse, and H. Wang. "Gaussian interference channel capacity to within one bit" *IEEE Transactions on Information Theory*, vol.54, No.12, pp.5534-5562, Dec. 2008.

[42] X. Shang, G. Kramer, and B. Chen. "A New Outer Bound and the Noisy-Interference Sum-Rate Capacity for Gaussian Interference Channels" *IEEE Transactions on Information Theory*, vol.55, No.2, pp. 689-699, Feb. 2009.

[43] J. Alexander, V. Pramod. "Cognitive Radio: An information-theoretic perspective" *IEEE Transactions on Information Theory*, Vol. 55, No. 9, pp. 3945-3958, Sept. 2009.

Appendices

A Sample Matlab Code for Overlay Synchronization

```
%-------------------------------------------------
% Define Parameters
%-------------------------------------------------
close all; clear all; clc;
[s1,s2] = RandStream.create('mrg32k3a','NumStreams',2);
fftLen = 2048;
cpLen = 512;
% Modulation order
modOrderPri = 4;
modOrderSec = 4;
continual_pilots = ...
       [ 0 48 54 87 141 156 192 201 255 279 282 333 ...
432 450 483 525 531 618 636 714 759 765 780 804 873 888...
918 939 942 969 984 1050 1101 1107 1110 1137 1140 1146...
1206 1269 1323 1377 1491 1683 1704]';
tps_set= [34 50 209 346 413 569 595 688 790 901 ...
       1073 1219 1262 1286 1469 1594 1687]';
pilots_secondary = [1:12:889 902 913:12:1704]'; % pilots in secondary signal
used_carriers = 1705;
used_carriers1 = 1705;
payload_carriers = 1512;
payload_carriers1 = 1371;
cplBoost = 4/3;
tpsBoost = 1;
nSymTx = 50;
pratio = 1/3; % secondary to primary ratio
alpha = [1 0.75 0.5 0.25 0]; % secondary splitting ratio
delay = [0 10 20,30]; %delay between primary and secondary % TXs
SNR = [0:2:36];
%-------------------------------------------------
% Create the the primary ( DVB-T)
%-------------------------------------------------
leftPad = ceil((fftLen-used_carriers)/2);
rightPad_start_pri = used_carriers + leftPad + 1;
payloadEnd = used_carriers + leftPad;
iniSeq = uint16( bin2dec('11111111111'));
g = [11, 2, 0];
wk = zeros(used_carriers,1);
for k = 1:length(wk)
    Bit = bitand(sum(bitget(iniSeq, g(2:end)+1 )), 1);
    wk(k) = bitand(iniSeq, 1);
    iniSeq = bitshift(iniSeq, -1);
    iniSeq = bitset(iniSeq, g(1), Bit);
end
h1 = modem.qammod(modOrderPri);
normFactorPri = ... (sum(abs(h1.Constellation).^2)/modOrderPri).^(-0.5);
priUsed = randi(s1,[0,modOrderPri-1],used_carriers,nSymTx);
priSymbolUsed = normFactorPri*qammod(priUsed, modOrderPri);
payload_datapri = zeros(payload_carriers, nSymTx);
pilot_set = zero(176,nSymTx);
payload_inxpri = zero(payload_carriers,nSymTx);
for sym_count = 0:nSymTx-1
    Kmin=0;
    pilot_set(:,sym_count+1) = union (continual_pilots, ...
                    Kmin + 3*rem(sym_count,4) + ...
                           12*(0:(used_carriers-12)/12));
```

```
    % Insert pilots and TPS and remember payload index
    v=1; % current input payload carrier index
    pilot=1; % current pilot index in pilot_set
    tps=1; % current tps index in tps_set
    for u = 1:used_carriers
        p = 1+pilot_set(pilot,sym_count+1);%get next pilot
        if tps <= length(tps_set) % get next tps
           t = 1+tps_set(tps);
        else
           t = 0;
        end
        if u == p % it's a pilot signal
           priSymbolUsed(u,sym_count+1)=cplBoost*2*(0.5...
                                          - wk(u) );
           pilot = pilot + 1;
        elseif u == t; % it's a TPS signal
               priSymbolUsed(u,sym_count+1) = ... tpsBoost*2*(0.5 - wk(u) );
               tps = tps + 1;
        else % it's a payload carrier
                payload_datapri(v,sym_count+1) =...
                                priSymbolUsed(u,sym_count+1);
                payload_inxpri(v,sym_count+1) = u;
                v = v + 1;
        end
    end
end
priSymbol =[zeros(leftPad,nSymTx);priSymbolUsed; ...
                        zeros(fftLen-payloadEnd,nSymTx)];

%-------------------------------------------------
% Create secondary OFDM
%-------------------------------------------------
cPilotsSec = cplBoost*2*(0.5 - wk(pilots_secondary+1) );
h2 = modem.qammod(modOrderSec);
normFactorSec = (sum(abs(h2.Constellation).^ ...
                    2)/modOrderSec).^(-0.5);
secMessage = randi(s2,[0,modOrderSec-1], fftLen, nSymTx);
secSymbol = normFactorSec*modulate(h2, secMessage);
% pad zeros
leftPad1 = ceil((fftLen-used_carriers1)/2);
rightPad_start_sec = used_carriers1 + leftPad1 + 1;
secSymbol(1:leftPad1,:) = 0; secSymbol(rightPad_start_sec:end,:) = 0;
secSymbol(leftPad1 + pilots_secondary + 1,:) = ...
                            repmat(cPilotsSec,1,nSymTx);
tps_mod = tps_set;
secSymbol(leftPad + tps_mod + 1,:) = 0;
secMessage(leftPad + tps_mod + 1,:) = -1;
for cnt = 1:nSymTx
    secSymbol(leftPad + pilot_set(:,cnt) + 1,cnt) = 0;
    secMessage(leftPad + pilot_set(:,cnt) + 1,cnt) = -1;
end
secMessage(leftPad1+pilots_secondary+1,:) = -1;
secMessage = secMessage(leftPad1+1:rightPad_start_sec-1,:);
secMessage(secMessage < 0) = [];
secMessage = buffer(secMessage,payload_carriers1);
for dd = 1:length(delay)
    figure('color','white')
    for ff = 1:5
```

```
Comb_symbol =(sqrt(1-alpha(ff)))*pratio*priSymbol+ ...
             (sqrt(alpha(ff)))*pratio*secSymbol;
Comb_symbol_noise = Comb_symbol;
midPoint = fftLen/2;
comb_ifftOut = ifft(circshift(Comb_symbol_noise,midPoint));
overlay_cpadded = [ comb_ifftOut(fftLen-cpLen+1:fftLen,:); comb_ifftOut];
Orig_ifftOut = ifft(circshift(priSymbol,midpoint));
Orig_cpadded =[Orig_ifftOut(fftLen-cpLen+1:fftLen,:);Orig_ifftOut];
comb_tx = [zeros(delay(dd),nSymTx);overlay_cpadded(1:end-delay(dd),:)] +...
           Orig_cpadded(:,1:nSymTx);
for snr_inx = 1:length(SNR)
 % Add noise to the symbol
 comb_tx_noise = comb_tx(:);
 comb_tx_noise =awgn(comb_tx_noise ...
                      ,SNR(snr_inx) - db(std(comb_tx_noise)));
 %-------------------------------------------------------------------------
 % Peak detection and synchronization ( Primary + Secondary )
 %-------------------------------------------------------------------------
 rhoinx = 10.0^(SNR(snr_inx)/10.0);
 rho = rhoinx / (rhoinx + 1.0);
 delayed_tx = [zeros(1,fftLen)';comb_tx_noise(1:end-fftLen)];
 magsqrd_tx = abs(comb_tx_noise).^2;
 magsqrd_delayed_tx = abs(delayed_tx).^2;
 adder_tx = magsqrd_tx + magsqrd_delayed_tx;
 delayed_conj_tx = conj(delayed_tx); % Delayed copy
 mixer_tx = comb_tx_noise.*delayed_conj_tx;
 correlation_tx = filter(ones(1,cpLen),1,mixer_tx); % Moving average filter
 corrMag_tx = abs(correlation_tx);
 CorrAngle_tx = angle(correlation_tx);
 power_tx = filter(rho/2*ones(1, cpLen),1, adder_tx);
 normCorr_tx = corrMag_tx./power_tx;
 [PeakCorr_tx,averages] = doPeakDetection(normCorr_tx);
 %-----------------------------------------------------------------
 % Sample and hold DVBT
 %-----------------------------------------------------------------
 sampledAndHold = zeros(size(CorrAngle_tx));
 indices  = 1:length(CorrAngle_tx);
 locations = indices(PeakCorr_tx == 1);
 for k = 1:(length(locations)-1)
     locations(k+1) = locations(k) + ( cpLen + fftLen);
 end
 PeakCorr_tx(:,1) = 0;
 PeakCorr_tx(locations,1) = 1;
 for idx = 1:(length(locations)-1)
     start_ = locations(idx);
     end_ = locations(idx+1) - 1;
     sampledAndHold(start_:end_) = CorrAngle_tx(start_);
 end
 sampledAndHold(end_+1:end) = CorrAngle_tx(end_+1);
 %-----------------------------------------------------------------
 % Freq offset correction DVBT
 %-----------------------------------------------------------------
 sensitivity = -1/fftLen;
 phase_ = zeros(size(sampledAndHold));
 for i = 1:length(sampledAndHold)
     phase_(i+1) = phase_(i) + sampledAndHold(i);
 end
 nco = cos(sensitivity*phase_(2:end)) + 1j*sin(sensitivity*phase_(2:end));
```

```
 freqCorrected = nco.*comb_tx_noise;
 delayed_comp = [zeros(1,fftLen)';freqCorrected(1:end-fftLen)];
 delayed_conj_comp = conj(delayed_comp); % Delayed copy
 mixer_comp = freqCorrected.*delayed_conj_comp;
 correlation_comp = filter(ones(1,cpLen),1,mixer_comp);% Moving average
 CorrAngle_comp = angle(correlation_comp);

 %-------------------------------------------------------------------------
 % Sampling DVBT
 %-------------------------------------------------------------------------
 peak_inx_ = find(PeakCorr_tx == 1);
 rcvd_samples = length(peak_inx_)*fftLen;
 d_time_sync = zeros(rcvd_samples,1);
 jj = 1;
 for ii = 1:length(peak_inx_)
     d_time_sync(jj:jj+fftLen-1) = freqCorrected((peak_inx_(ii)- ...
                fftLen+1):peak_inx_(ii) - 0);
     jj = jj + fftLen;
 end

%-------------------------------------------------------------------------
% FFT DVBT
%-------------------------------------------------------------------------
sampled = reshape(d_time_sync,fftLen,length(peak_inx_));
midPoint = round(fftLen/2);
fftOutComb = circshift( fft(sampled), midPoint);
pilot_len = size(pilot_set,1);
[fftOutComb,carrier_angle,carrier_mag,nSym] = ...
               Equalize(fftOutComb,used_carriers,leftPad,...
               pilot_set,priSymbol,rightPad_start_pri,pilot_len);
figure('color','w')
plot(fftOutComb(leftPad+1:rightPad_start_pri-1,10),'.');
title('QPSK constellations at primary receiver for relayed ...
                     overlay(equalized)');
xlabel('Real');
ylabel('Imaginary');

%-------------------------------------------------------------------------
% Primary receiver
%-------------------------------------------------------------------------
[fftOutCombMod,PriDemodMssg]= ...
                    MessageMoDem(fftOutComb,leftPad,used_carriers, ...
                          payload_carriers,continual_pilots,...
                               tps_set,normFactorPri,modOrderPri,...
                                wk,cplBoost,tpsBoost,rightPad_start_pri);
priDataDemapped = gray2bin(PriDemodMssg(:,1:nSym),'qam',modOrderPri);
rxDataBitsPri    = de2bi(priDataDemapped,'left-msb');
MssgDemod = qamdemod((1/normFactorPri)*payload_datapri,modOrderPri);
txDatadeMappedpri = gray2bin(MssgDemod(:,1:nSym),'qam',modOrderPri);
txDataBitsPri = de2bi(txDatadeMappedpri,'left-msb');
for tpri = 1:nSym
    [nErr ber(snr_inx,tpri)] = biterr(txDataBitsPri((tpri-1)* ...
                payload_carriers+1:tpri*payload_carriers), ...
                      rxDataBitsPri((tpri-1)* ...
                        payload_carriers+1:tpri*payload_carriers))
end
```

```
    %-------------------------------------------------------------------------
    % Secondary receiver
    %-------------------------------------------------------------------------
    ResidualData = fftOutComb - fftOutCombMod;
    ResidualData(leftPad+1:rightPad_start_pri-1,1:nSym) =  ...
     ResidualData(leftPad+1:rightPad_start_pri-1,1:nSym).*(carrier_mag);
    ResidualData(leftPad+1:rightPad_start_pri-1,1:nSym) = ...
     ResidualData(leftPad+1:rightPad_start_pri-1,1:nSym)./...
                        (cos(carrier_angle) - 1j*sin(carrier_angle));
    pilot_len_sec = length(pilots_secondary);
    [ResidualData,carrier_angle,carrier_mag,nSym] =  ...
                       secEqualize(ResidualData,used_carriers1,...
                           leftPad1, pilots_secondary,...
                             secSymbol,rightPad_start_sec,pilot_len_sec);

    figure('color','w')
    plot(ResidualData(leftPad+1:rightPad_start_pri-1,10),'.');
    title('QPSK at secondary receiver for relayed overlay(equalized)');
    xlabel('Real');
    ylabel('Imaginary');
    %-------------------------------------------------------------------------
    % Demodulation (Secondary)
    %-------------------------------------------------------------------------
    for cnt = 1:nSym
        ResidualData(leftPad + pilot_set(:,cnt) + 1,cnt) = 100;
    end
    ResidualData(leftPad + tps_set + 1,:) = 100;
    ResidualDataMesg = ResidualData(leftPad1+1:rightPad_start_sec-1,:);
    ResidualDataMesg(pilots_secondary + 1,:) = 100;
    ResidualDataMesg(ResidualDataMesg==100) = [];
    ResidualDataMesg = buffer(ResidualDataMesg,payload_carriers1);
    mesSym = size(ResidualDataMesg,2);
    ResidualDemod = qamdemod((1/normFactorSec)*ResidualDataMesg,modOrderSec);
    resDataMapped = gray2bin(ResidualDemod(:,1:mesSym-1),'qam',modOrderSec);
    resDataBits = de2bi(resDataMapped,'left-msb');
    txDatadeMappedsec = gray2bin(secMessage(:,1:mesSym-1),'qam',modOrderSec);
    txDataBitssec = de2bi(txDatadeMappedsec,'left-msb');
    for tsec = 1:nSym-1
         [nErrsec bersec(snr_inx,tsec)] = biterr(txDataBitssec((tsec-1)*...
           payload_carriers1+1:tsec*payload_carriers1),resDataBits((tsec-1)*...
                                payload_carriers1+1:tsec*payload_carriers1));
     end
end
%-------------------------------------------------------------------------
% BER plots for recived signal at the primary and secondary receivers
%-------------------------------------------------------------------------
if (ff == 1)
        semilogy(EbNo,mean(ber,2),'-b','MarkerSize',10,'LineWidth',2)
        hold on
        semilogy(EbNo,mean(bersec,2),'-r','MarkerSize',10,'LineWidth',2)
        grid on;
        xlabel('SNR in dB');
        ylabel('Bit Error Rate')
else if (ff == 2)
         semilogy(EbNo,mean(ber,2),'-bx','MarkerSize',10,'LineWidth',2)
         semilogy(EbNo,mean(bersec,2),'-rx','MarkerSize',10,'LineWidth',2)
else if (ff == 3)
         semilogy(EbNo,mean(ber,2),'-bo','MarkerSize',10,'LineWidth',2)
```

```
            semilogy(EbNo,mean(bersec,2),'-ro','MarkerSize',10,'LineWidth',2)
    else if (ff == 4)
            semilogy(EbNo,mean(ber,2),'-bd','MarkerSize',10,'LineWidth',2)
            semilogy(EbNo,mean(bersec,2),'-rd','MarkerSize',10,'LineWidth',2)
    else
            semilogy(EbNo,mean(ber,2),'--b','MarkerSize',10,'LineWidth',2)
            semilogy(EbNo,mean(bersec,2),'--r','MarkerSize',10,'LineWidth',2)
                end
            end
        end
    end
end

function [corrPeaks averages  ratios] = doPeakDetection(normCorr)

%-------------------------------------------------------------------------
% Peak detection
%-------------------------------------------------------------------------
corrPeaks = zeros(size(normCorr));
averages = zeros(size(normCorr));
ratios = zeros(size(normCorr));

peak_val = -Inf;
peak_ind = 0;
state = 0;
i = 1;
avg =-1;
avg_alpha = 0.000001;
threshold_factor_fall = 0.8;
threshold_factor_rise = 0.7;
normCorr_ = normCorr - 1;
while i <= length(normCorr_)

    if state == 0  % below threshold
          if normCorr_(i) > avg*threshold_factor_rise
                state = 1;
          else
                avg = (avg_alpha)*normCorr_(i) + (1-avg_alpha)*avg;
                averages(i) = avg;
                ratios(i) = normCorr_(i)/avg;
                i = i+1;
          end

    elseif state == 1   % above threshold, have not found peak
            if normCorr_(i) > peak_val
                peak_val = normCorr_(i);
                peak_ind = i;
                avg = (avg_alpha)*normCorr_(i) + (1-avg_alpha)*avg;
                averages(i) = avg;
                ratios(i) = normCorr_(i)/avg;
                i = i+1;
            else
                if normCorr_(i) > avg*threshold_factor_fall
                  avg = (avg_alpha)*normCorr_(i) + (1-avg_alpha)*avg;
                  averages(i) = avg;
                  ratios(i) = normCorr_(i)/avg;
                  i = i+1;
```

```
                else
                    corrPeaks(peak_ind) = 1;
                    state = 0;
                    peak_val = -Inf;
                end
            end
    end
end
function[fftOutMod,MssgDemod]=
MessageMoDem(fftData,LeftPad,used_carriers,payload_carriers,...
continual_pilots,tps_set,normFactor,modOrder,w,cpBoost,tpBoost,rightPad_star)
num_sym = size(fftData,2);
payload_data = zeros(payload_carriers, num_sym);
payload_inx = zeros(payload_carriers,num_sym);
fftOutUsed = fftData(LeftPad+1:rightPad_start-1,:);
for sym_count = 0:num_sym-1
    Kmin=0;
    pilot_set = union (continual_pilots, ...
                    Kmin + 3*rem(sym_count,4) + ...
            12*(0:(used_carriers-12)/12));
    % separate data from pilots and TPS
    v=1; % current input payload carrier index
    pilot=1; % current pilot index in pilot_set
    tps=1; % current tps index in tps_set
    for u = 1:used_carriers % for all output carriers
        p = 1+pilot_set(pilot); % get next pilot
        if tps <= length(tps_set) % get next tps
           t = 1+tps_set(tps);
        else
           t = 0;
        end
        if u == p % it's a pilot signal
           fftOutUsed(u,sym_count+1) = cpBoost*2*(0.5 - w(u) );
           pilot = pilot + 1;
        elseif u == t; % it's a TPS signal
             fftOutUsed(u,sym_count+1) = tpBoost*2*(0.5 - w(u) );
             tps = tps + 1;
            else % it's a payload carrier
              payload_data(v,sym_count+1) = fftOutUsed(u,sym_count+1);
              payload_inx(v,sym_count+1) = u;
              v = v + 1;
            end
        end
    end
MssgDemod = qamdemod((1/normFactor)*payload_data,modOrder);
MssgMod = normFactor*qammod(MssgDemod,modOrder);
fftOutMod = fftData;
for jj = 1:num_sym
    sym_payload_inx = payload_inx(:,jj);
    fftOutUsed(sym_payload_inx,jj) = MssgMod(:,jj);
end
fftOutMod(LeftPad+1:rightPad_start-1,:) = fftOutUsed;

% Primary Equalizer
function[fftOutComb,carrier_angle,carrier_mag,nSym] = ...
                Equalize(fftOutComb,used_carriers,leftPad, ...
                    pilot_set,txSymbol,right_pad_start,pilot_length)
```

```
%------------------------------------------------------------------------
% Equalization Primary
%------------------------------------------------------------------------
nSym = size(fftOutComb,2);
carrier_angle = zeros(used_carriers,nSym);
carrier_mag = zeros(used_carriers,nSym);
pilots_rx = zeros(pilot_length,nSym);
pilot_tx = zeros(pilot_length,nSym);
for cnt = 1:nSym
    pilots_rx(:,cnt) = fftOutComb(leftPad + pilot_set(:,cnt) + 1,cnt);
    pilot_tx(:,cnt) = txSymbol(leftPad + pilot_set(:,cnt) + 1,cnt);
    h = pilots_rx(:,cnt)./pilot_tx(:,cnt);
    pilot_mag = abs(h);
    pilot_angle = angle(h);
    for kk = 1:size(pilot_angle,1)-1
         denom = pilot_set(kk+1,cnt)-pilot_set(kk,cnt);
         tmp = pilot_angle(kk+1);
         for jj = 1:denom-1
             if (pilot_angle(kk+1) - pilot_angle(kk)) > pi
                 pilot_angle(kk+1) = pilot_angle(kk+1) - 2*pi;
             else if (pilot_angle(kk+1) - pilot_angle(kk)) < -pi
                     pilot_angle(kk+1) = pilot_angle(kk+1) + 2*pi;
                 end
             end
             carrier_angle(1+pilot_set(kk,cnt)+jj,cnt) = (1-(jj/denom)).*...
                           pilot_angle(kk) + (jj/denom).*pilot_angle(kk+1);
             carrier_mag(1+pilot_set(kk,cnt)+jj,cnt) = (1-(jj/denom)).*...
                            pilot_mag(kk) + (jj/denom).*pilot_mag(kk+1);
             if carrier_angle(1+pilot_set(kk,cnt)+jj,cnt) > pi
                carrier_angle(1+pilot_set(kk,cnt)+jj,cnt) = carrier_angle(1+...
                                          pilot_set(kk,cnt)+jj,cnt) - 2*pi;
             else if carrier_angle(1+pilot_set(kk,cnt)+jj,cnt) < -pi
                     carrier_angle(1+pilot_set(kk,cnt)+jj,cnt) = 2*pi + ...
                                  carrier_angle(1+pilot_set(kk,cnt)+jj,cnt);
                 end
             end
         end
         pilot_angle(kk+1) = tmp;
    end
    carrier_angle(1+pilot_set(:,cnt),cnt) = pilot_angle;
    carrier_mag(1+pilot_set(:,cnt),cnt) = pilot_mag;
end
fftOutComb(leftPad+1:right_pad_start-1,1:nSym) = fftOutComb(leftPad+...
                             1:right_pad_start-1,1:nSym).*...
                              (cos(carrier_angle) - 1j*sin(carrier_angle));
fftOutComb(leftPad+1:right_pad_start-1,1:nSym) = fftOutComb(leftPad+...
                                1:right_pad_start-1,1:nSym)./(carrier_mag);

%Secondary Equalizer
function[resData,carrier_angle,carrier_mag,nSym] = ...
                    secEqualize(resData,used_carriers,leftPad, pilot_set,...
                    txSymbol,right_pad_start,pilot_length)
%------------------------------------------------------------------------
% Equalization Secondary
%------------------------------------------------------------------------
nSym = size(resData,2);
carrier_angle = zeros(used_carriers,nSym);
carrier_mag = zeros(used_carriers,nSym);
```

```
pilots_rx = zeros(pilot_length,nSym);
pilot_tx = zeros(pilot_length,nSym);
for cnt = 1:nSym
    pilots_rx(:,cnt) = resData(leftPad + pilot_set + 1,cnt);
    pilot_tx(:,cnt) = txSymbol(leftPad + pilot_set + 1,cnt);
    h = pilots_rx(:,cnt)./pilot_tx(:,cnt);
    pilot_mag = abs(h);
    pilot_angle = angle(h);
    for kk = 1:size(pilot_angle,1)-1
         denom = pilot_set(kk+1)-pilot_set(kk);
         tmp = pilot_angle(kk+1);
         if (pilot_angle(kk+1) - pilot_angle(kk)) > pi
                 pilot_angle(kk+1) = pilot_angle(kk+1) - 2*pi;
         else if (pilot_angle(kk+1) - pilot_angle(kk)) < -pi
                     pilot_angle(kk+1) = pilot_angle(kk+1) + 2*pi;
              end
         end
         for jj = 1:denom-1
             carrier_angle(1+pilot_set(kk)+jj,cnt) = (1-(jj/denom)).*...
                    pilot_angle(kk) + (jj/denom).*pilot_angle(kk+1);
             carrier_mag(1+pilot_set(kk)+jj,cnt) = (1-(jj/denom)).*...
                         pilot_mag(kk) + (jj/denom).*pilot_mag(kk+1);
             if carrier_angle(1+pilot_set(kk)+jj,cnt) > pi
                carrier_angle(1+pilot_set(kk)+jj,cnt) = carrier_angle(1+ ...
                                                  pilot_set(kk)+jj,cnt) - 2*pi;
             else if carrier_angle(1+pilot_set(kk)+jj,cnt) < -pi
                     carrier_angle(1+pilot_set(kk)+jj,cnt) = 2*pi + ...
                                   carrier_angle(1+pilot_set(kk)+jj,cnt);
                 end
             end
         end
         pilot_angle(kk+1) = tmp;
    end
    carrier_angle(1+pilot_set,cnt) = pilot_angle;
    carrier_mag(1+pilot_set,cnt) = pilot_mag;
end
resData(leftPad+1:right_pad_start-1,1:nSym) = resData(leftPad+1:...
       right_pad_start-1,1:nSym).*(cos(carrier_angle) - 1j*sin(carrier_angle));
resData(leftPad+1:right_pad_start-1,1:nSym) = resData(leftPad+1:...
                             right_pad_start-1,1:nSym)./(carrier_mag);
```

B Sample Matlab Code for LTE cell search and Synchronization

```
%=====================================================
%   Cell search and synchronization in LTE
%=====================================================
% Initialize LTE Parameters
Main_LTE_params;
global LTE_params;
%-----------------------------------------------
% Primary sequence generation
%-----------------------------------------------
BSID = 1;
NID1 = floor(BSID/3);
NID2 = mod(BSID,3);

%% Primary synchronization signal
switch NID2
    case 0
        u = 25;
    case 1
        u = 29;
    case 2
        u = 34;
    otherwise
         error('invalid BSID Specification.');
end

Prim_seq_half = zeros(31,2);
for n=1:31
    Prim_Seq_half(n,1) = exp(-1i*pi*u*(n-1)*n/63);
    PrimSync_half(n,2) = exp(-1i*pi*u*(n+31)*(n+32)/63);
end

PriSeq = reshape(Prim_seq_half,62,[]);

% Primary synchronization signal mapping and used resource
elements per
% resource blocks
% Nrb is No of resource blocks, Nsc No of sub carriers per RB
and Ns is OFDM % symbols in a sub-frame

PriSeq_Mapping = false(Nrb*Nsc,Ns);
Sync_Used = zeros(Nrb,2);
```

```
k = zeros(62,1);
for n=1:62
    k(n)=n-32+Nrb*Nsc/2;
end
k = k+1;    % corrected to matlab indices (zero excluded)
PriSeq_Mapping(k,Ns/2)=1;
Sync_Used(ceil(k(1)/Nsc),1) = 2*(ceil(k(1)/Nsc)*Nsc-k(1)+1);
if(mod(k(end),Nsc) == 0)
    Sync_Used (ceil(k(1)/Nsc)+1:ceil(k(end)/Nsc),1) = 2*12;
else
    Sync_Used (ceil(k(1)/Nsc)+1:ceil(k(end)/Nsc)-1,1) = 2*12;
    Sync_Used (ceil(k(end)/Nsc),1) = 2*12- ...
        2*(ceil(k(end)/Nsc)*Nsc-k(end));
end

%% Secondary synchronization signal
qq = floor(NID1/30);
q = floor((NID1+qq*(qq+1)/2)/30);
m = NID1+q*(q+1)/2;
m0 = mod(m,31);
m1 = mod(m0+floor(m/31)+1, 31);

PN_gen = commsrc.pn('GenPoly',        [1 0 0 1 0 1], ...
                    'InitialStates', [1 0 0 0 0],   ...
                    'Shift',          0,    ...
                    'NumBitsOut',     31);
PN_seq_half = generate(PN_gen).';
PN_seq = 1-2*PN_seq_half;

SC_gen1 = commsrc.pn('GenPoly',        [1 0 1 0 0 1], ...
                    'InitialStates', [1 0 0 0 0],   ...
                    'Shift',          0,    ...
                    'NumBitsOut',     31);
SC_seq1_temp = generate(SC_gen1).';
SC_seq1 = 1-2*SC_seq1_temp;
SC_gen2 = commsrc.pn('GenPoly',        [1 1 0 1 1 1], ...
                    'InitialStates', [1 0 0 0 0],   ...
                    'Shift',          0,    ...
                    'NumBitsOut',     31);
SC_seq2_temp = generate(SC_gen2).';
SC_seq2 = 1-2*SC_seq2_temp;
```

```
SecSync = zeros(62,1);
for n=0:30
  switch subframe
     case 1
       SecSync(2*n+1) = PN_seq(mod(n+m0,31)+1).* ...
                              SC_seq1(mod(n+NID2, 31)+1);
       SecSync(2*n+2) = PN_seq(mod(n+m1,31)+1).* ...
                            SC_seq1(mod(n+NID2+3,31)+1).* ...
                              SC_seq2(mod(n+mod(m0,8),31)+1);
    case 6
       SecSync(2*n+1) = PN_seq(mod(n+m1,31)+1).* ...
                                    SC_seq1(mod(n+NID2, 31)+1);
       SecSync(2*n+2) = PN_seq(mod(n+m0,31)+1).* ...
                              SC_seq1(mod(n+NID2+3,31)+1).* ...
                                SC_seq2(mod(n+mod(m1,8),31)+1);
    end
end

% Secondary synchronization signal mapping
Sec_Mapping = false(Nrb*Nsc,Ns);
k = zeros(62,1);
for n=1:62
    k(n)=n-32+Nrb*Nsc/2;
end
k = k+1;
Sec_Mapping(k,Ns/2-1)=1;
ResUsedElements = zeros(Nrb*2,1);
for i2 = 1:2
    for i1 = 1:Nrb
        ResUsedElements(i1+(i2-1)*Nrb) = ...
                      sum(sum(ReservedMapping((i1-1)*...
                      Nsc+1:i1*Nsc,(i2-1)*Ns/2+1:Ns/2*i2)));
    end
end
ResNElements = sum(sum(ResUsedElements));


% Read received data stream combined from three BSs with BSIDs
1, 2, 3.
fid = fopen('RxData3ModOrd1.dat','rb');
data = fread(fid,'float'); fclose(fid);
```

```
% Create complex samples from real and imaginary parts
d =data(1:2:end) + 1j*data(2:2:end);

%-----------------------------------------
%       Primary synchronization
%-----------------------------------------
pr1 = LTE_params.Sync_Signal(1,1).PrimSync;
pr2 = LTE_params.Sync_Signal(2,1).PrimSync;
pr3 = LTE_params.Sync_Signal(3,1).PrimSync;
% Plot cross-correlation output of pr1 and d
figure('color','w');
subplot(3,2,1)
[normPrimcorr] = doCorrelation(d, pr1);
plot(normPrimcorr,'r')
ylabel('Primary syncrhonization, q = 29')
[PeakCorr averages  ratios] = doPeakDetection(normPrimcorr);
hold on;
plot(averages(LTE_params.Nfft+1:end), 'k');
plot(ratios(LTE_params.Nfft+1:end), 'g');
stem(100*PeakCorr,'c.');
title('Normalized Magnitude ')
% plot the output of the cross-correlation of pr2 and d
subplot(3,2,2)
[normPrimcorr] =   doCorrelation(d, pr2);

plot(normPrimcorr,'r')
ylabel('Primary syncrhonization, q = 34')
[PeakCorr averages  ratios] = doPeakDetection(normPrimcorr);
hold on;
plot(averages(LTE_params.Nfft+1:end), 'k');
plot(ratios(LTE_params.Nfft+1:end), 'g');
stem(100*PeakCorr,'c.');
title('Normalized Magnitude')



% plot the output of the cross-correlation of pr3 and d
subplot(3,2,3)
[normPrimcorr] =   doCorrelation(d, pr3);
plot(normPrimcorr,'r')
ylabel('Primary syncrhonization, q = 25')
```

```
title('Normalized Magnitude')
[PeakCorr averages  ratios] = doPeakDetection(normPrimcorr);
hold on;
plot(averages(LTE_params.Nfft+1:end), 'k');
plot(ratios(LTE_params.Nfft+1:end), 'g');
stem(100*PeakCorr,'c.');

sec1 = LTE_params.Sync_Signal(1,1).SecSync;
sec2 = LTE_params.Sync_Signal(2,1).SecSync;
sec3 = LTE_params.Sync_Signal(3,1).SecSync;
sec4 = LTE_params.Sync_Signal(4,1).SecSync;

%-----------------------------------------
%       Secondary synchronization
%-----------------------------------------
% plot the output of the cross-correlation of sec1 and d
figure('color','w');
subplot(4,2,1);
[normSec_corr] =   doCorrelation(d, sec1);
plot(normSec_corr,'r')
ylabel('Secondary syncrhonization, BS1')
title('Normalized Magnitude')
% plot the output of the cross-correlation of sec2 and d
subplot(4,2,2)
[normSec_corr] =   doCorrelation(d, sec2);
plot(normSec_corr,'r')
ylabel('Secondary syncrhonization, BS2')
title('Normalized magnitude')
% plot the out put of the cross-correlation of sec3 and d
subplot(4,2,3)
[normSec_corr] =   doCorrelation(d, sec3);
plot(normSec_corr,'r')
ylabel('Secondary syncrhonization, BS3')
title('Normalized Magnitude')
% plot the output of the cross-correlation of sec4 and d
subplot(4,2,4)
[normSec_corr] =   doCorrelation(d, sec2);
plot(normSec_corr,'r')
ylabel('Secondary syncrhonization, BTS4');
title('Normalized Magnitude')
```

```
%-------------------------------------------------------------
% Secondary peak detection
%-------------------------------------------------------------
function [normCorr] =   doCorrelation(d, seq)
% Performs correlation of input data stream 'd' with the given
% synchronization sequence 'seq', Ntot: used carriers in the
% system
global LTE_params;
% let's perform shifted ifft on the synch sequence
padede_seq = padarray(seq,5);
zero_dc_seq = [padded_seq(1:LTE_params.Ntot/2); zeros(1,1); ...
                    padded_seq(LTE_params.Ntot/2+1:end)];
seq_tmp = [zero_dc_seq; zeros(LTE_params.Nfft- ...
         LTE_params.Ntot-1,size(zero_dc_seq,2))];
shifted_seq =  circshift(seq_tmp,-LTE_params.Ntot/2);
shifted_seq_ifft = ifft(shifted_seq _Circpadded);
correlation_Sum = abs(filter(flipud(conj(shifted_seq_ifft)),...
                            1, d )).^2 ;
power = abs(filter(ones(1,length(shifted_seq_ifft)),1, ...
                              d.*conj(d)) );
normCorr = corrSum./power;


function [corrPeaks averages  ratios] =
                              doPeakDetection(normCorr)
% Perform peak detection on the normalized correlation output
'normCorr'
global LTE_params;
corrPeaks = zeros(size(normCorr));
averages = zeros(size(normCorr));
ratios = zeros(size(normCorr));
peak_val = -Inf;
peak_ind = 0;
state = 0;
i = 1;
avg = 0.01;
avg_alpha = 0.01;
threshold_factor_fall = 5;
threshold_factor_rise = 15;
while i <= length(normCorr)
    if state == 0  % below threshold
```

```
            if normCorr(i) > avg*threshold_factor_rise
                  state = 1;
            else
                  avg = (avg_alpha)*normCorr(i) + (1- ...
                                avg_alpha)*avg;
                  averages(i) = avg;
                  ratios(i) = normCorr(i)/avg;
                  i = i+1;
            end
      elseif state == 1   % above threshold, have not found peak
             if normCorr(i) > peak_val
                  peak_val = normCorr(i);
                  peak_ind = i;
                  avg = (avg_alpha)*normCorr(i) + ...
                                (1-avg_alpha)*avg;
                  averages(i) = avg;
                  ratios(i) = normCorr(i)/avg;
                  i = i+1;
             else
                  if normCorr(i) > avg*threshold_factor_fall
                     avg = (avg_alpha)*normCorr(i) + (1-
                           avg_alpha)*avg;
                     averages(i) = avg;
                     ratios(i) = normCorr(i)/avg;
                     i = i+1;
                  else
                      corrPeaks(peak_ind) = 1;
                      state = 0;
                      peak_val = -Inf;
                  end
             end
      end
end
```

C DVB-T Continual and TPS pilot positions for 2K and 8K Modes

Continual pilot carrier positions (index number N)														
2K mode							8K mode							
0	48	54	87	141	156	192	0	48	54	87	141	156	192
201	255	279	282	333	432	450	201	255	279	282	333	432	450
483	525	531	618	636	714	759	483	525	531	618	636	714	759
765	780	804	873	888	918	939	765	780	804	873	888	918	939
942	969	984	1 050	1 101	1 107	1 110	942	969	984	1 050	1 101	1 107	1 110
1 137	1 140	1 146	1 206	1 269	1 323	1 377	1 137	1 140	1 146	1 206	1 269	1 323	1 377
1 491	1 683	1 704					1 491	1 683	1 704	1 752	1 758	1 791	1 845
							1 860	1 896	1 905	1 959	1 983	1 986	2 037
							2 136	2 154	2 187	2 229	2 235	2 322	2 340
							2 418	2 463	2 469	2 484	2 508	2 577	2 592
							2 622	2 643	2 646	2 673	2 688	2 754	2 805
							2 811	2 814	2 841	2 844	2 850	2 910	2 973
							3 027	3 081	3 195	3 387	3 408	3 456	3 462
							3 495	3 549	3 564	3 600	3 609	3 663	3 687
							3 690	3 741	3 840	3 858	3 891	3 933	3 939
							4 026	4 044	4 122	4 167	4 173	4 188	4 212
							4 281	4 296	4 326	4 347	4 350	4 377	4 392
							4 458	4 509	4 515	4 518	4 545	4 548	4 554
							4 614	4 677	4 731	4 785	4 899	5 091	5 112
							5 160	5 166	5 199	5 253	5 268	5 304	5 313
							5 367	5 391	5 394	5 445	5 544	5 562	5 595
							5 637	5 643	5 730	5 748	5 826	5 871	5 877
							5 892	5 916	5 985	6 000	6 030	6 051	6 054
							6 081	6 096	6 162	6 213	6 219	6 222	6 249
							6 252	6 258	6 318	6 381	6 435	6 489	6 603
							6 795	6 816					

TPS pilots carrier positions (Index number N)													
2K mode					8K mode								
34	50	209	346	413	34	50	209	346	413	569	595	688
569	595	688	790	901	790	901	1 073	1 219	1 262	1 286	1 469	1 594
1 073	1 219	1 262	1 286	1 469	1 687	1 738	1 754	1 913	2 050	2 117	2 273	2 299
1 594	1 687				2 392	2 494	2 605	2 777	2 923	2 966	2 990	3 173
					3 298	3 391	3 442	3 458	3 617	3 754	3 821	3 977
					4 003	4 096	4 198	4 309	4 481	4 627	4 670	4 694
					4 877	5 002	5 095	5 146	5 162	5 321	5 458	5 525
					5 681	5 707	5 800	5 902	6 013	6 185	6 331	6 374
					6 398	6 581	6 706	6 799				